Response of Metals and Metallic Structures to Dynamic Loading

National Materials Advisory Board

Commission on Sociotechnical Systems

NMAB-341

NATIONAL RESEARCH COUNCIL
COMMISSION ON SOCIOTECHNICAL SYSTEMS

NATIONAL MATERIALS ADVISORY BOARD

Chairman

Mr. Julius J. Harwood
Director, Materials Science Laboratory
Engineering and Research Staff
Ford Motor Company
P.O. Box 2053
Dearborn, Michigan 48121

Past Chairman

Dr. Seymour L. Blum
Director, Energy and Resources Management
The MITRE Corporation
P.O. Box 208
Bedford, Massachusetts 01730

Members

Dr. George S. Ansell
Dean, School of Engineering
Rensselaer Polytechnic Institute
Troy, New York 12181

Dr. Alan G. Chynoweth
Executive Director, Electronic Device, Process and Materials Division
Bell Laboratories
Murray Hill, New Jersey 07974

Dr. Arthur C. Damask
Professor, Physics Department
Queens College of New York City
Flushing, New York 11367
(Mail Address)
29 Brewster Lane
Bellport, N.Y. 11713

Mr. Selwyn Enzer
Associate Director
Center for Futures Research
University of Southern California
Los Angeles, California 90007

Dr. Joseph N. Epel
Director, Plastics Research and Development Center
Budd Corporation
356 Executive Drive
Troy, Michigan 48084

Dr. Herbert I. Fusfeld
Director of Research
Kennecott Copper Corporation
161 E. 42nd Street
New York, New York 10017

Dr. Robert E. Hughes
Professor of Chemistry
Executive Director, Materials Space Center
Department of Chemistry
Cornell University
Ithaca, New York 14850

Dr. James R. Johnson
Executive Scientist and Director
Advanced Research Programs Laboratory
3M Company
P.O. Box 33221
St. Paul, Minnesota 55133

Mr. Lawrence Levy
President
Northern Energy Corp.
70 Memorial Drive
Cambridge, Massachusetts 02142

Mr. William D. Manly
Senior Vice President
Cabot Corporation
1020 West Park Avenue
Kokomo, Indiana 46901

Dr. Frederick T. Moore
Industrial Advisor
Industrial Development and Finance Department, Room D422
World Bank
1818 H Street, N.W.
Washington, D.C. 20431

Dr. Harold W. Paxton
Vice President-Research
U.S. Steel Corporation
600 Grant Street
Pittsburgh, Pennsylvania 15219

Mr. Nathan E. Promisel
Consultant
12519 Davan Drive
Silver Spring, Maryland 20904

Dr. Jason M. Salsbury
Director
Chemical Research Division
American Cyanamid Company
Berdan Avenue
Wayne, New Jersey 07470

Dr. Raymond L. Smith
President
Michigan Technological University
1400 College Avenue
Houghton, Michigan 49931

Dr. William M. Spurgeon
Director, Manufacturing and Quality Control
Bendix Corporation
24799 Edgemont Road
Southfield, Michigan 48075

Dr. Morris A. Steinberg
Director, Technology Applications
Lockheed Aircraft Corporation
Burbank, California 91520

Dr. Giuliana C. Tesoro
Adjunct Professor
Massachusetts Institute of Technology
278 Clinton Avenue
Dobbs Ferry, New York 10522

Dr. John E. Tilton
Professor
Department of Mineral Economics
221 Walker Building
The Pennsylvania State University
University Park, Pennsylvania 16802

Dr. John B. Wachtman, Jr.
Director
Center for Materials Science
National Bureau of Standards
Room B306, Materials Building
Washington, D.C. 20234

NMAB Staff:

W. R. Prindle, Executive Director
R. V. Hemm, Executive Secretary

3/3/78

UNCLASSIFIED

SECURITY CLASSIFICATION OF THIS PAGE (When Data Entered)

REPORT DOCUMENTATION PAGE

READ INSTRUCTIONS BEFORE COMPLETING FORM

1. REPORT NUMBER: NMAB-341	2. GOVT ACCESSION NO.
3. RECIPIENT'S CATALOG NUMBER	
4. TITLE (and Subtitle): Response of Metals and Metallic Structures to Dynamic Loading	5. TYPE OF REPORT & PERIOD COVERED: Final Report
6. PERFORMING ORG. REPORT NUMBER: NMAB-341	
7. AUTHOR(s): NMAB Committee on the Dynamic Response of Materials Subjected to High Strain Loading	8. CONTRACT OR GRANT NUMBER(s): MDA 903-78-C-0038
9. PERFORMING ORGANIZATION NAME AND ADDRESS: National Materials Advisory Board, National Academy of Sciences, Washington, D.C. 20418	10. PROGRAM ELEMENT, PROJECT, TASK AREA & WORK UNIT NUMBERS
11. CONTROLLING OFFICE NAME AND ADDRESS	12. REPORT DATE: May 1978
	13. NUMBER OF PAGES: 179
14. MONITORING AGENCY NAME & ADDRESS (if different from Controlling Office)	15. SECURITY CLASS. (of this report): UNCLASSIFIED
	15a. DECLASSIFICATION/DOWNGRADING SCHEDULE

16. DISTRIBUTION STATEMENT (of this Report)

This report has been approved for public release and sale; its distribution is unlimited.

17. DISTRIBUTION STATEMENT (of the abstract entered in Block 20, if different from Report)

18. SUPPLEMENTARY NOTES

19. KEY WORDS (Continue on reverse side if necessary and identify by block number)

High Strain Rate
Dynamic Response of Materials
Fracture
Fracture Mechanics
Failure Prediction
Stress Analysis

20. ABSTRACT (Continue on reverse side if necessary and identify by block number)

Dynamic response of metals and metallic structures is reviewed with respect to current procedures and understanding in order to identify research needs. Emphasis is placed on response in military environments which involve very high loading rates, such as those due to air blasts and underwater explosions. Included in this review is discussion of basic inelastic deformation mechanisms, mechanical properties, fracture analysis and testing, structural analysis (including consideration of buckling response) and scale modeling. The principal conclusions and recommendations are given in Section II.

DD FORM 1 JAN 73 1473 EDITION OF 1 NOV 65 IS OBSOLETE

UNCLASSIFIED

SECURITY CLASSIFICATION OF THIS PAGE (When Data Entered)

RESPONSE OF METALS AND METALLIC STRUCTURES TO DYNAMIC LOADING

Report of

The Committee on the Response of Metals and Metallic Structures to Dynamic Loading

NATIONAL MATERIALS ADVISORY BOARD
Commission on Sociotechnical Systems
National Research Council

Publication NMAB-341

National Academy of Sciences

Washington, D. C.

1978

NOTICE

The project that is the subject of this report was approved by the Governing Board of the National Research Council, whose members are drawn from the Councils of the National Academy of Sciences, the National Academy of Engineering, and the Institute of Medicine. The members of the Committee responsible for the report were chosen for their special competence and with regard for appropriate balance.

This report has been reviewed by a group other than the authors according to procedures approved by a Report Review Committee consisting of members of the National Academy of Sciences, National Academy of Engineering, and the Institute of Medicine.

This study by the National Materials Advisory Board was conducted under Contract No. MDA 903-78-C-0038 with the Department of Defense and the National Aeronautics and Space Administration.

This report is for sale by the National Technical Information Service, Springfield, Virginia 22151.

Printed in the United States of America.

COMMITTEE ON THE RESPONSE OF METALS AND METALLIC STRUCTURES TO DYNAMIC LOADING

Chairman

RICHARD A. SCHAPERY, Director, Mechanics and Materials Research Center, and Professor of Civil and Aerospace Engineering, Texas A&M University, College Station, Texas

Members

MELVIN F. KANNINEN, Senior Researcher, Applied Solid Mechanics Section, Battelle Columbus Laboratories, Ohio

ULRIC S. LINDHOLM, Director, Department of Material Sciences, Southwest Research Institute, San Antonio, Texas

ARTHUR J. McEVILY, Jr., Department of Metallurgy, School of Engineering, University of Connecticut, Storrs, Connecticut

ROBERT J. McGRATTAN, Chief, Ocean Science and Engineering, Electric Boat Division, General Dynamics, Corp., New London, Connecticut

GEORGE C. SIH, Professor and Director, Institute of Fracture Mechanics, Lehigh University, Bethlehem, Pennsylvania

Liaison Representatives

SHUN-CHIN CHOU, Mechanics Research Laboratory, Army Materials and Mechanics Research Center, Watertown, Massachusetts

GEORGE C. DEUTSCH, Director, Materials and Structures Division, National Aeronautics and Space Administration, Washington, D. C.

L. R. HETTCHE, Engineering Materials Division, Naval Research Laboratory, Department of the Navy, Washington, D. C.

THEODORE NICHOLAS, Metals Behavior Branch, Metals and Ceramics Division, Air Force Materials Laboratory, Wright-Patterson Air Force Base, Ohio

EDWARD PALMER, Head, Underwater Explosion Research Division, D. W. Taylor Naval Ship Research and Development Center, Portsmouth, Virginia

JEROME PERSH, Staff Specialist, Materials and Structures (Engineering Technology), ODDR&E, Department of Defense, Washington, D. C.

GEORGE SORKIN, Director, Materials and Mechanics Division, Naval Sea Systems Command, Washington, D. C.

Advisor to the Committee

AJAYA K. GUPTA, Senior Research Engineer, Structural Analysis, IIT Research Institute, Chicago, Illinois

NMAB Staff

DONALD G. GROVES, Staff Engineer

ACKNOWLEDGMENTS

The committee would like to thank the following persons for giving generously of their time in making presentations before the committee:

W. E. Baker, Southwest Research Institute, San Antonio, Texas

G. T. Hahn, Battelle-Columbus Laboratories, Columbus, Ohio

E. A. Lange, Naval Research Laboratory, Department of the Navy, Washington, D. C.

Dr. A. K. Gupta, IIT Research Institute, participated in some of the committee meetings and made significant contributions to the report, for which the members are very grateful.

The committee also received considerable help from their associates and many others through personal discussions and by providing pertinent publications and data. The invaluable staff support of Donald G. Groves in the committee deliberations and report preparation is also gratefully acknowledged.

R. A. Schapery
Chairman
NMAB Committee on Response
of Metals and Metallic
Structures to Dynamic Loading

ABSTRACT

Dynamic response of metals and metallic structures is reviewed with respect to current procedures and understanding in order to identify research needs. Emphasis is placed on response in military environments which involve very high loading rates, such as those due to air blasts and underwater explosions. Included in this review is discussion of basic inelastic deformation mechanisms, mechanical properties, fracture analysis and testing, structural analysis (including consideration of buckling response) and scale modeling. The principal conclusions and recommendations are given in Section II.

CONTENTS

I. INTRODUCTION

The Department of Defense (DoD) has a major interest in structural evaluation, design, and testing of equipment. Current approaches involve, to varying degrees, modern methods of structural analysis, linear elastic fracture mechanics, and nondestructive inspection, as well as the more traditional methods of impact testing of specimens and scale modeling.

This report concentrates on military environments that involve very high loading rates, such as those due to air blasts and underwater explosions. In these problems, valid approaches must incorporate the strain rate and temperature sensitivity of inelastic behavior possessed by many structural alloys. There is presently a considerable amount of research underway to improve the various technologies and their interaction in dynamic problems. However, the state of the art is quite limited, especially for the problems involving dynamic elastic-plastic response and failure. Furthermore, in many cases where theoretical methods exist there are insufficient mechanical and fracture property data in the high strain rate regime to permit implementation and verification of the analyses.

Being cognizant of these factors, the DoD requested that the National Materials Advisory Board (NMAB) appoint a committee to recommend areas where current procedures and understanding should be strengthened. Special attention was directed to the examination of:

- Materials tests which reflect more advanced concepts in the mechanics of failure,

- Developments which could successfully merge material property testing with modern methods of computational structural mechanics,

- Developments which will lead to quantitative analysis procedures for assessing the flaw and load severity in defense engineering systems, and

- Development of small-scale testing and evaluation procedures which will reduce the need for large model or full-scale testing.

Important benefits accruing from implementation of the Committee's recommendations are:

- Reduction in testing costs,
- More rapid assessment of materials feasibility, and
- Development of better materials, processing, and fabrication to cope with dynamic loads.

As a practical matter, considering the very broad interdisciplinary nature of the study, this Committee decided to restrict its assessment to metallic structures and to deal with only nominal strain rates of loading up to 10^3 seconds^{-1}; this latter restriction excludes phenomena such as those produced by high-speed projectile penetration and particle impact. Fatigue also is excluded from this study.

It is believed that significant improvements in the state of the art can be achieved through a proper understanding and application of the various interrelated disciplines which are involved: metallurgy, mechanical property characterization, fracture analysis and testing, structural analysis (including consideration of buckling response) and scale modeling. This report addresses each of these areas to the extent believed necessary to respond to the aforementioned DoD request and provide the basis for the Conclusions and Recommendations given in Section II. (For the reader's convenience, individual sets of conclusions are also listed at the end of the most lengthy subsections; however, only the main ones are collected in Section II.) Figure I-1 depicts the way in which the several disciplines interact in the assessment of damage tolerance of structures.

The time variation of the loading is obviously an important consideration in dynamic problems. Therefore, background information on the nature of some transient load environments is given in Section III. Current understanding of dynamic response of materials and approaches employed in its investigation are discussed in

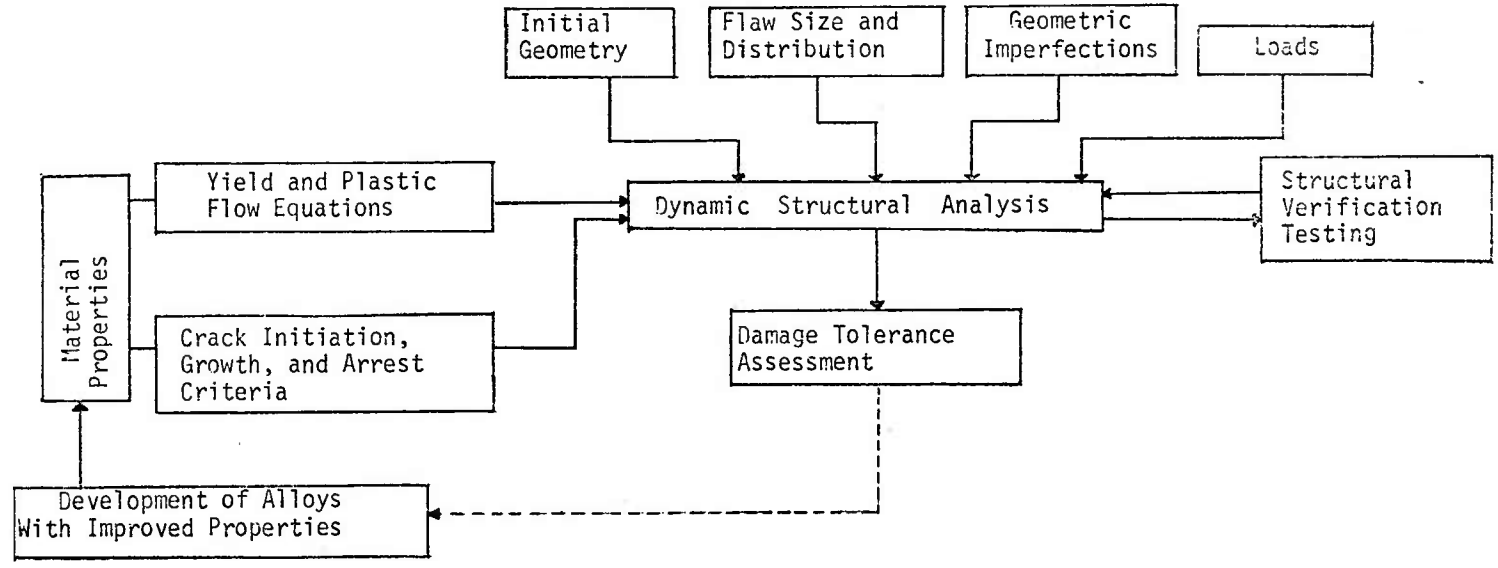

FIGURE I-1 A Typical Flow Diagram for Damage Tolerance Assessment

Section IV. Of the various areas, dynamic fracture mechanics and related testing are covered in the most detail; the committee believes this emphasis is necessary because of the complexity of the subject and the fact that there have been many important developments in just the past few years that are not summarized elsewhere.

There are many important problems in which the failure mode is excessive deformation and/or buckling. Prediction of this type of failure for ductile materials subjected to large impulse loading can often be made quite simply and accurately, using the assumption of rigid-plastic behavior. Inasmuch as Jones (1975, 1976, 1978) and Jones and Okawa (1976) have recently reviewed both theoretical and experimental studies in this area, it is not covered in this report. They discuss relatively simple formulas which provide physical insight into dynamic behavior and quite accurate estimates of a variety of responses, including failure of beams, plates, shells, and rings, and slamming and ice damage of ships. The importance of such dynamic plastic analyses cannot be overemphasized; they often are entirely adequate in the early stages of a preliminary design, provide guidelines for the selection a meaningful set of parameters for an experimental program, and can serve as special cases for checking more general numerical procedures.

The reader will see that different sets of units are used in this report. Many figures are reproduced from publications, and conversion of data and units would be rather time-consuming and costly. Therefore, we implore the indulgence of the reader and offer a brief conversion table between English, metric, and SI units in Table I-1.

TABLE I-1 Standard International Values of Some U.S. Units

1 in. = .0254 m
1 ft. = .3048 m
1 lbf = 4.448 N
1 kgf = 9.807 N
1 dyne = 10 E-6 N

1000 psi = 6.895 MN/m^2
1 bar = E 6 $dyne/cm^2$ = .1 MN/m^2
1 atm = .1013 MN/m^2
1 torr = 1 mm Hg = 133.3 N/m^2
1 kgf/mm^2 = 9.807 MN/m^2

1000 psi $\sqrt{in.}$ = 1.099 $MN/m^{3/2}$
1 lbf/in. = 175.1 N/m

1 lbm = .4536 kg
1 ft lbf = 1.356 Nm
1 erg = 1 dyne cm = .1E-6 Nm
1 hp = 745.7 Nm/s
1 kw = 1000 Nm/s

1 $lbm/in.^3$ = 27.68 E 3 kg/m^3
1 gm/cm^3 = 1000 kg/m^3
1 centipoise = .001 N s/m^2
1 lbf s/ft^2 = 47.88 N s/m^2

c_{air} = 344 m/s
c_{water} = 1470 m/s
c_{steel} = 5000 m/s
c_{light} = 299.8 E 6 m/s

g = 9.807 m/s^2
γ = 66.70 E-12 Nm^2/kg^2
or $m^3/kg\text{-}s^2$

P R E F I X E S

atto	femto	pico	nano	micro	milli	kilo	mega	giga	tera
a	f	p	n	μ	m	k	M	G	T
10^{-18}	10^{-15}	10^{-12}	10^{-9}	10^{-6}	10^{-3}	10^{-3}	10^{6}	10^{9}	10^{12}

REFERENCES - INTRODUCTION

Jones, N., "A Literature Review of the Dynamic Plastic Response of Structures," The Shock and Vibration Digest, The Shock and Vibration Information Center, Naval Research Laboratory, Washington, D. C., Vol. 7, No. 8, p. 89, 1975.

Jones, N., "Plastic Behavior of Ship Structures," Presented at Annual Meeting of the Society of Naval Architects and Marine Engineers, 1976.

Jones, N., and Okawa, D.M., "Dynamic Plastic Buckling of Rings and Cylindrical Shells," Nuclear Engineering and Design, Vol. 37, p. 125, 1976.

Jones, W., "Recent Progress in the Dynamic Plastic Behavior of Structures," Report Number 78-1, Massachusetts Institute of Technology, Cambridge, Massachusetts, 1978.

II. CONCLUSIONS AND RECOMMENDATIONS

These conclusions and recommendations represent the composite opinion of the committee. Every effort was made to be objective in the evaluation of the recent literature and current activities in the field.

As an aid to the reader, section numbers in which the relevant background discussion appears are indicated in parentheses.

A. Conclusions

1. A reasonable understanding of the processes governing constant strain rate and temperature effects on yield and stable plastic response has been achieved. Experimental techniques and data are available for many structural materials in the ranges of strain rate and temperature of engineering interest. However, existing constitutive equations and data are not adequate for predicting inelastic response under conditions of unloading and reloading into the plastic state. (Sections IV.B.1-3.)

2. One of the oldest ideas in fracture control is the certification of materials for service by testing under high rates of loading. Impact tests such as the Charpy test, the drop-weight tear test, and the dynamic tear test have been (and continue to be) widely used. These tests were originally intended to give qualitative information only, such as the transition temperature. Recently, however, it has become widely realized that it may be possible to extract useful quantitative information from the results of impact tests. What is not yet generally recognized is that the conventional analytical interpretation of such tests via a completely static point of view can be substantially in error. Recent research work using dynamic (i.e., inertia forces included) analyses described in this report have clearly shown this for precracked charpy specimens and for the drop-weight tear test. Hence, there is a strong need for additional dynamic analyses to accompany high strain

rate testing. These will likely lead to improved specimen design and test techniques to evaluate fracture properties of more direct use in engineering structural design (Section IV.B.4.)

3. The two main approaches in dynamic fracture analysis and testing are: 1) the dynamic propagation of a crack initiated under quasi-static loading conditions, and 2) initiation of crack growth under dynamic loading. Obviously, a full and proper treatment of dynamic fracture must combine dynamic initiation, propagation and arrest of cracks; such a capability does not yet exist. (Sections IV. B.4-6.)

4. Provided the loading is known, or can be established if structural coupling exists, prediction of dynamic response without flaw growth and large deformations can be made for many engineering structures. (Section IV.B.6.)

5. Large and full-scale models are currently used for structural evaluation despite the high costs and time consumption, generally because there is a lack of confidence in small scale model tests. However, analytical and numerical techniques to predict scale model and prototype response have improved dramatically in recent years. These techniques have led to a significant increase in understanding of dynamic structural response and of the way in which flaws and geometric inperfections, respectively, influence fracture and buckling behavior. Although uncertainties still exist, the progress made so far appears to provide the basis for significant cost and time savings through greater reliance on analysis and scale models in structural design and evaluation. (Sections IV.B.6 and IV.C.)

6. Similitude analysis is vital to the success of any scale model test, even though it may prove impossible to match all geometric, kinematic dynamic, and constitutive similitude parameters. Many materials of DoD interest exhibit moderate to high toughness values; however, similitude analysis and testing is not restricted to linear elastic behavior and can be extended to treat elastic-plastic behavior. (Section IV.C.)

B. Recommendations

The two most critical needs are concerned with fracture criteria and scale modeling:

1. Establish criteria and associated tests for the initiation, propagation, and arrest of cracks in tough structural materials. Current dynamic fracture mechanics can treat linear elastic behavior only. Both experimental and mathematical analysis work needs to be done to identify and establish the appropriate material parameters needed for a dynamic elastic-plastic fracture mechanics methodology and to verify the basic concepts. (Section IV.B.4-6.)

2. Develop methods of structural model testing which incorporate fracture mechanics principles. In view of the importance of flaws in the damage tolerance of structures subjected to dynamic loading, model tests must be able to incorporate flaws in sensitive areas. To circumvent the difficulty arising from thichness dependence of the fracture toughness, a research program addressed to toughness-scaled materials should be conducted. This program should include analysis and experiment in order to select appropriate scaling parameters and to verify that model tests using toughness-scaled materials will give reliable information on actual structures with flaws. (Section IV.C.)

Additional recommendations follow. (It should be noted that recommendations 3 and 4 are made with little support given in the body of the report because of the paucity of information reported in the open literature.)

3. Further work is needed to develop better analysis techniques to handle shock wave-structure interaction problems. These analyses should be verified by experiment-model and prototype. (Section III.)

4. For close-in explosions, such as contact mines or other near field problems with high peak pressure, additional definition of reflected shock parameters is needed (Section III.)

5. Where gaps exist in data for dynamic flow stress of structural materials of interest, they should be filled and a catalog of data prepared by one of the appropriate DoD information centers such as MCIC. (Section IV.B.2)

6. Through experimental and theoretical investigations, develop improved constitutive equations for dynamic inelastic behavior under multiaxial stresses and time varying strain rates. (Section IV.B.3)

7. Standardization of test methods for measuring stress-strain behavior at high rates should be considered before these data are used in critical design applications. (Section IV.B.3)

8. Develop improved analysis methods for prediction of dynamic buckling and large deformation response of shell structures. This work should include both theoretical and scale-model investigations. (Section IV.B.6)

III. LOADING

The starting point of any dynamic response analysis is a definition of the geometry of the structure, the physical properties of the materials from which the structure is fabricated, and the nature of the loading. The details of structural geometry are generally prescribed and known within the accuracy limits of manufacturing tolerances. For statically loaded metallic structures, the set of material properties needed to adequately describe the elastic, inelastic and fracture behavior is relatively well defined. In the dynamic loading regime, there remain some uncertainties as to the adequacy of our ability to describe material behavior. Proper prescription of dynamic material properties will be a major concern of remaining sections of this report. The remaining prerequisite, that of load definition, will be the subject of this section.

The committee has restricted its attention to a regime of high strain-rate loading which excludes high velocity projectile or particle impact. These latter problems involve localized, intense deformation which produces very high strain rates and therefore should be treated separately. The present report is concerned with dynamic loading sources which produce gross structural damage, such as impingement by a propagating blast wave, structural impact or collision, or the sudden release of energy as in propellant expansion. These loading sources generally produce impulse durations on the order of milliseconds. The response depends, of course, on the overall stiffness and mass distribution of the structure. Typical inelastic strain rates associated with permanent damage are of the order of 1-100 sec^{-1}, with local rates at strain concentration sites (notches, corners, cracks, etc.) reaching and perhaps exceeding 1000 sec^{-1}. Our review of material constitutive properties will concentrate, therefore, on the strain-rate range between "static" and 1000 sec^{-1}.

In this section some typical dynamic loading sources of interest to DoD are described. This characterization is intended only to illustrate the nature of the loading function and the relative range of the load defining parameters. The values presented represent typical ranges and therefore are not recommended for use in specific problems.

TABLE III-1 Ranges of Pressures, Durations, Impulse for Various Surface Ship Loadings

Source	Range of Pressures, psi	Range of Durations, seconds	Range of Impulses, psi-sec.	Strain Rate (sec^{-1})
Explosion in Air				
a. Nuclear	5-1000	0.1-10	0.05-250	
b. Non-nuclear	5-5000	10^{-3}-10^{-1}		
Underwater Explosion				
a. Nuclear	500-3000	10^{-2}-0.1	1-100	1-5
b. Non-nuclear	500-10^{4}	$5x10^{-5}$-10^{-2}	0.5-10	10-50
Mechanical Impact	500-3000	$5x10^{-3}$	1-10	10-50
Ship Hull Slamming				
a. Large Surface Ship	1-50	10^{-3}-10^{-1}		
b. High-Performance Craft	1-150	$5x10^{-2}$-10^{-1}		
Muzzle Blast				
a. Interior	10^{4}-10^{5}	10^{-3}-10^{-2}		
b. Exterior	0.5-20	10^{-3}-10^{-2}		
Land Mine	$2x10^{4}$-$1.5x10^{5}$	0.1-10		

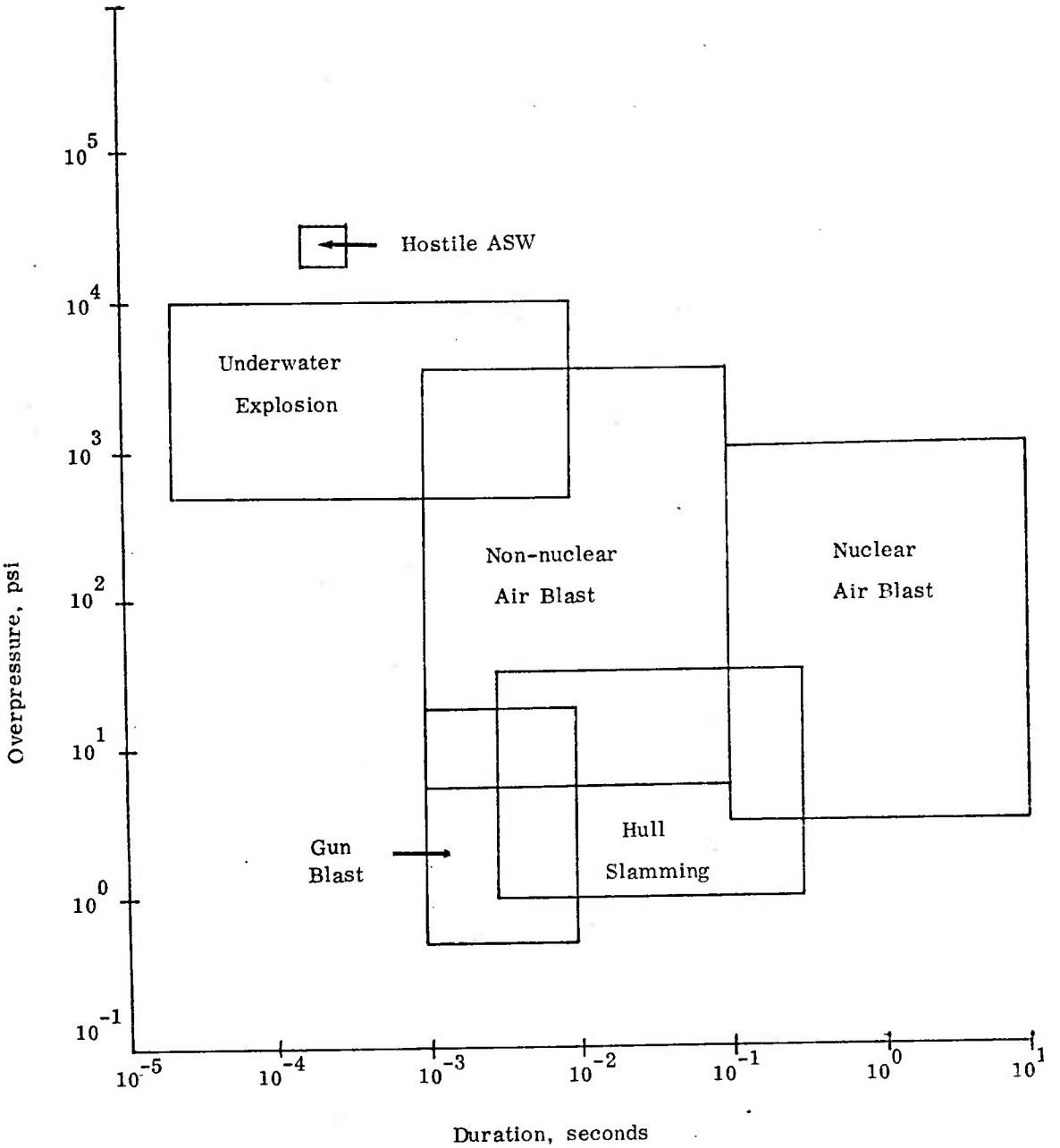

FIGURE III-1 Overpressure vs. Duration for Loading Conditions Cited in Table III.1

Table III-1 presents a list of dynamic loading sources of concern to military structures or components with a typical range of peak pressures, load durations and total impulses for each source. Most problems of the type we are considering involve a single loading event; in some cases, however, the impact load may be repetitive. Examples of the latter are ship hull slamming in rough seas or repetitive firing of a weapon. In such cases, damage is cumulative and failure may occur only after long time periods (number of impacts). Figure III-1 plots the peak overpressure versus duration for sources listed in Table III-1.

The details of the pressure pulses from various sources are illustrated in subsequent figures. For an air blast, either from conventional or nuclear sources, the idealized pressure wave is as given in Figure III-2. It has a sharp rise time followed by a positive and then a negative pressure phase. From a structural point of view, the critical parameters are the peak positive pressure, the duration, and total impulse of the positive phase. Figures III-3a, b, and c give the magnitude of these parameters for different standoff distances for nuclear and scaled TNT equivalents (Baker, 1973). Reflected pressures from the exposed surface of a structure in the field of a blast wave may be many times the free field pressure. The pressure-time history can be modified as well by the presence of surrounding reflecting or refracting surfaces, such as the ground.

Underwater explosion loading (Cole, 1965) is normally of two types: plane waves of moderate peak pressure with a slow exponential decay and spherical waves with rapid exponential decay, as illustrated in Figure III-4. The plane wave is associated with a nuclear explosion located at a considerable distance from the structure and the spherical wave is associated with a conventional chemical explosion located close to the structure. For the case of the chemical explosion, the loading is much different than the free field wave, as shown in Figure III-5 due to non-linear interaction between the structure and the shock wave (Barton and Pilkey, 1974). This nonlinear interaction is associated with the deformation of the shell. Also, local cavitation occurs as the shell responds to the shock wave. Typically, a few milliseconds after shock wave arrival a

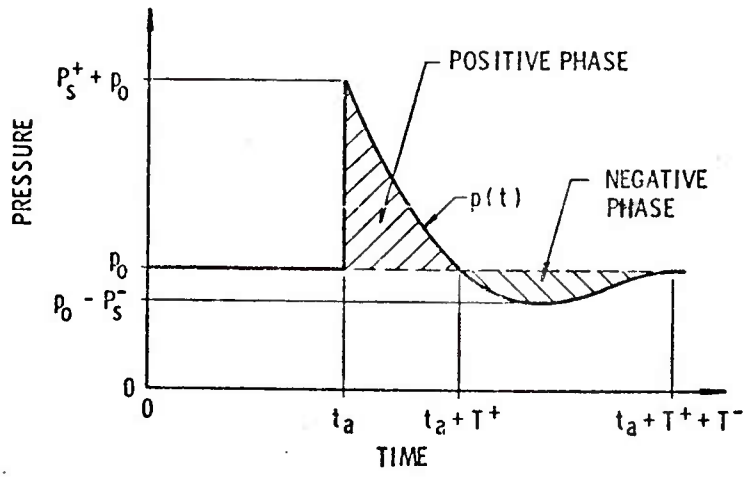

FIGURE III-2 Idealized Blast Wave

SOURCE: Baker, W.E., 1973

reloading occurs due to closing of the cavitation. Other secondary loads due to surface reflected waves or bottom reflected waves can also occur.

In the case of plane wave excitation (Huang, 1969) due to an underwater nuclear explosion at a considerable distance from the structure, the response of a typical cylindrical shell consists primarily of rigid body motion, beam whipping, and axisymmetric (breathing mode) motion. Other motions, such as asymmetric shell bending modes, contribute to a lesser extent.

In terms of strain response, the strain rate for the nuclear explosion is an order of magnitude less than the strain rate for a conventional chemical explosion (cf. Table III-1). The spherical wave from the chemical explosion excites the high frequency shell bending modes, resulting in a high frequency strain response. The order of magnitude difference in strain rates is based on both analytical and experimental data (Cole, 1965).

For the case of mechanical impact on underwater structures, the structure is subjected to a high impulse loading over a small area and for fairly long durations. For both mechanical impact and chemical explosions, impulses on the order of 1 to 10 psi-sec are typical (cf. Table III-1).

In rough seas, the impact of the ship hull (International Ship Structures Congress, 1976) against the free water surface can produce pressures which results in

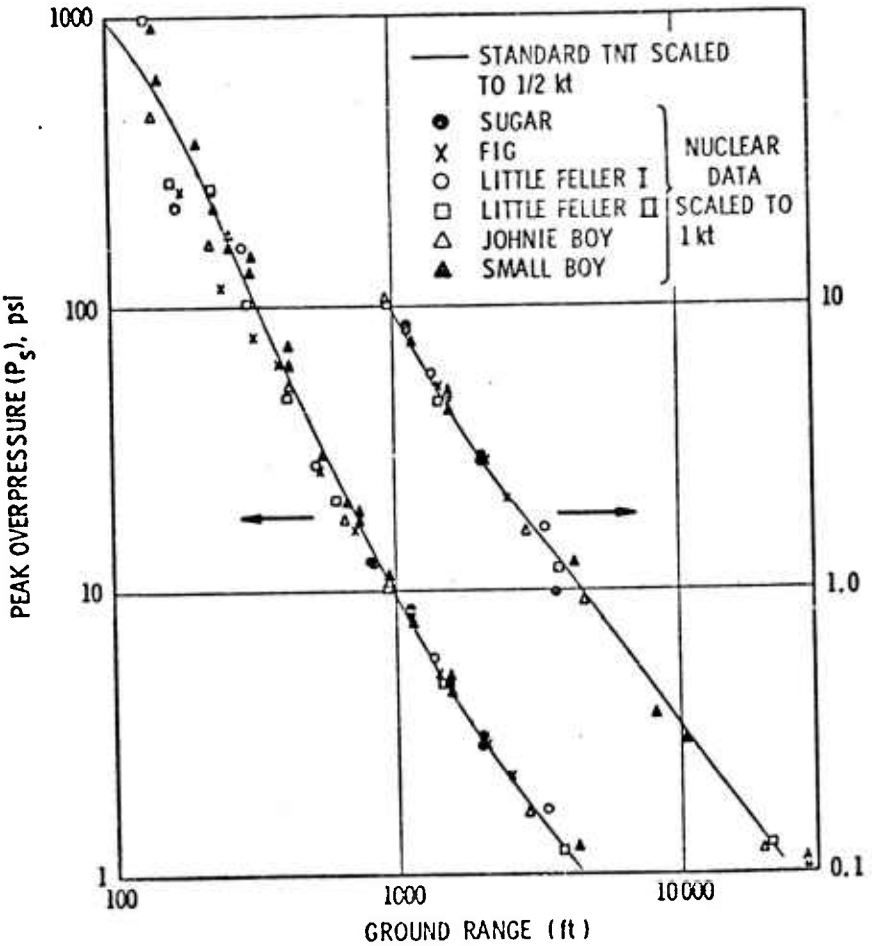

FIGURE III-3a Scaled Peak Overpressure vs. Ground Range

SOURCE: Baker, W.E., 1973

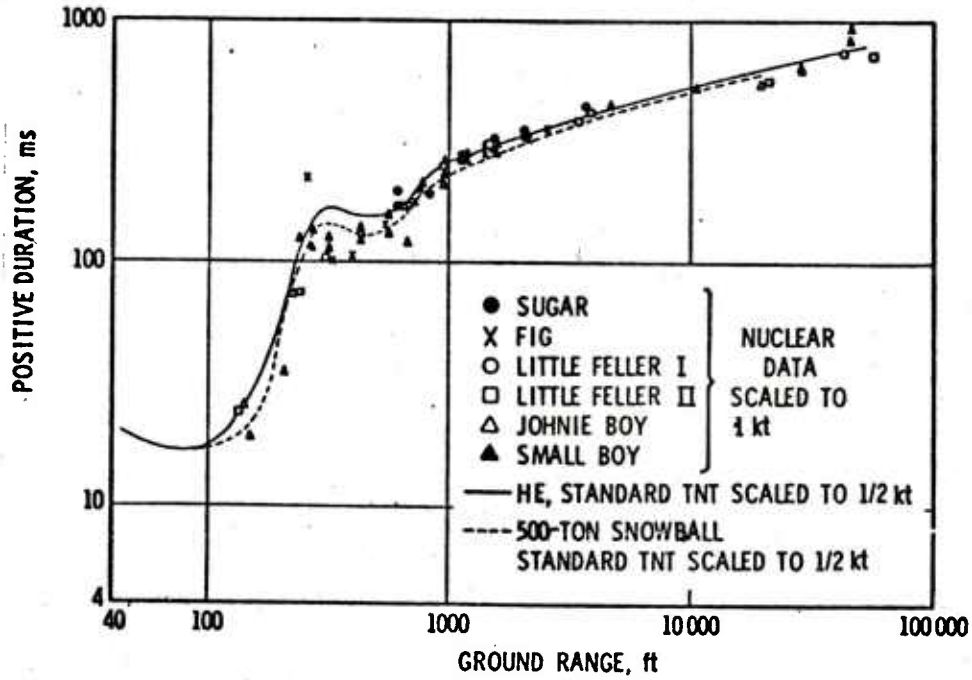

FIGURE III-3b Scaled Positive Duration vs. Ground Range

SOURCE: Baker, W. E., 1973

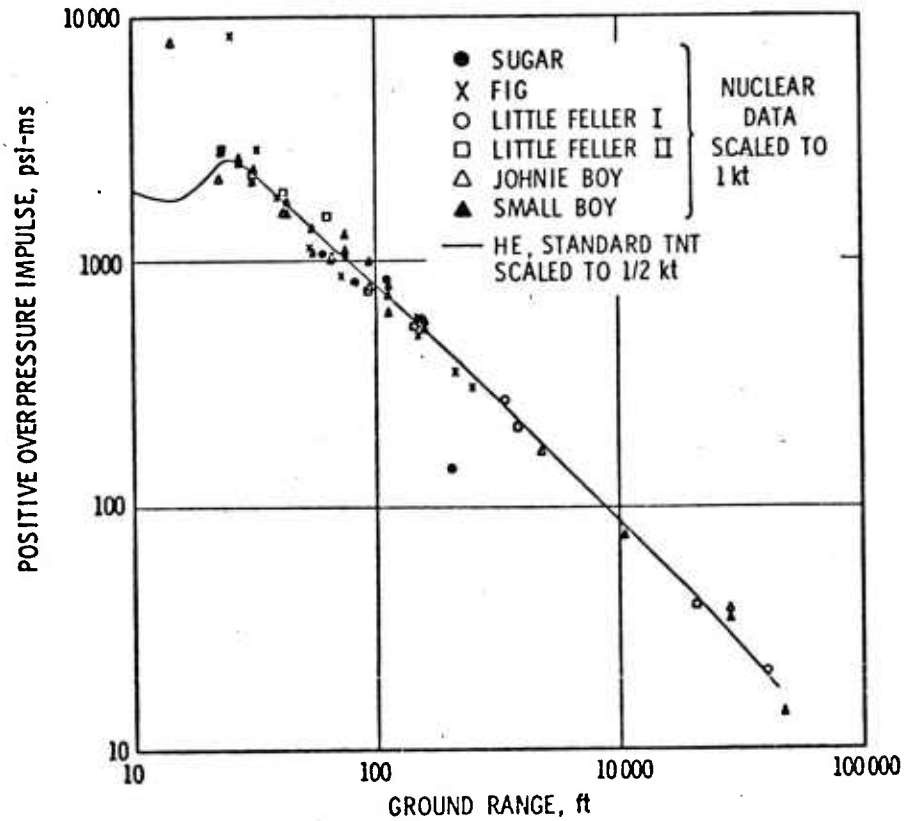

FIGURE III-3c Scaled Positive Impulse vs Ground Range

SOURCE: Baker, W. E., 1973

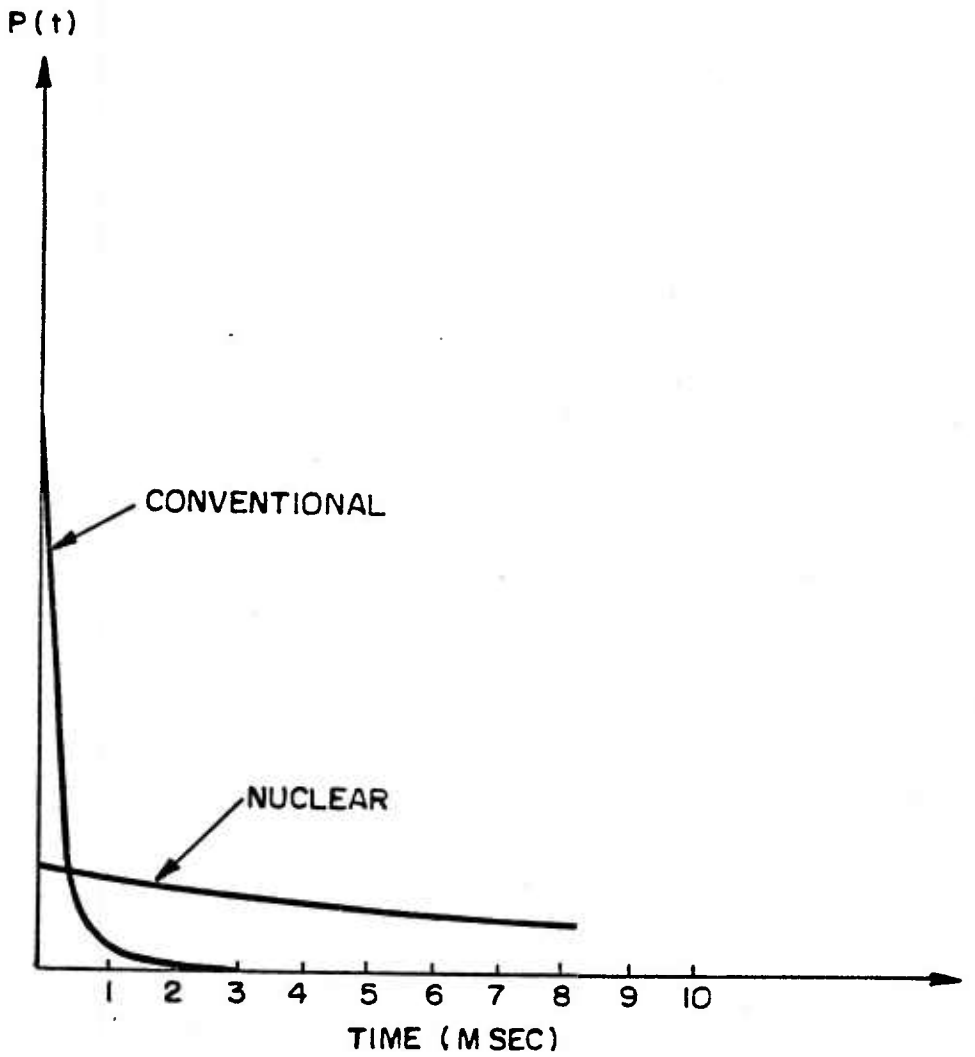

FIGURE III-4. Free Field Pressure for Conventional and Nuclear Explosions

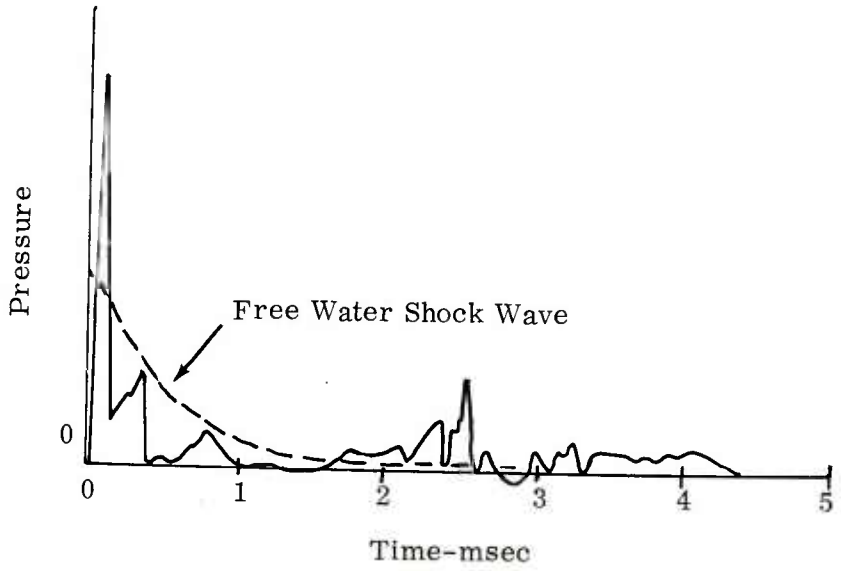

FIGURE III-5 Shock Wave Pressure History on a Cylindrical Shell

permanent hull plating damage. Figures III-6a, b, and c show the nature of this ship slamming problem for a typical large ore carrier. For high-speed surface effects ships, data have been taken for slamming events and are reproduced in Figure III-7. Slamming represents a repetitive impact which may lead to damage accumulation.

The detonation of propellant in guns and other projectile launch systems is another source of impulse loading. Interior ballistics is concerned with the pressure-time loading within the breech and the launch tube (barrel). In some cases, the transient pressure field external to the muzzle, created as the projectile exits, may significantly affect surrounding structures. A particular example of the latter is that of heavy weapons externally mounted on light weight aircraft such as helicopters. Figure III-8 illustrates typical conditions for internal ballistics of a calibre .30 gun (Handbook AMCP 706-342, 1970).

A severe threat to military land vehicles is the buried mine. Severe shock pressures may be experienced by tank hull bottom plating due to mine explosions. In this case, the total impulse is produced both by the expanding gases and by the added momentum of the soil mass carried by the explosion (Westline, 1972). The pressure-time history can

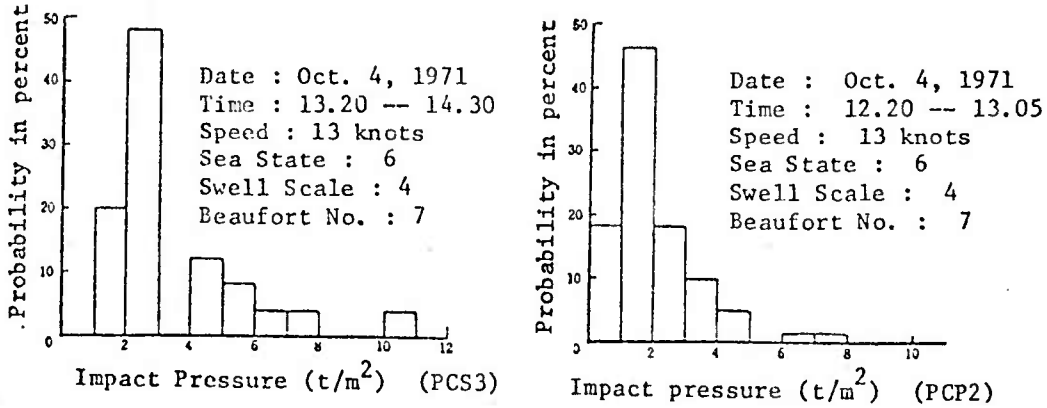

FIGURE III-6a Frequency Distribution of Impact Pressure on Bow Flare of Large Ore Carrier

SOURCE: Baker, W. E., 1973

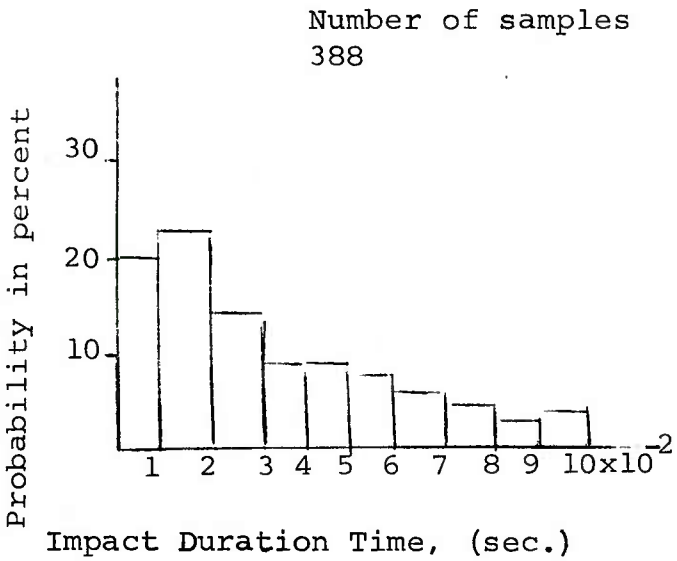

FIGURE III 6-b Frequency Distribution of Duration Time of Impact Pressure on Bow Flare of Large Ore Carrier

SOURCE: 6th International Ship Structure Congress, 1976

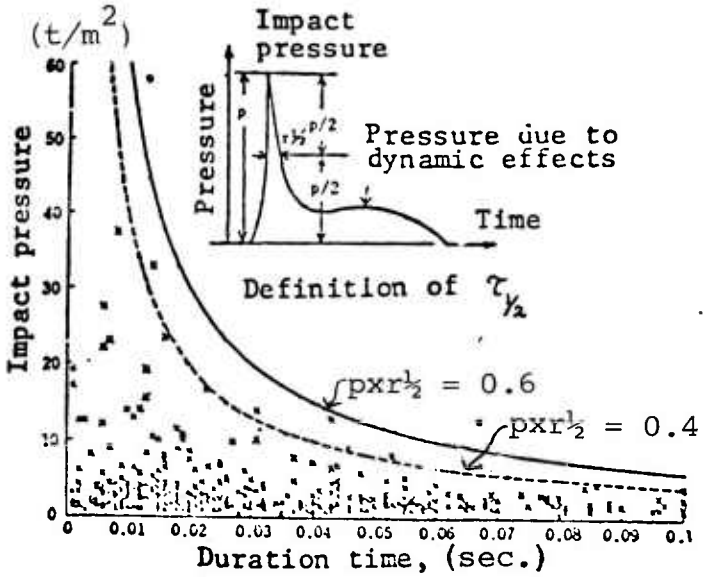

FIGURE III-6c Relationship Between Magnitude and Duration of Impact Pressure Observed on Bow Flare of Large Ore Carrier

SOURCE: 6th International Ship Structure Congress, 1976

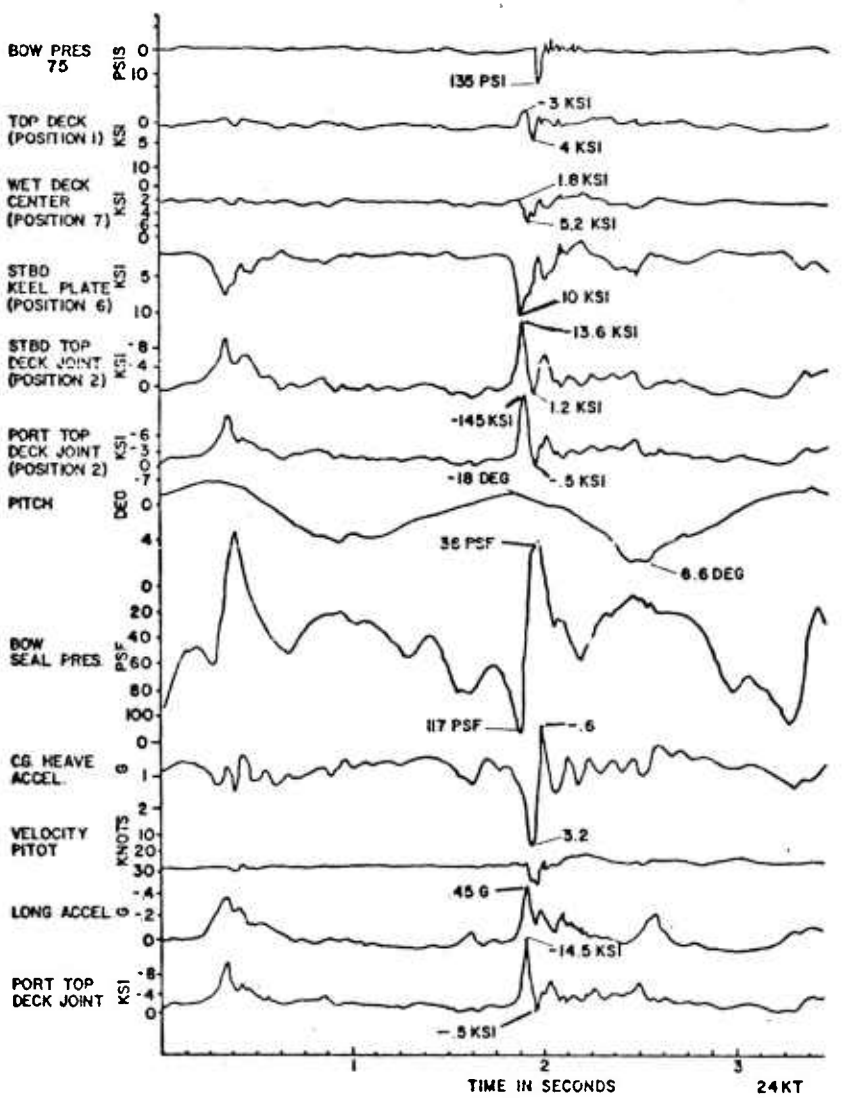

FIGURE III-7 Manned Testcraft XR-1C Slamming Event (24 Knots, Significant Wave Height 0.8 - 0.9 m, Head Seas)

SOURCE: 6th International Ship Structure Congress, 1976

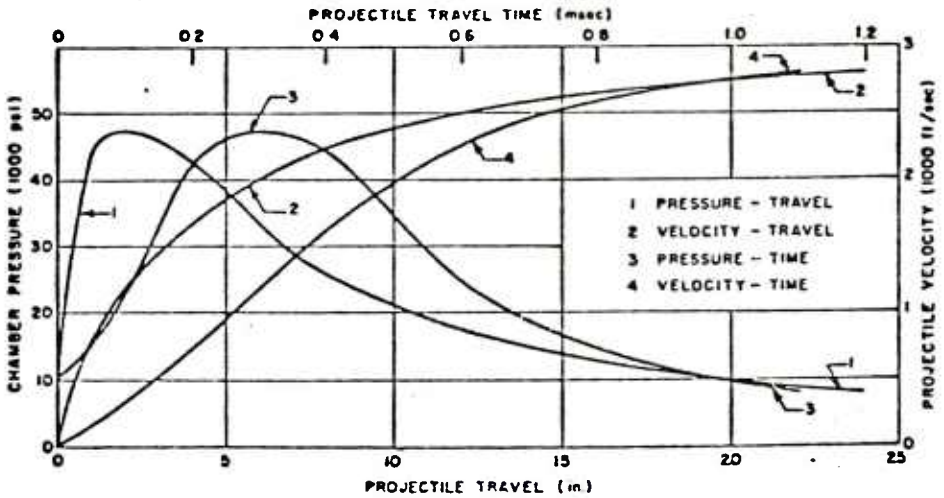

FIGURE III-8 Interior Ballistics of Caliber .30 Gun

SOURCE: Handbook AMCP 706 -342, 1970

be very complex relative to an air blast, with the total impulse being a function of charge weight, stand-off distance and depth of burial.

The preceding discussion illustrates, by example, the nature of some typical loading sources. Several points are important to keep in mind. First, if the load duration is short in comparison with the fundamental response time of the structure, then it may be considered as an impulse. The dynamic structural analysis is then greatly simplified in that the loading can be treated simply as an initial velocity condition and load-structure interactions are not important. In many cases, however, the load duration is comparable to the structural response time (e.g., the fundamental period of vibration of the structure in the dominant excited mode). In these cases, the analysis can become very complex, including nonlinear interactions between the loading and the deformation. A complete solution in this case may require solving the transient field equations in the surrounding medium as well as in the structure. Adequate analyses for many problems of this type do not as yet exist.

REFERENCES - SECTION III

Baker, W. E., Explosions in Air, University of Texas, Austin, Texas (1973).

Barton, F. W. and Pilkey, W. D., "Underwater Shock Survey - A Summary of the Unclassified Literature Related to the Transient Fluid-Structure Interaction Problems," Technical Report 14, Weidlinger Associates under Office of Naval Research Contract N00014-72-C-0119, (Sept. 1974).

Cole, R. H., Underwater Explosions, Dover Publications, New York (1965).

Handbook AMCP 706-342, Chapter 6, "Gun Tube Design," (1970).

Huang, H., "Exact Linear Analysis of the Transient Response of an Elastic Cylindrical Shell of Infinite Length to Plane Underwater Shock Waves," Report MACHLAB 163, Naval Ship Research and Development Laboratory (June 1969).

International Ship Structures Congress (6th), "Slamming and Impact," Report of Committee II.3, Boston, Massachusetts, (1970).

Westline, P. S., "The Impulse Imparted to Targets by the Detonation of Land Mines," Shock and Vibration Bulletin, No. 42, (Jan. 1972).

IV. CURRENT UNDERSTANDING AND APPROACHES

A. Introduction

In order to design adequately for damage tolerance one usually needs a mathematical description of elastic and inelastic deformation behavior and associated structural analysis techniques for the expected range of deformation rates. (As used here, damage tolerance is the ability of a structure or component to absorb mechanical energy without failure. In turn, failure is defined as a loss in functional capability according to some specified criterion: e.g., excessive deformation (transient or residual), structural instability (collapse), or loss of residual strength (fracture). The use of material screening tests for dynamic fracture resistance (Charpy, dynamic-tear, drop-weight tear test, etc.), normally assures that fracture in dynamically loaded structures is accompanied by large inelastic deformations. Therefore, with tough materials a major need exists for realistic models of rate-dependent plastic deformation and fracture. The dynamic fracture problem involves prediction of initiation of crack growth under rapid loading as well as dynamic crack propagation and arrest. Section IV will include discussions on the modeling of these deformation and fracture phenomena.

The overall problem considered is that of describing the behavior of materials and structures when subjected to the dynamic loading of the type illustrated in Section III. This loading is essentially of short duration and high intensity. We are interested in both the transient and the residual or permanent deformation of the structure. The permanent deformation also includes the creation of new surface area if separation or fracture of initially continuous structural elements has taken place.

Analytical modeling of the entire process of deformation and fracture is a complex process which is often broken up into subelements; e.g., "elasticity," "plasticity," and "fracture mechanics," which are studied separately. This introductory discussion will emphasize the problems of developing constitutive behavior models for a continuum which contains a range of internal defects of varying scale.

For analytical purposes, materials are usually modeled by taking a finite (but perhaps irreducibly small) element for which there can be defined a deterministic relation between the applied surface tractions and body forces and the resulting deformations or deformation rates. Usually, this element is taken to be homogeneous and continuous. This homogeneous assumption is certainly satisfactory for problems in elasticity; however, for plasticity and for material failure it is the local nonhomogeneities which govern the behavior. Therefore, let us think of a material element constructed of the following components:

1. Ideal crystalline lattice.
2. Point defects - interstitials, vacancies, etc.
3. Line defects - dislocations.
4. Areal defects - grain boundaries, twin boundaries, cracks.
5. Volume defects - inclusions, pores.

Thus, the volume element consists of a continuous, homogeneous crystalline lattice interspersed with a variety of localized nonhomogeneities or "defects." Elastic behavior is based upon the reversible small distortions of the crystalline matrix. Strength behavior is governed by the much more complex phenomena associated with the nucleation, migration, growth, interaction, and coalescence of the multiplicity of defects.

In particular experimental situations, we may be able to isolate a deformation process where a single mechanism is operating alone or is dominant. For example, very small deformation where only reversible lattice distortions occur allows us to measure the constants in the elastic constitutive law. A second example is a single crystal of a pure metal or solid solution alloy where irreversible deformation results from dislocation glide only. This is the simplest form of plasticity. A specimen with a single large crack is a third example; if stressed to a level sufficient to extend the crack, but not sufficient to produce large scale plastic deformation, this specimen provides the data required for the application of linear elastic fracture mechanics.

Generally, however, we are faced with developing a constitutive model for a structural, polycrystalline alloy which contains a finite population of many of the defects listed above. The response of this defect structure to a given load environment is very complex and depends on the

relative population and distribution of defect species and their modes of interaction. Analytical description with relatively good accuracy is available for each of the isolated individual mechanisms: e.g., interstitial or vacancy diffusion, dislocation glide, twinning, grain boundary sliding, crack propagation, etc. The challenge is to better understand the nature of the interaction of these mechanisms and thereby develop constitutive and fracture relations for real materials when a multiplicity of effects are occurring simultaneously. Little progress has been made in this direction.

The alternative has been to rely on stress-deformation response measurements of bulk specimens; such measurements effectively integrate all of the internal defect motions. The constitutive relations derived from this empirical process then relate only the stimulus to the response of a "black-box" material element (test specimen); analytical relationships are fit to a variety of specific mechanical test data corresponding to typical load or deformation histories such as creep, constant strain rate, fatigue, impact, etc. This approach, although it has proven useful, suffers from a lack of predictive capacity for "untested" situations. Improvement must come from constitutive modeling based, as nearly as possible, on actual physical phenomena.

Obviously, the matter of scale is critical when defining a basic material element for the purposes of developing constitutive models. The scale of many of the defects which play a significant, if not critical, role in the constitutive behavior is of the same dimension as the lattice parameter (spacing between nearest neighbor atoms). Therefore, unless we reduce the problem to a discrete lattice model (individual atoms bound together by pair-wise potentials), our minimum material element must contain a distribution of defects (inhomogeneities).

Finally, it is important to consider the nonhomogeneities to be structural defects, having not only specific geometrical configurations but also to have associated with them local residual stress fields produced by distortions of the surrounding matrix, usually assured to be an elastic continuum. In addition, the deformation-induced stress field may be further intensified by the presence of other local structural inhomogeneities (inclusions, porosity,

ect.). The development and interaction of these small-scale inhomogenities are the factors which control both plastic deformation and fracture.

B. Analytical Modeling and Related Materials Property Tests

1. Basic Deformation Mechanisms

Let us consider those processes in metals which are dependent upon the plastic strain rate. In considering the underlying causes of plasticity, one normally deals with the effect of stress and temperature on the initiation and propagation of dislocations. In fracture, one is concerned at least with the effect of the same variables on the initiation and propagation of cracks in brittle materials or of voids and ductile materials. If the problem is one of solely elastic deformation, structural analysis is greatly simplified because the material properties are by definition independent of the time-dependence of the deformation. Inelastic deformation in metals is primarily the result of the motion of dislocations and their interactions with other internal defects in the lattice. The rate controlling mechanisms for this process are outlined in this section.

Table IV-1 and Figures IV-1 and IV -2 summarize the known plastic deformation rate controlling mechanisms which apply to metals over the entire rance of temperature and stress. The four basic mechanisms are viscous drag, thermal activation, athermal stress barriers, and diffusion. Several specific examples of each mechanism are given in Table IV-1. Figure IV-1, which is a modified version of deformation map as used by Ashby, (1972) illustrates curves of constant strain-rate in the stress τ - temperature (T) plane. Stress and temperature are normalized by the shear modulus, μ, and melting temperature, T_m, respectively. The curves are for constant values of dislocation velocity, v, normalized by the shear wave velocity, C_s. This parameter, v/c_s, can be related to plastic shear strain rate, $\dot{\gamma}$, by the kinematic relation:

$$\dot{\gamma} = \rho b v \qquad \text{(IV-1)}$$

where ρ is the density of mobile dislocations and b is the Burger's vector of the dislocations. In Figure IV-1, the

TABLE IV-1 Basic Deformation Mechanisms

1. Viscous Drag on Dislocations
   - Thermoelastic
   - Phonon scattering
   - Phonon viscosity
   - Electron viscosity
2. Thermal Activation of Dislocations Past Short-Range Barriers
   - Dislocation intersection
   - Solute atoms
   - Peierls mechanisms
   - Cross slip
3. Athermal Stress Fields
   - Long-range stress fields
   - Incoherent precipitates
4. Diffusion Controlled Dislocation Motion
   - Dislocation climb
   - Nabarro-Herring creep
   - Coble creep

dimensional scales are roughly appropriate for aluminum where the dislocation density is taken as $10^{10}cm^{-2}$. Figure IV-2 shows curves of constant homologous temperature for the same material.

The four basic mechanisms can be separated roughly by stress level. At the highest stresses, $\tau > \tau_o$, dislocations are not impeded by other defects and the only drag forces are those generated by the interaction of the high velocity dislocations with the basic crystalline lattice. This interaction can result in several dissipative mechanisms as

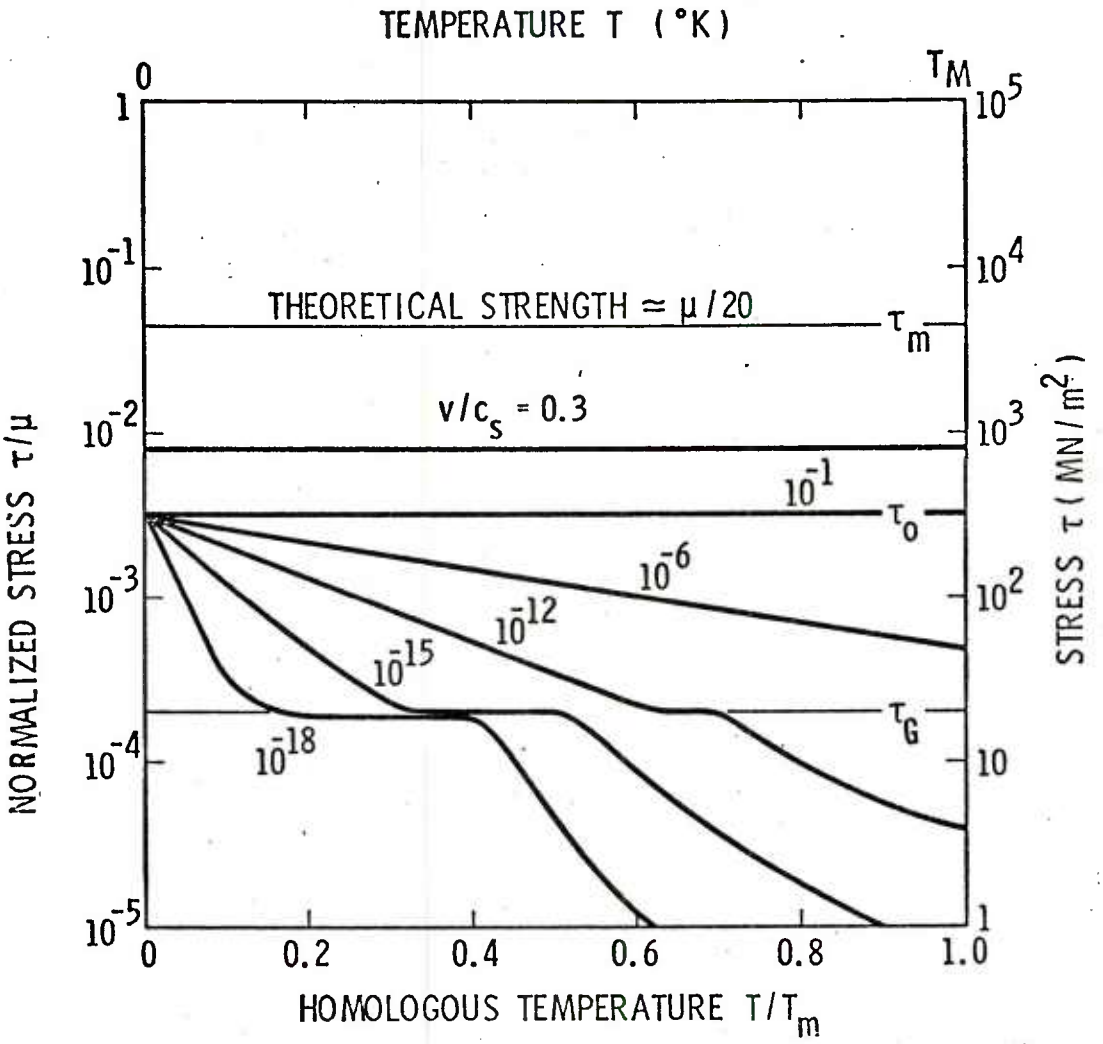

FIGURE IV-1 Deformation Map. Dimensional Parameters Correspond Roughly to Aluminum

SOURCE: Adapted from Ashby, 1972

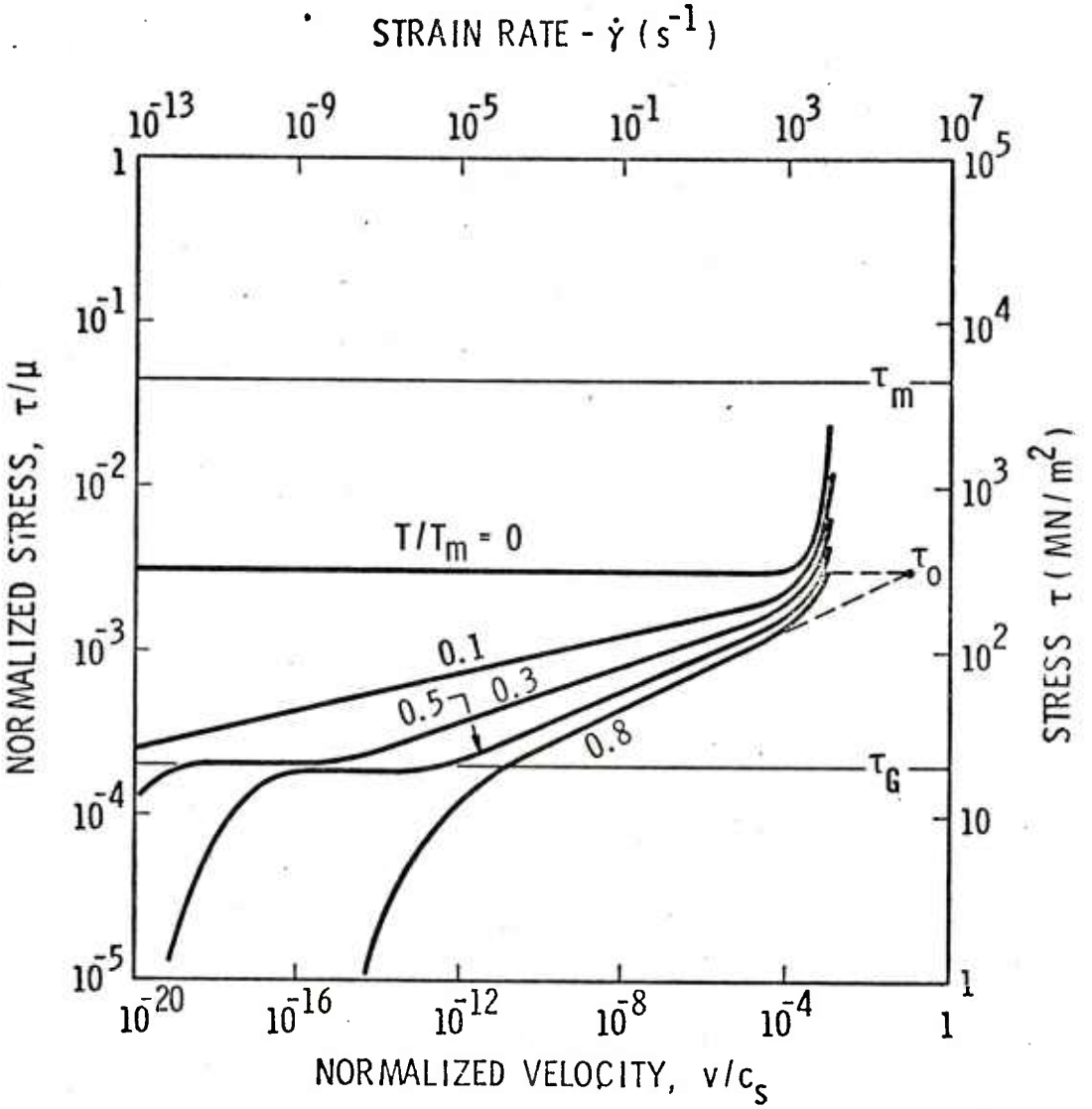

FIGURE IV-2 Deformation Map in Terms of Dislocation Velocity or Strain Rate. Alternate Presentation of Figure IV-1

SOURCE: Adapted from Ashby, 1972

listed in Table IV-1, all of which yield a linear vicous relation between dislocation velocity (or strain rate) and applied shear stress; viz.,

$$b\tau = Bv \qquad \text{(IV-2)}$$

where $B = B(T)$ is a net drag coefficient. The magnitude of this coefficient is such that only the viscous force is significant at very high dislocation velocities.

For stresses in the range $\tau_G < \tau < \tau_O$, the dominant rate controlling mechanism is thermal activation of dislocations past short-range obstacles, shown schematically in Figure IV-3. In this range, the governing equation is of the Arhennius form

$$\dot{\gamma} = B' \exp\left[\frac{U(\tau)}{kT}\right] \qquad \text{(IV-3)}$$

where the coefficient B' of the exponential is often taken as a constant but must contain the number of activation sites, area swept out by a successful activation event, the Burger's vector, and the attempt frequency. $U = U(\tau)$ is the stress-dependent thermal activation energy and k is the Boltzmann constant.

Thermal activation is effective for only short range stress fields with dimensions of the order of the lattice spacing. Movement of dislocations through internal stress fields of longer range can be accomplished only by supplying the energy by means of the applied stress. The athermal stress, τ_G, is a mean stress required to overcome such long range internal barriers.

The total picture given above is useful conceptually, but it should be kept in mind that within a given range of parameters a number of distinct defect interactions are probable, only a few of which are listed in Table IV-1. Therefore, in reality, especially for commercial alloys, the situation is more complex than shown. Obviously, a simple constitutive equation cannot account for all possible internal defect interactions explicitly. Therefore, for each alloy we must have some guidelines as to the dominant controlling mechanisms for a given set of the independent variables. This is the intent of the Ashby type deformation map. In the same sense, fracture maps may be constructed also (Ashby, 1977).

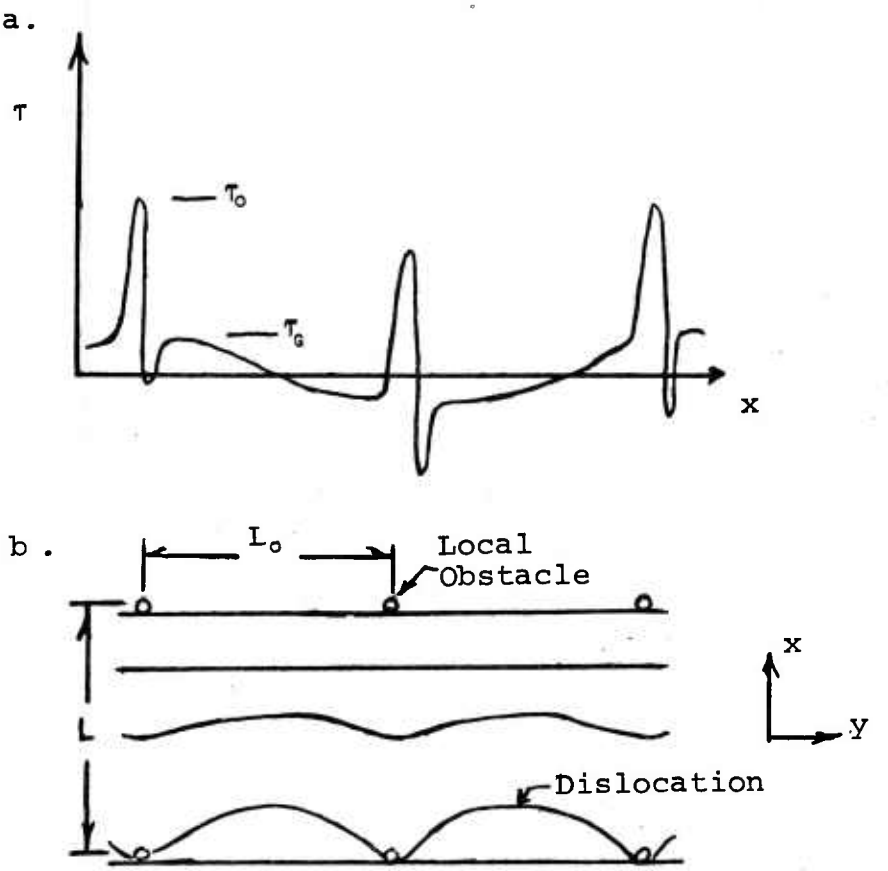

FIGURE IV-3 Thermal Activation Past Square Array of Localized Obstacles

a. stress vs. displacement

b. successive positions of dislocation in plan of motion with regular array of obstacles

2. Metallurgical Aspects of Strain Rate Sensitivity

As discussed above, the stress associated with plastic flow of a material is customarily represented as a function of two external variables, the instantaneous plastic strain rate and the temperature (cf. Figure IV-2). The degree of sensitivity to these variables depends very much upon the material as well as its thermo-mechanical history. For example, the variation in this "flow stress" with either plastic strain rate or temperature is much more pronounced in low strength as compared to high strength steels, and the dependence upon these variables is much greater in body-centered cubic metals (e.g., iron) than in face-centered cubic metals (e.g., aluminum). There are important practical ramifications to this dependence of the flow stress on these variables, as in high speed manufacturing operations where the flow stress at the strain rate involved rather than the static strength determines the requisite machine capacity. In addition, the fracture process in steels, one matter which will be of concern herein, can be deleteriously influenced by either an increase in strain rate or a decrease in temperature. This review will be primarily directed at strain-rate sensitivity, which is almost always coupled to temperature sensitivity, and will focus on the controlling factors giving rise to a dependence of the flow stress of an alloy on these parameters. In addition, the influence of strain rate and temperature on fracture behavior of precracked alloys will also be considered. In order to set some bounds on the range of the variables considered, the temperatures of interest will be well below the creep range, and an upper limit in strain rate of 10^3/sec will be set so that consideration of shock phenomena which can involve strain rates of up to 10^9/sec will be excluded.

In the strain rate range of interest;i.e., below 10^3/sec, the principal factors leading to a strain rate effect are temperature and the time available for thermal activation of dislocation motion; for aluminum see Figure IV-2. The sensitivity of the fracture process to strain rate and temperature results directly from the fact that the fracture toughness of an alloy depends upon the extent of plastic deformation involved in the rupture process; normally, the greater the amount of localized plastic deformation, the tougher the material, and any factor which inhibits plastic deformation can be expected to also lower

the fracture toughness. Further, in materials that can fail by cleavage, below a critical temperature an increase in strain rate will promote brittle behavior if the local stresses at a notch or crack rise rapidly enough to satisfy a fracture criterion before sufficient time has elapsed to permit the thermal activation of enough plastic deformation to relax these high stresses. For such materials, whenever fracture under dynamic loading conditions is of concern it is important that the factors responsible for strain-rate sensitivity be understood, and the magnitude of related strain-rate effects be established.

Before going into a more detailed consideration of the underlying causes of strain-rate sensitivity, a few examples will be given to illustrate the extent to which strain rate can influence the flow stress. In Figure IV-4 a comparison

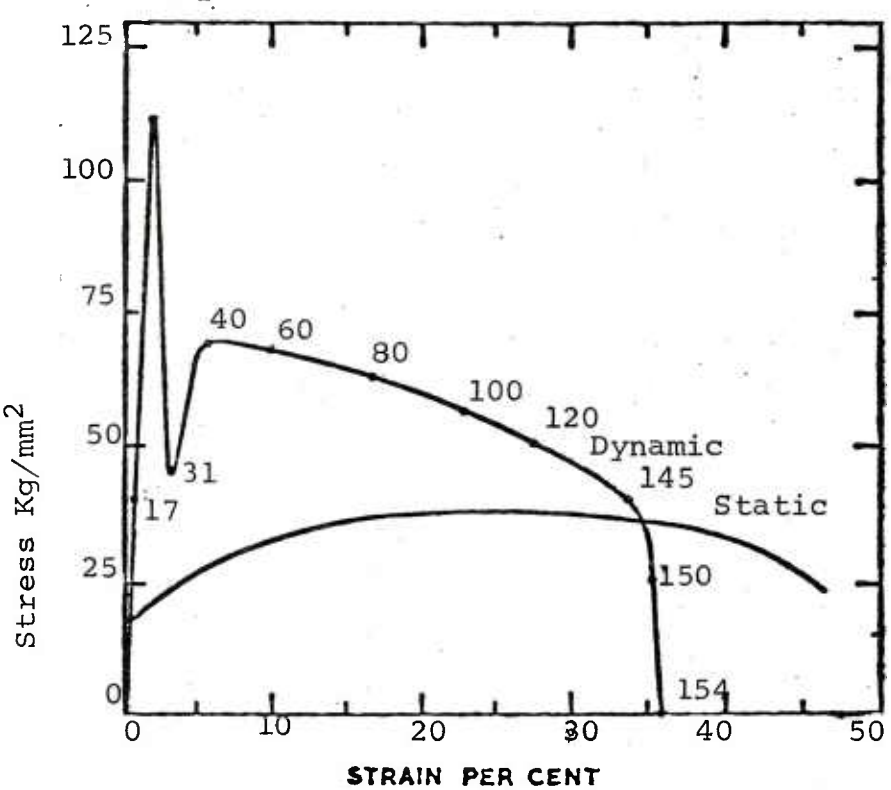

FIGURE IV-4 Stress-Strain Curves of Low Carbon Steel Under Static and Dynamic Loading. Times in Microseconds are Shown on Dynamic Curve

SOURCE: Campbell & Harding, 1960

is given of flow stress of a low carbon steel under conditions of static ($\simeq 10^{-4}$/sec) and dynamic ($\simeq 2 \times 10^{3}$/sec) tensile straining conditions (Campbell and Harding, 1961). In this material, plastic deformation initially involves the spread of a Luders band, and the increase in the upper yield point with strain rate comes about because dislocations are initially locked by interstitial atoms and a finite time is required to initiate dislocation motion and the spread of this Luders band. The dip in the dynamic stress-strain curve is related to the spread of this band. Beyond the yield region, the flow stress initially rises and then slowly falls off and approaches the static curve at higher strains. This falloff in strain-rate sensitivity with increasing strain, but without a decrease in the flow stress itself, also occurs in the case of iron tested in compression as shown in Figure IV-5 (Hockett and Zukas, 1973). With high-purity aluminum, Figure IV-6, at least over the strain range tested, this trend is not followed (Hauser, et al., 1961).

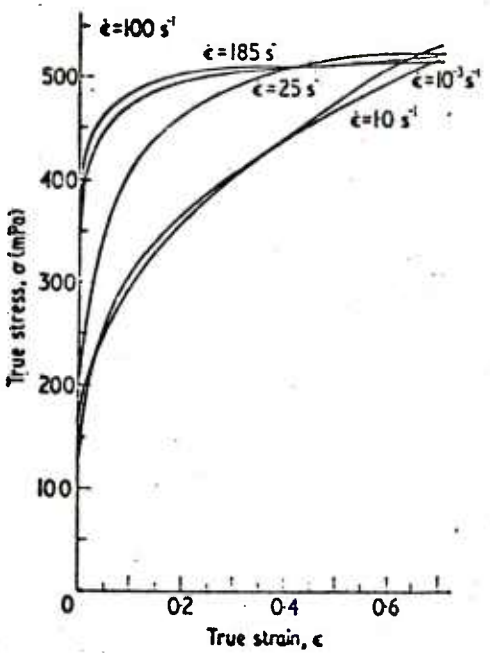

FIGURE IV-5 True Stress Against True Strain Curves for Iron Compressed at 295 K at the Indicated Constant True Strain Rates

SOURCE: Hockett and Zukas, 1973

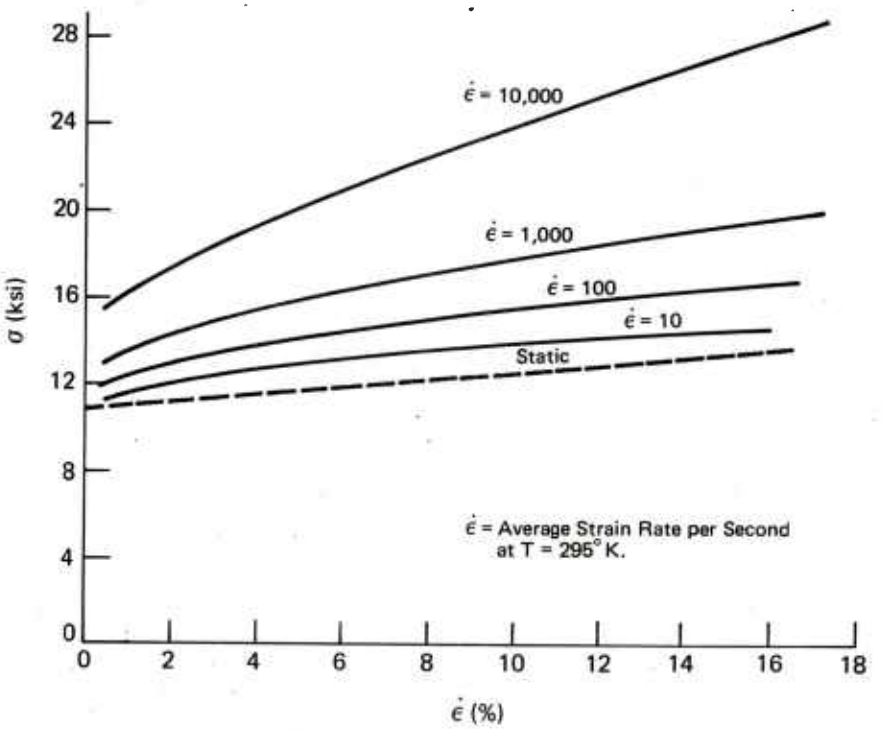

FIGURE IV-6 Effect of Strain on Stress at Constant Strain Rate

SOURCE: Hauser et al, 1961

In Figure IV-7, the dependency of the lower yield of a low carbon steel is shown as a function of grain size, radiation dosage, and impact velocity (Campbell and Harding, 1961). The stress given by the intersection of straight lines with the ordinate is known as the friction stress and it is seen that the large increase in flow stress with increasing velocity is due to an increase in the thermally activated friction stress. The grain size dependency is independent of strain rate, and hence independent of thermal activation, since it is due to a long-range stress associated with grain boundaries. Additional examples of the influence of strain rate and temperature on the lower yield stress of a 0.2 weight percent carbon steel are given in Figure IV-8 and IV-9 (Taylor and Malvern, 1961). The strong dependency of the lower yield stress on those test variables is evident.

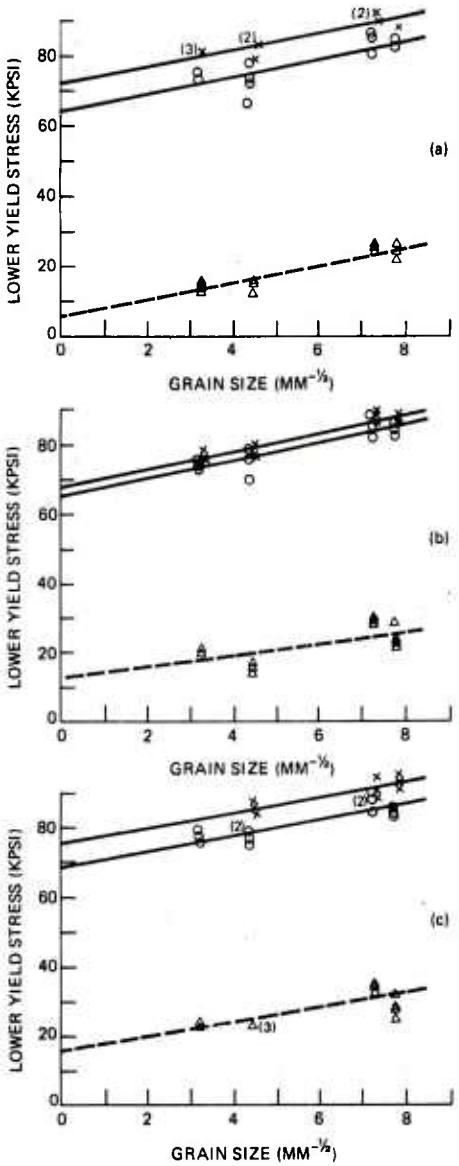

FIGURE IV-7 Lower Yield Stress of Steel: (a) unirradiated; (b) radiation dose 8 x 10^{17} neutrons/sq. cm; (c) radiation dose 5 x 10^{18} neutrons/sq. cm.
Δ = static loading
o = impact velocity 198 ips
x = impact velocity 507 ips

SOURCE: Campbell and Harding, 1961

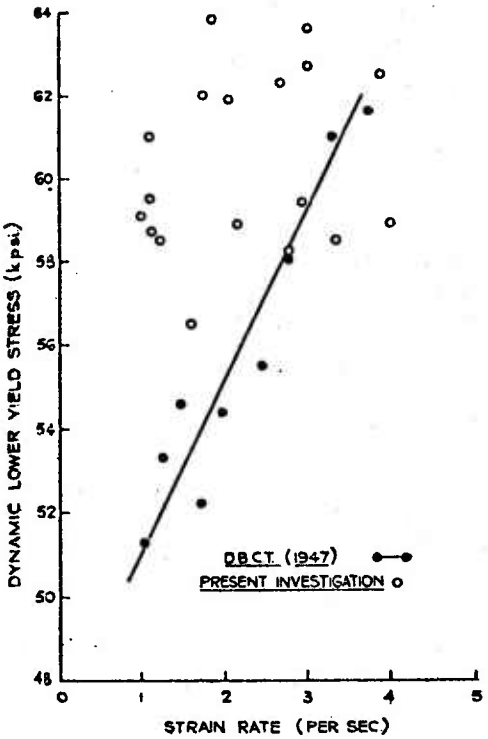

FIGURE IV-8 Dynamic Lower Yield Stress as a Function of Specimen Strain Rate for Normalized (Present Investigation) and Unnormalized (Taylor) Mild Steel at Room Temperature. (0.26 steel)

SOURCE: Taylor and Malvern, 1961

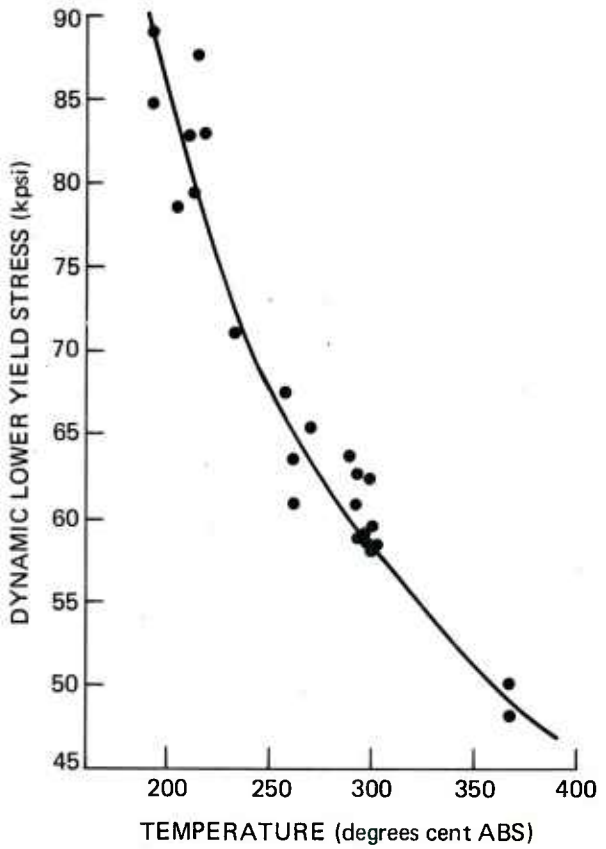

FIGURE IV-9 Dynamic Lower Yield Stress as a Function of Test Temperature (.2c steel)

SOURCE: Taylor and Malvern, 1961

In order to understand the basis for strain-rate sensitivity, it is useful to consider again the interaction of a dislocation with the various types of barriers in a material which oppose the motion of the dislocation under stress. These barriers to dislocation motion can be divided into two groups according to the distance over which they interact with glide dislocations (Basinski, 1959, and Basinski and Christian, 1960). In face-centered cubic metals such as copper and aluminum, the principal obstacles exerting short-range forces, such as forest dislocations or jogs, can be overcome at finite temperatures with the help of

thermal fluctuations, even though the force on the glide dislocations is smaller than the force exerted by the obstacles. This type of interaction will lead to a temperature and strain-rate dependent flow stress. On the other hand, the activation energies involved when the dislocation moves under adverse stress over a large distance would be outside the range of thermal fluctuations at ordinary temperatures. We must expect, therefore, that the flow stress originating from long-range elastic interactions between dislocations should be independent of the strain rate, and depend upon the temperature only through the elastic moduli.

Body-centered cubic metals such as iron differ from face-centered cubic metals in that there is an additional important type of barrier known as the Peierls-Nabarro stress which results from an interaction of a dislocation with the lattice. This barrier is of a short-range type and can be overcome with the aid of thermal fluctuations. Additionally, dislocation interaction with interstitial atoms such as carbon and nitrogen can occur, but it appears that the Peierls-Nabarro stress rather than an interstitial effect gives rise to significant friction stress and is responsible for the high degree of temperature and rate sensitivity in bcc metals.

The following type of equation was proposed by Seeger (1957) to account for the temperature and strain rate sensitivity of the flow stress in the presence of a particular short-range barrier such as the cutting of a glide dislocation by forest dislocations. An applied shear stress, τ, can aid in the motion of the dislocation through this type of barrier; however, a portion of the applied stress, τ_G, may be needed to overcome long-range barriers due to the stress fields of parallel dislocations. In this model, the number of activated sites is independent of temperature. The plastic strain rate, $\dot{\gamma}$, is expressed as

$$\dot{\gamma} = B' \exp\left[-\frac{U_0 - v_0(\tau - \tau_G)}{kT}\right] \qquad \text{(IV-4)}$$

where $B'=bA'N\nu_0$, and b is the Burgers vector, A' is the area swept out, N is the number of activated sites, ν_0 is a frequency factor which depends upon the obstacle and the way it is overcome, k is Boltzmann's constant, U_0 is the

constant activation energy, and v_o is known as the activation volume. From Equation IV-4, the following expression can be derived from the shear stress for flow,

$$\tau = \tau_G + \frac{U_o - kT\ln(Na'b\nu_o/\dot{\gamma})}{V_o} : T \leq T_o \qquad \text{(IV-5a)}$$

$$\tau = \tau_G \qquad : T \geq T_o$$

where $$T_o \equiv \frac{U_o}{k\ln(Na'b\nu_o/\dot{\gamma})} \qquad \text{(IV-5b)}$$

The dependency of the flow stress upon temperature and strain rate based on this equation is shown in Figure IV-10, which depicts a limited region of interest of Figure IV-1. The linear dependency of the flow stress on temperature at

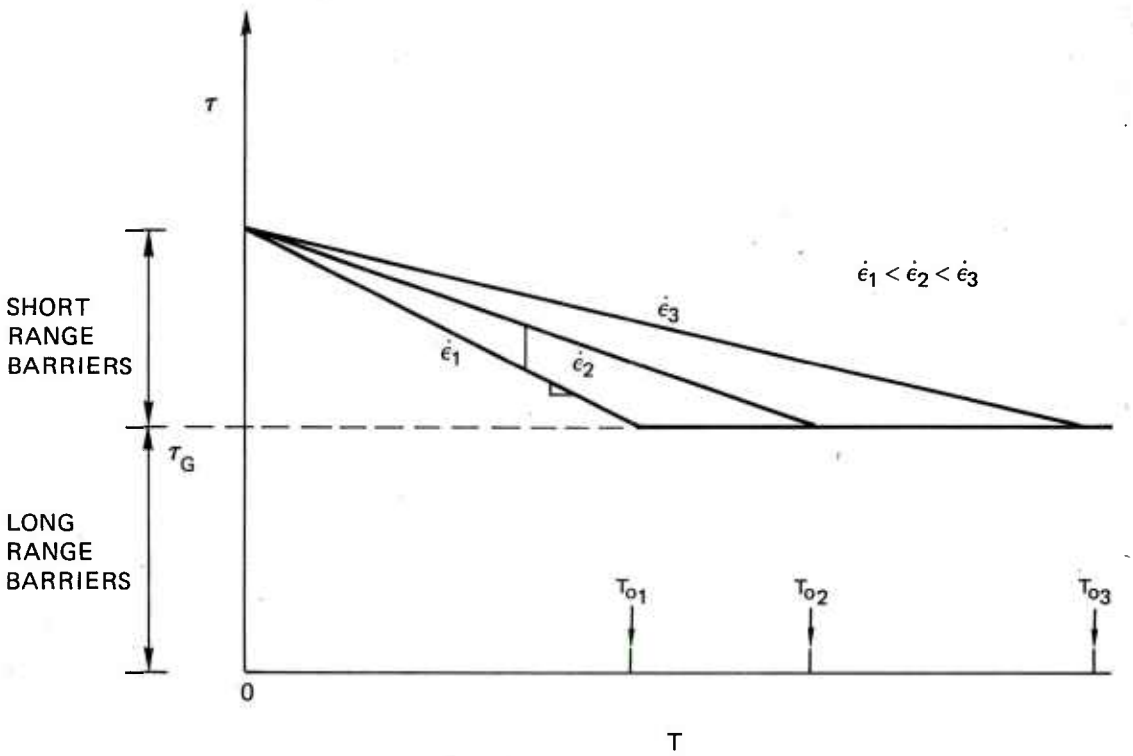

FIGURE IV-10 Dependence of the Flow-Stress on Temperature as Predicted by Equation IV-5

a given strain rate as predicted by Equation IV-5a is in general agreement with observations on the hexagonal of trigonal metals; e.g., magnesium, zinc, cadmium, and bismuth, and on the face-centered cubic metal aluminum (Seeger, 1957). In the case of titanium, a hexagonal metal, the variation is not linear but the thermal and athermal regions are apparent as shown in Figure IV-11 (deMeester, et al., 1975). It is clear from Equation IV-5a that temperature and strain rate effects are interrelatable, and the following parametric relationships, derivable from Equation IV-5a have been used to correlate the uniaxial strain rate $\dot{\epsilon}$ and temperature sensitivity of the uniaxial

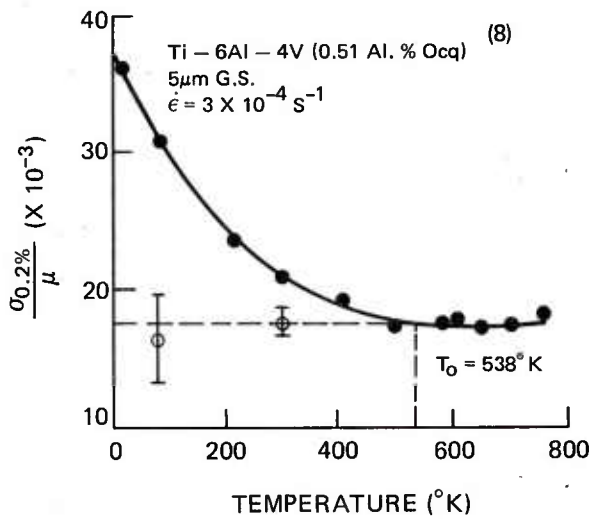

FIGURE IV-11 The 0.2 Percent Yield Stress Divided by the Shear Modulus Versus Temperature. Also included are values of the athermal component of the flow stress divided by the modulus, as determined by various methods

SOURCE: deMeester et al, 1975

flow stress, σ, with σ and $\dot{\epsilon}$ equated to 2τ and $2\dot{\gamma}/3$, respectively:

$$\sigma = f_1 \left(T \ln A/\dot{\epsilon}\right) \qquad \text{(IV-6a)}$$

or, equivalently,

$$\sigma = f_2(T_M') \text{ where } T_M' \equiv \left(1 - \alpha \ln \frac{\dot{\epsilon}}{\dot{\epsilon}_0}\right) T \qquad \text{(IV-6b)}$$

where A, α, and $\dot{\epsilon}_0$ are constants, and T_M' is the velocity-modified temperature of MacGregor and Fisher (1945).

Figure IV-12 is an example of the use of Equation IV-6a (Bennett and Sinclair, 1966). Figures IV-13 and IV-14 are illustrations of the use of the velocity-modified temperature approach (MacGregor and Fisher, 1945).

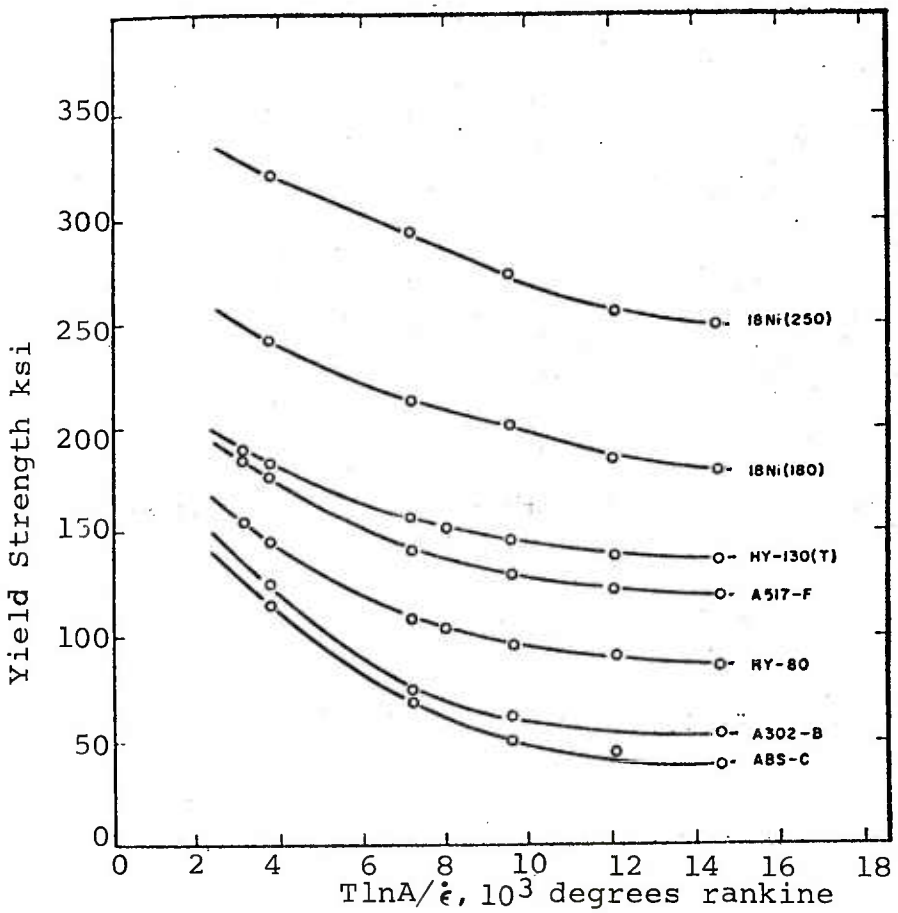

FIGURE IV-12 Yield Strength for Seven Steels in Terms of the Rate-Temperature Parameter, TlnA/$\dot{\epsilon}$. A = 10^8 sec

SOURCE: Bennett and Sinclair, 1966

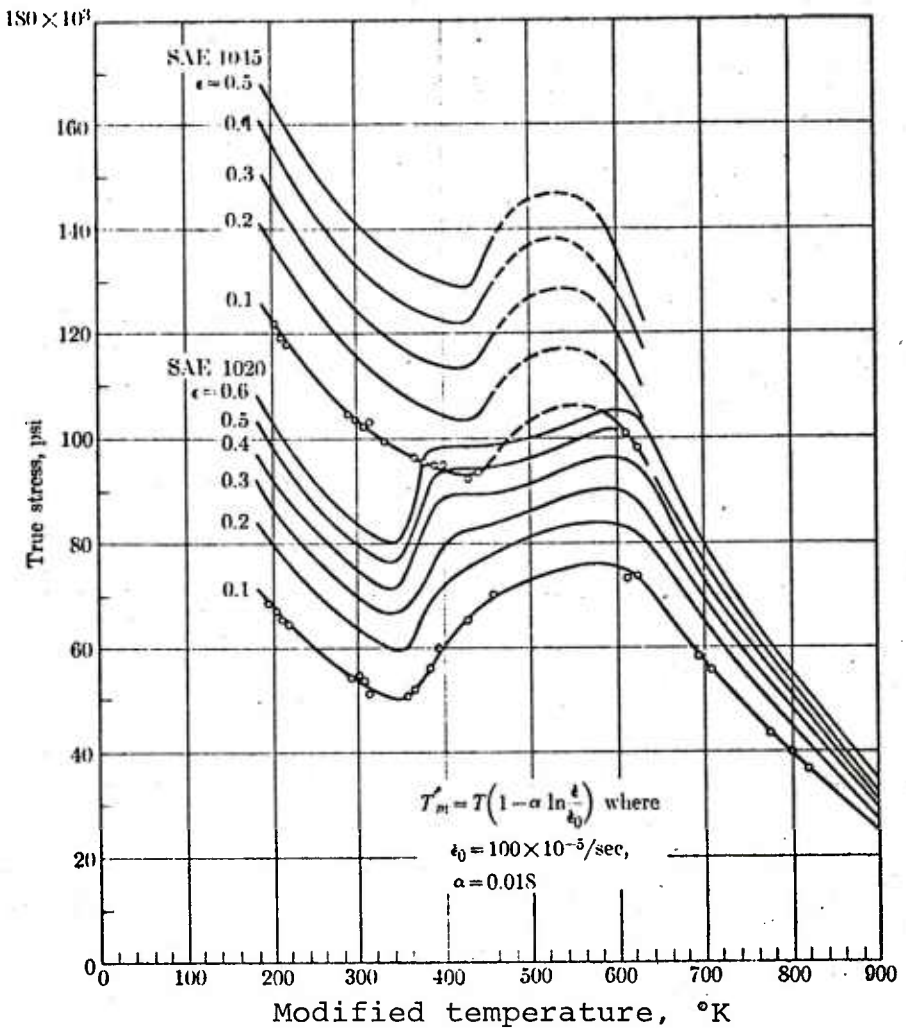

FIGURE IV-13 Stress as a Function of True Strain and Velocity-Modified Temperature for Annealed 1020 and 1045 Steels. Strain rates from 5 to 500 x 10^{-5}/sec are correlated on each curve

SOURCE: MacGregor and Fisher, 1945

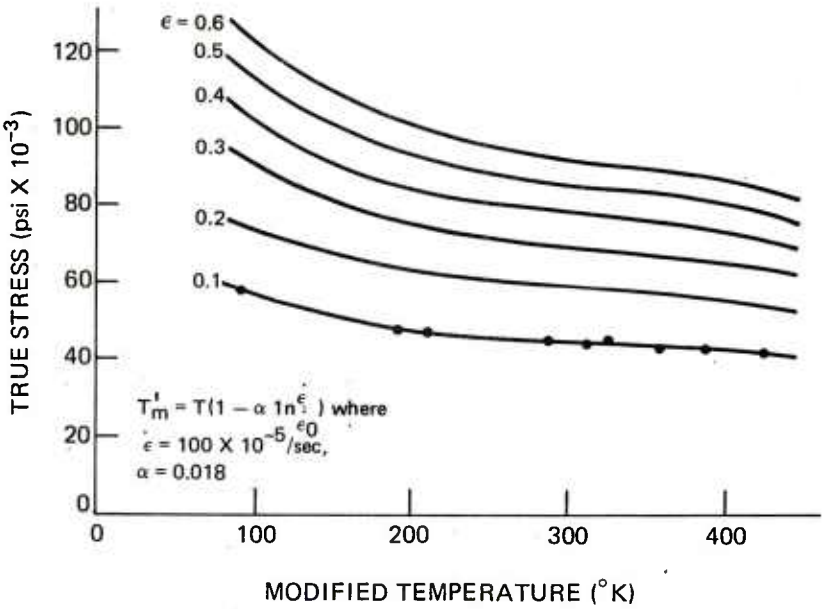

FIGURE IV-14 Stress as a Function of True Strain and Velocity-Modified Temperature for Annealed Brass

SOURCE: MacGregor and Fisher, 1945

Basinski (1959) has used a modified form of Equation IV-4 in the analysis of the temperature and strain-rate sensitivity of face-centered cubic metals. This analysis allows for an increase in the number of activated sites with an increase in temperature and also includes consideration of the decrease of the elastic moduli with temperature. Again dislocation intersections are considered to be the important barriers. Basinski and Christian (1960) have also analyzed the behavior of decarburized iron and iron containing a small amount of carbon and nitrogen (0.0027% carbon and 0.004% nitrogen). The principal barrier to dislocation motion in these materials was found to be the Peierls-Nabarro stress, and the equation for the strain rate was similar to that employed by Seeger, Equation IV-4, but with a modified dependency of the activation energy on stress. The variation of the flow stress with temperature for iron is shown in Figure IV-15a. Basinski's analysis which is confirmed by the data leads to the conclusion that the strain-rate sensitivity $\left(\frac{\delta \sigma}{\delta \dot{\epsilon}}\right)_{T, \epsilon}$ should vary as

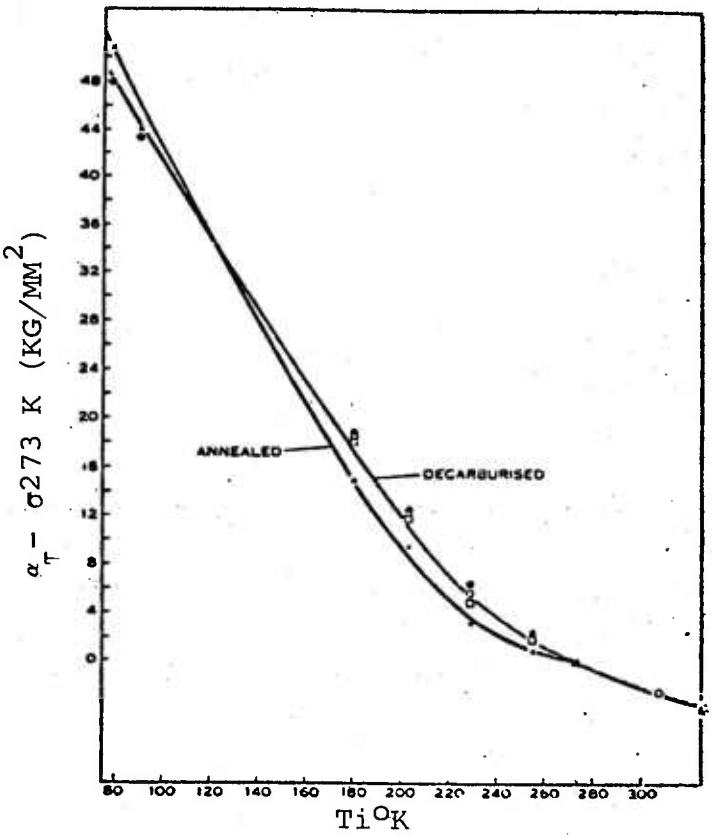

FIGURE IV-15a Temperature Dependence of Reversible Flow Stress in Iron. ●, Represent Points Taken at 2 Percent Strain; O, Represent Points Taken at 10 Percent Strain; □ Represent Points Taken at 20 Percent Strain. $\dot{\varepsilon} = 10^{-4}$/sec

SOURCE: Basinski and Christian, 1960

$$\left(\frac{\delta\sigma}{\delta\dot{\varepsilon}}\right)_{T,\dot{\varepsilon}} = CT - DT^2 \qquad \text{(IV-7)}$$

where C and D are independent of temperature. The strain-rate sensitivity should therefore rise at low temperatures and then fall off at higher temperatures as a critical temperature T_0 is approached. This behavior is shown in Figure IV-15b. We note that the degree of strain-rate sensitivity in iron is much greater than for aluminum and

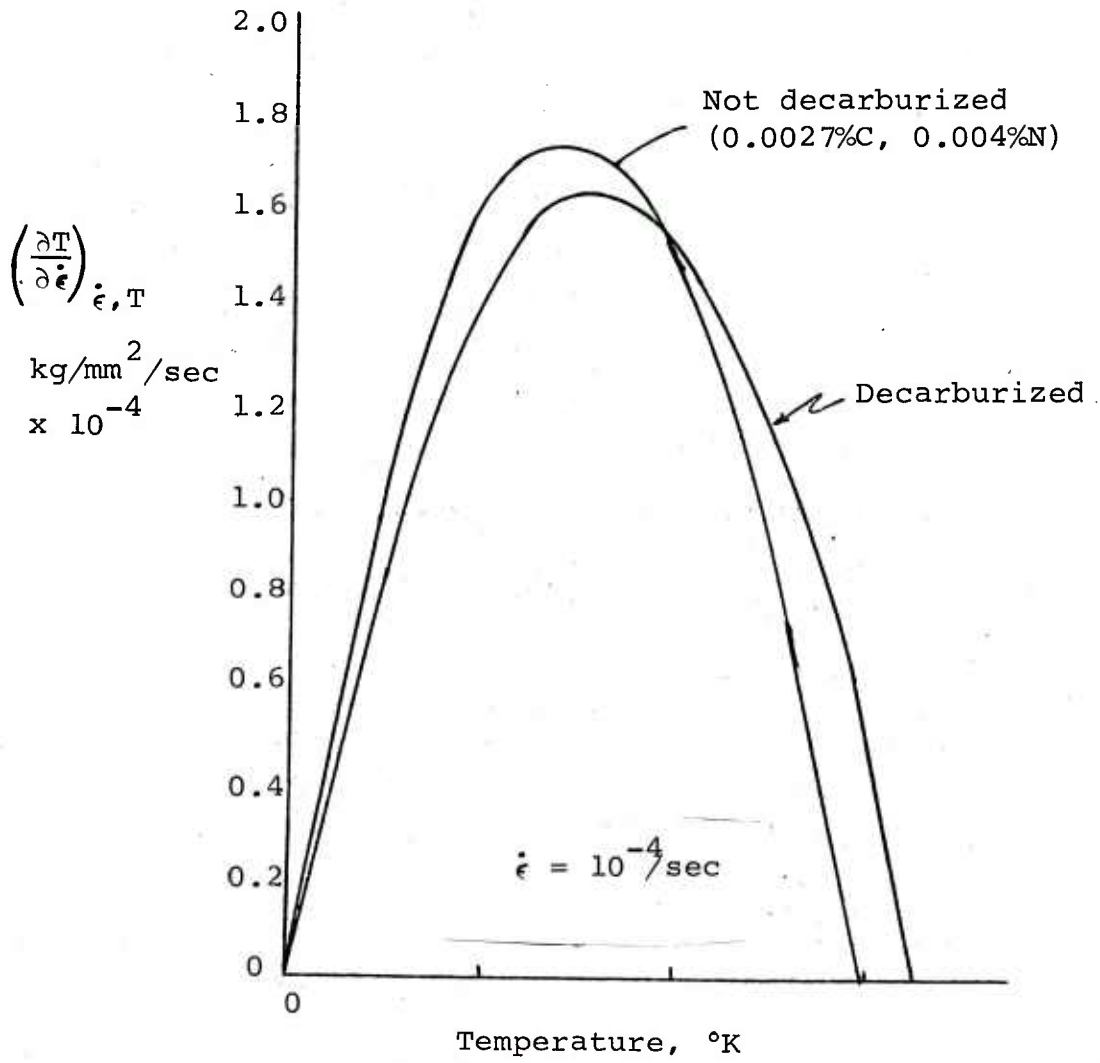

FIGURE IV-15b Strain Rate Sensitivity of the Flow Stress of Polycrystalline Iron

SOURCE: Basinski and Christian, 1960

other face-centered cubic metals also studied by Basinski. Also, the fact that the strain-rate sensitivity of decarburized iron is quite similar to that of non-decarburized iron provides further evidence of the importance of the Peierls-Nabarro stress rather than some interstitial effect in controlling the strain-rate sensitivity (Basinski and Christian, 1960).

Next let us consider results of Davies and Magee (1975) from constant strain rate tests carried out at room temperature on a variety of steels and aluminum alloys. These results are shown in Figures IV-16 through IV-21. At strain

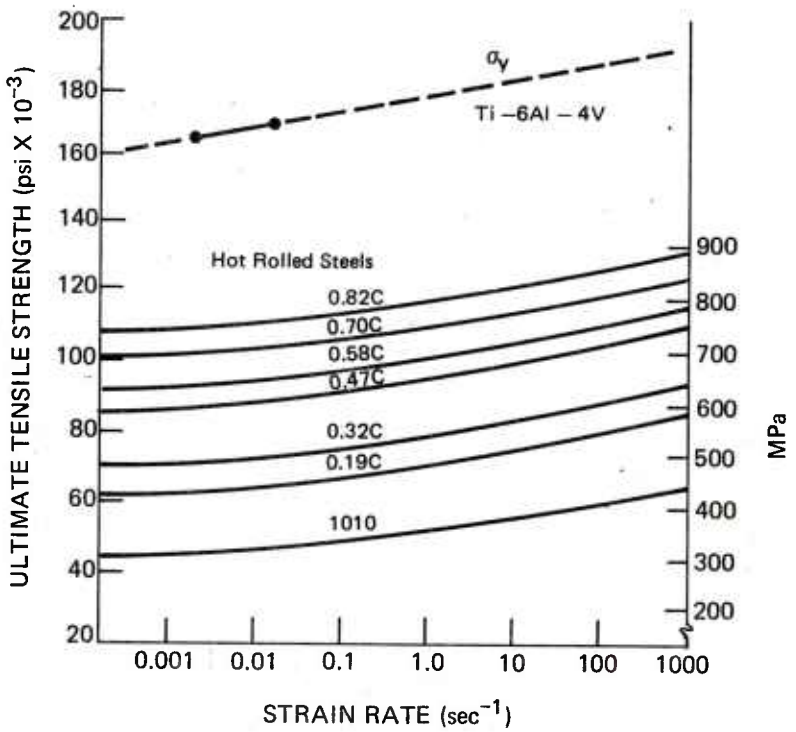

FIGURE IV-16 Ultimate Tensile Strength as a Function of Strain Rate for the Series of Hot-Rolled Steels Containing 0.10 to 0.82 Percent Carbon

SOURCE: Davies and Magee, 1975

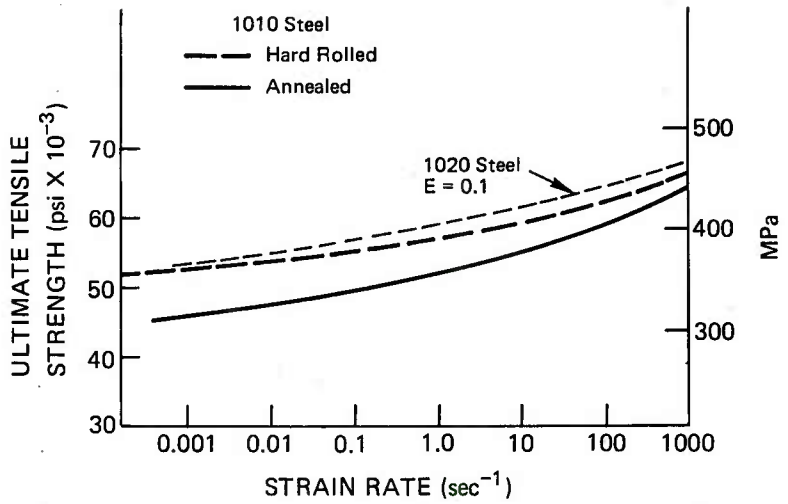

FIGURE IV-17 Ultimate Tensile Strength as a Function of Strain Rate for Annealed and Hard Rolled 1010 Steel, Showing Reduction in Strain Rate Sensitivity with Prior Cold Work

SOURCE: Davies and Magee, 1975

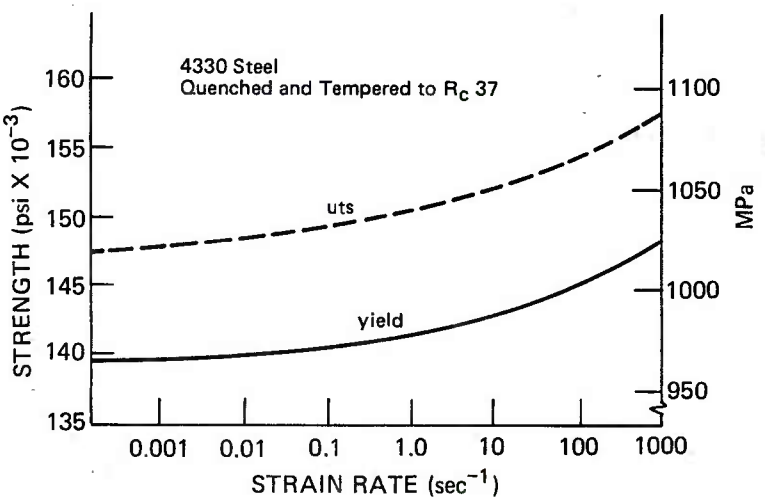

FIGURE IV-18 The Yield and Ultimate Tensile Strength as a Function of Strain Rate for 4330 Steel that was Quenched and Tempered to R_c 37

SOURCE: Davies and Magee, 1975

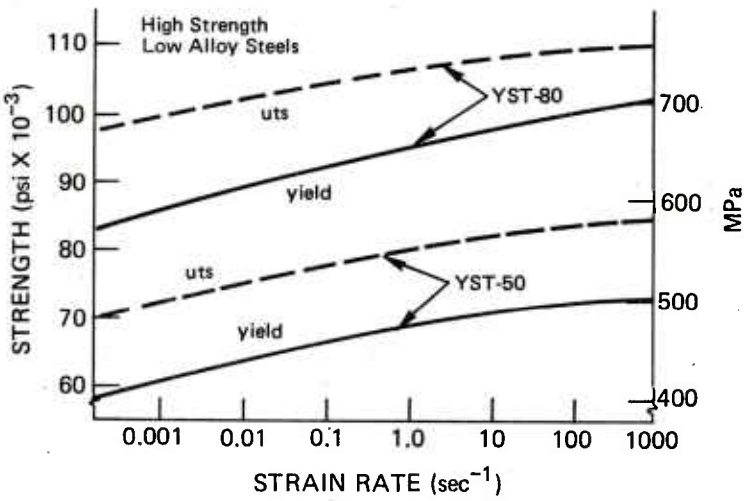

FIGURE IV-19 Yield and Ultimate Tensile Strength as a Function of Strain Rate

SOURCE: Davies and Magee, 1975

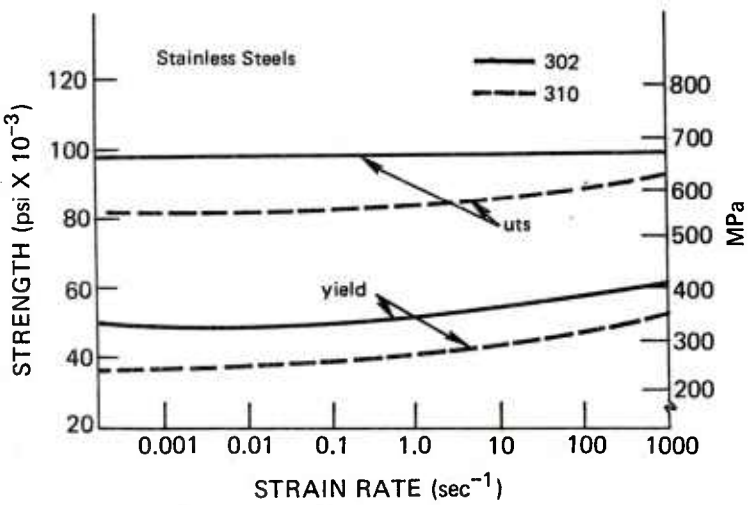

FIGURE IV-20 Yield and Ultimate Tensile Strength as a Function of Strain Rate for 302 and 310 Stainless Steel

SOURCE: Davies and Magee, 1975

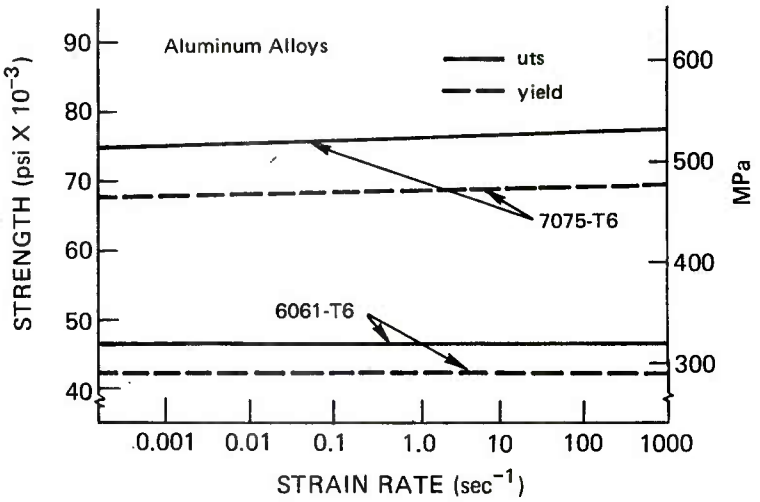

FIGURE IV-21 Yield and Ultimate Tensile Strength as a Function of Strain Rate for the Fully Hardened Aluminum Alloys 7075 and 6061

SOURCE: Davies and Magee, 1975

rates in excess of 80/sec reflection of elastic waves ("ringing") occurred which interfered with the determination of the flow stress at low strains, but beyond 100 percent elongation this effect died out and therefore the ultimate tensile strength rather than the yield strength is plotted in some of these figures. For comparison, data for Ti-6Al-4V are also shown (Hatch, 1965) as are the results of MacGregor and Fisher (1945) from Figure IV-13 for the flow stress of 1020 steel.

From equation IV-5a, at constant temperature uniaxial stress σ can be expressed as

$$\sigma = \sigma_G + C_1 \ln \dot{\epsilon}/\dot{\epsilon}_0 \qquad \text{(IV-8a)}$$

which predicts that the flow stress should vary linearly with the log of the strain rate; this behavior seems to be true for aluminum alloy (cf. Figure IV-21), but not true for the steels (cf. Figures IV-16 through IV-20).

If both sides of Equation IV-8a are divided through σ_G, then

$$\frac{\sigma}{\sigma_G} = 1 + \frac{C_1}{\sigma_G} \ln \dot{\epsilon}/\dot{\epsilon}_0 \qquad \text{(IV-8b)}$$

or

$$R = 1 + K_R \ln \dot{\epsilon}/\dot{\epsilon}_0 \qquad \text{(IV-8c)}$$

where $R \equiv \sigma/\sigma_G$, $K_R \equiv C_1/\sigma_G$. The quantities R and K_R are thus indices of strain-rate sensitivity. Values for both R and K_R from Figures IV-16 through IV-21 are given in Table IV-2. It can be seen that the value of R decreases with increasing strength level. Note that the strain-rate sensitivity of the titanium alloy appears to be greater than that of a steel of comparable strength level.

With respect to the influence of strain rate on fracture behavior of precracked steel specimens, it is of interest to note that the trends in fracture behavior have been related to the same parameter T ln $A/\dot{\epsilon}$ (Equation IV-6a) which has been used to correlate the strain rate and temperature dependence of the flow stress, Figure IV-12. The fracture toughness K_{Ic} (cf. Section IV-4) of several steels as a function of this parameter is shown in Figures IV-22a,b, and c (Hatch, 1965). The degree of correlation is quite good

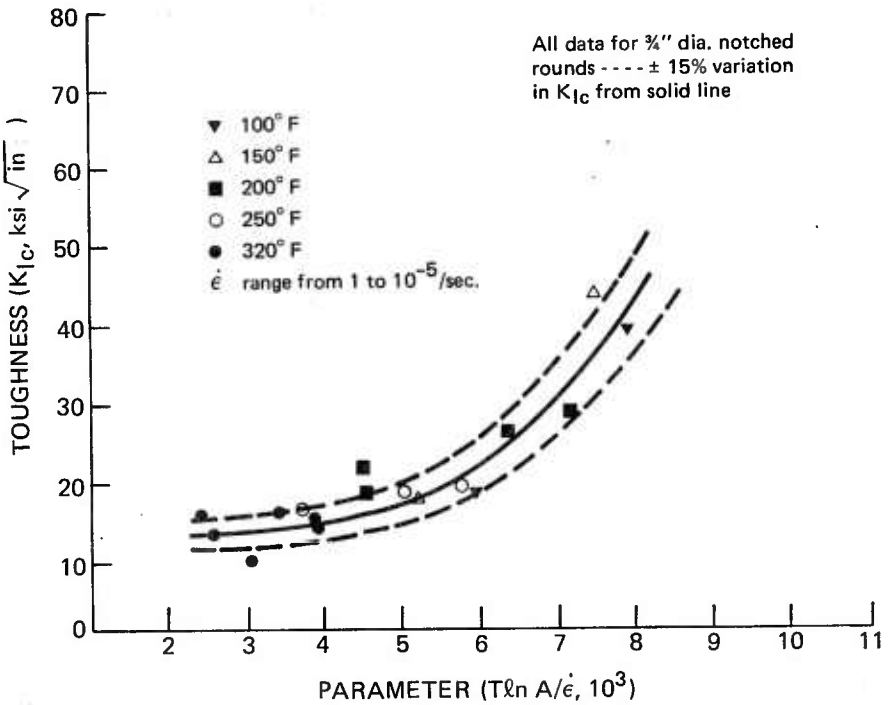

FIGURE IV-22a Crack Toughness as a Function of the Parameter for E Steel, $A = 10^8$/sec

SOURCE: Corten and Shoemaker, 1967

TABLE IV-2 Dynamic Factors for Several Alloys

Material	Dynamic Factor, R $UTS_{833/SEC}/UTS_{0.016/SEC}$	K_R UTS	Dynamic Factor, R $YS_{833/SEC}/YS_{0.016/SEC}$	K_R YS
Hot-rolled steel				
0.10C	1.37	0.0870		
0.19	1.32	0.0622		
0.32	1.26	0.0549		
0.47	1.23	0.0456		
0.58	1.20	0.0415		
0.70	1.19	0.0384		
0.82	1.18	0.0363		
Hard-rolled 1010 steel	1.19	0.0413		
Quenched and tempered,				
4330	1.07	0.0110		
Fine pearlitic steel	1.12	0.0264		
HSLA-YST-50	1.12	0.0291		
YST-80	1.10	0.0191		
Stainless steel-302	1.00	0.0		
310	1.12	0.0146		
Aluminum alloys-6061	1.00	0.0		
7075	1.03	0.0038		
Ti-6Al-4V [12]			0.025	1.12
1020 steel [9]			0.05	1.25

SOURCE: Davies and Magee, 1975

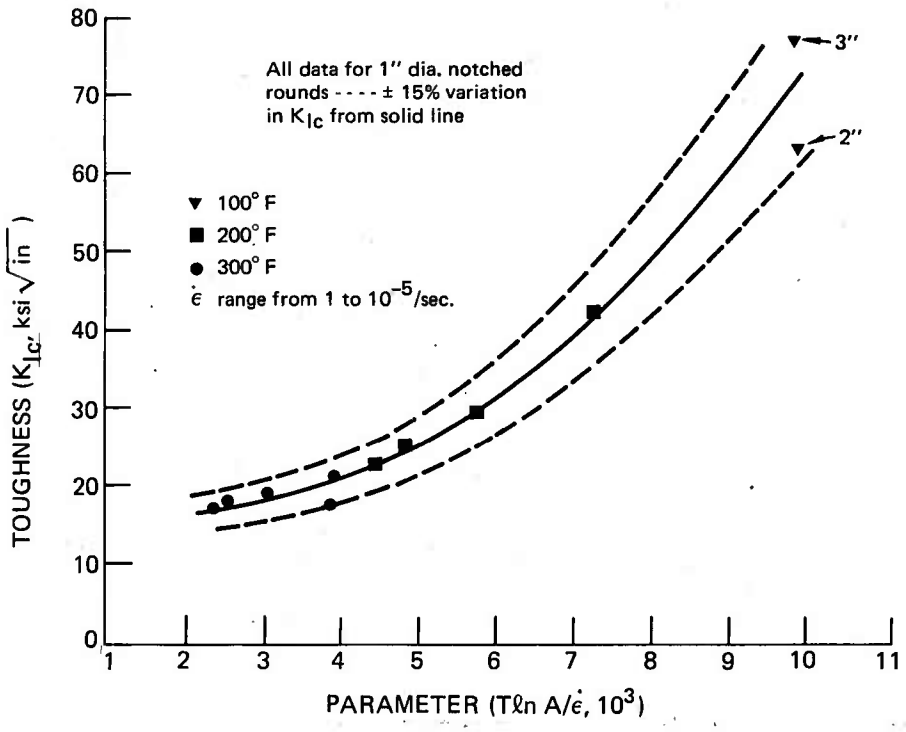

FIGURE IV-22b Crack Toughness as a Function of the Parameter for A302B Steel, A = 10^9/sec

SOURCE: Corten and Shoemaker, 1967

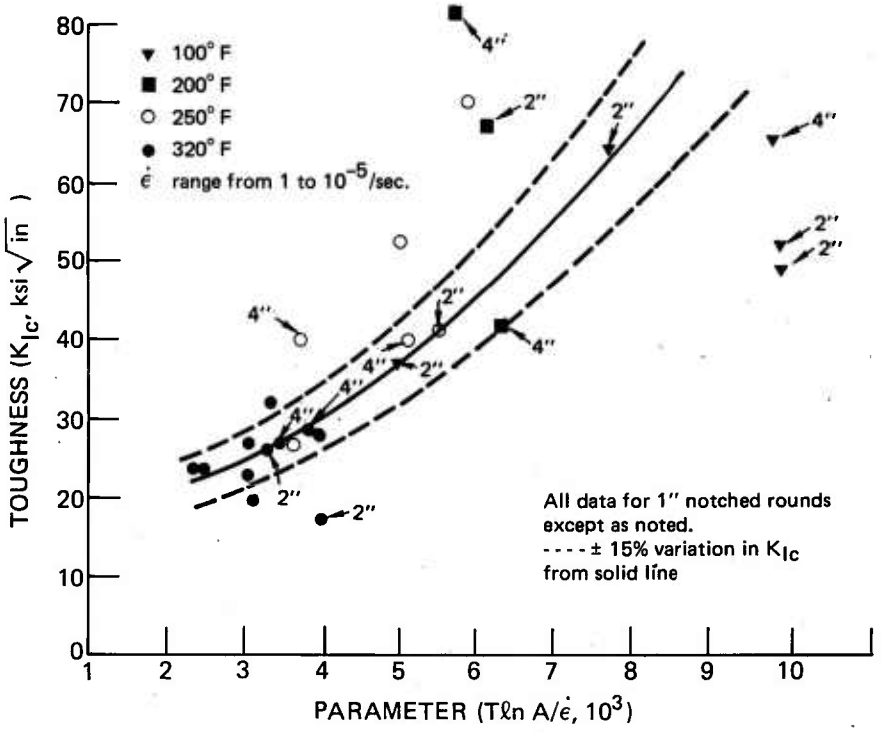

FIGURE IV-22c Crack Toughness as a Function of the Parameter for ABS Class C Steel $A = 10^8/sec$

SOURCE: Corten and Shoemaker, 1967

for two of the steels, but the extent of the scatter in the data for the third steel does not enable a conclusion to be drawn as to the degree of correlation. (In this analysis the strain rates used were correlated with a point within the plastic zone using an assumed elastic stress distribution. The strain rate for other points such as on the elastic-plastic boundary were also used without any significant shift in data correlation.) A good correlation implies that there is a strong interrelationship between the strain rate and temperature sensitivity of the flow stress and fracture toughness.

On a plot of the fracture toughness or impact energy absorbed versus temperature, an increase in the rate of loading often leads to a shift of the toughness-temperature curve to lower temperature, as illustrated in Figure IV-23;

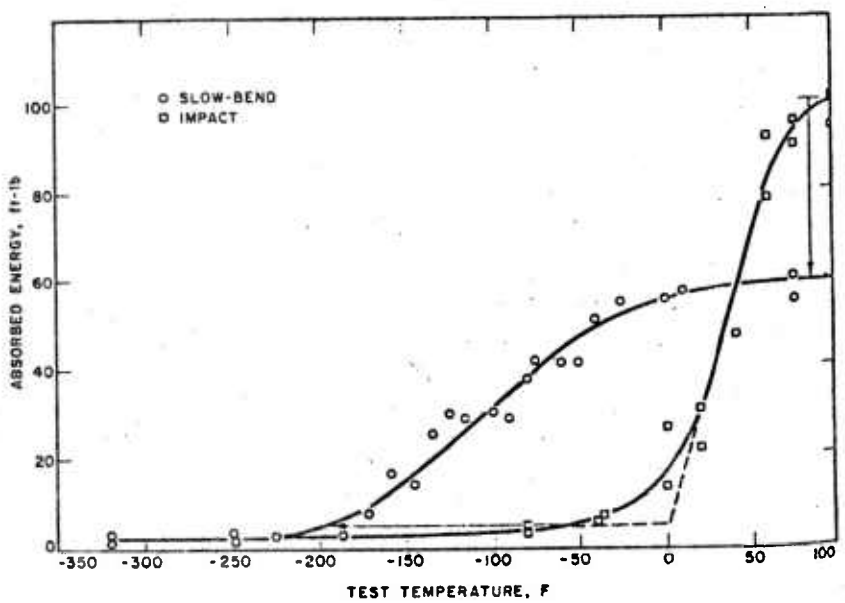

FIGURE IV-23 Slow-Bend and Impact CVN Test Results for ABS-C Steel, σ_Y = 39 ksi

SOURCE: Rolfe and Barsom, 1977

no significant shift exists for the high-strength steel of Figure IV-24. Barsom (1975) has developed a useful empirical relationship to account for the magnitude of this shift in °F:

$$T_{shift} = 215 - 1.5\ \sigma_{ys} \quad \text{for } 36 < \sigma_y < 140 \text{ ksi} \qquad \text{(IV-9)}$$

and

$$T_{shift} = 0.0 \quad \text{for } \sigma_y > 140 \text{ ksi}$$

Referring to Figure IV-23, this shift is the horizontal distance between the intersection of the dashed lines (tangent lines drawn from the lower shelf level and the transition region for the impact test) to the onset of the transition on the static curve. This relationship was originally developed for Charpy V-notch specimens but as Figures IV-25

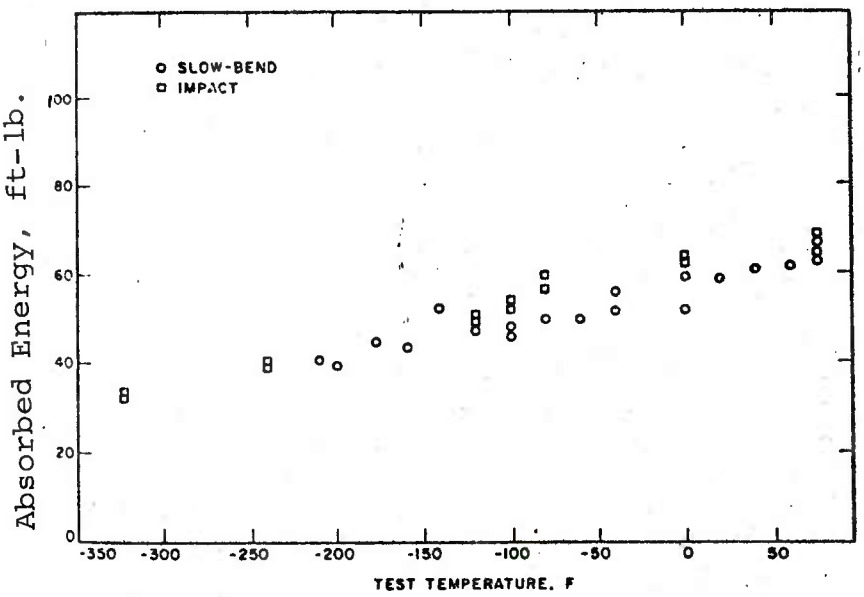

FIGURE IV-24 Slow-Bend and Impact CVN Test Results for 18Ni(180) Steel
σ_Y = 180 ksi

SOURCE: Rolfe and Barsom, 1977

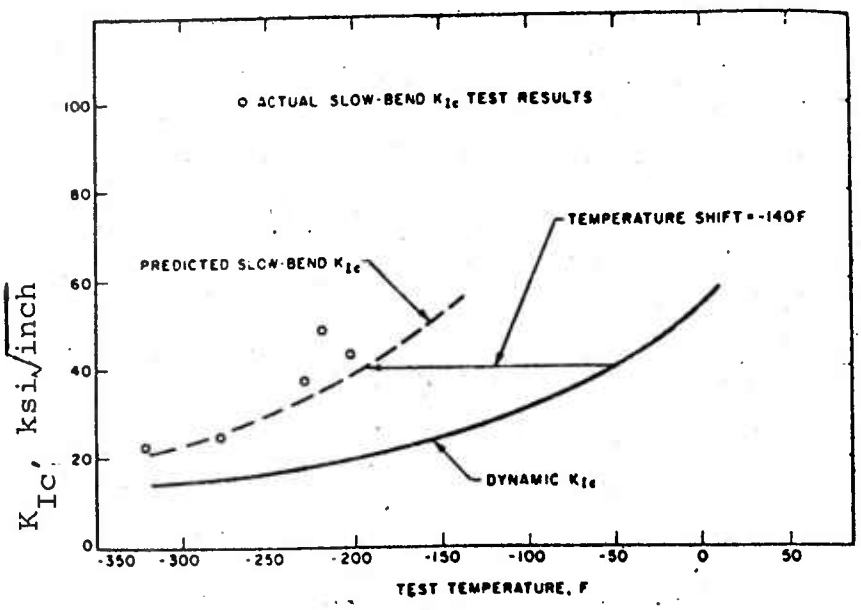

FIGURE IV-25 Use of CVN Test Results to Predict the Effect of Loading Rate on K_{Ic} for ABS-C Steel. σ_Y = 50 ksi

SOURCE: Rolfe and Barsom, 1977

IV-26 (Rolfe and Barsom, 1977) indicate it has also been applied to fracture toughness tests. We again note that strain rate effects are much more pronounced for low-strength steels as compared to high-strength steels. In the ductile region above the transition range it is believed that the increase in flow stress with strain rate produces the increase in toughness of these alloys (cf. Figure IV-23).

In conclusion, it appears that a reasonable understanding of the processes governing strain rate effects on flow stress has been achieved, and that experimental results are available for a range of engineering materials of interest. The situation with respect to a basic understanding of the dependence of the fracture process on strain rate is not as well established as for flow behavior. However, it is encouraging that in certain cases the trends in fracture behavior with temperature and strain rate have been related to the same parameter ($T \ln A/\dot{\epsilon}$) which has been used to correlate the flow stress; also, experimental results are available to assist in the assessment of the effects of strain rate in particular instances.

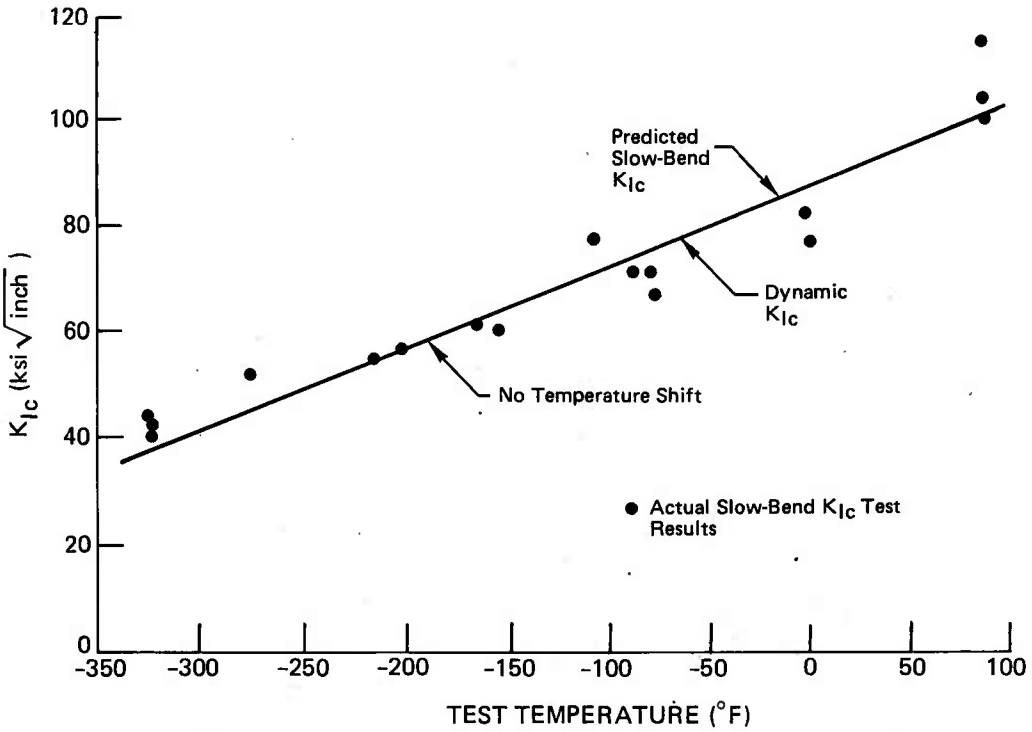

FIGURE IV-26 Use of CVN Test Results to Predict the Effect of Loading Rate on K_{Ic} for 18 Ni (250) Maraging Steel, σ_Y = 246 ksi

SOURCE: Rolfe and Barsom, 1977

3. Dynamic Test Techniques and Constitutive Equations

The previous section has dealt with metallurgical related phenomena which result in plastic strain rate sensitivity. This section will review briefly the test techniques which allow us to measure quantitatively the strain-rate effect in bulk specimens and the continuum constitutive equations which are used to include strain-rate sensitivity in dynamic structural analysis.

An extensive review and bibliography of high strain-rate test techniques has been given by Lindholm (1971). The early work in this area, which began during and after World War II, initially emphasized measurements of large amplitude plastic waves in bars. Plastic wave profiles (strain or particle velocity) were measured as functions of time or position in the bar. Derivation of the constitutive properties of the bar material from such measurements required the solution of the transient initial and boundary value problem using an a priori assumed form of the constitutive relation. This is a consequence of the fact that stress is not measured directly and independently in the experiment. Adequacy of the assumed form of the constitutive relation must then be based upon the degree of agreement between the analysis and other experimental information on wave profiles not used as part of the material characterization procedure. Two critical problems arise with this method. First, it has been found that the plastic wave profiles are not strongly sensitive to the explicit form of the rate-dependent terms in the constitutive relation. Thus, the experiment is not very discriminating in terms of the material property of interest. Secondly, as the wave propagates, the strain rate can vary widely; however, a constant strain-rate test is normally desired in order to minimize strain-history effects. These factors, and others, led to considerable uncertainty and some confusion during the 50s and 60s regarding the importance of strain rate in dynamic plasticity.

A significant advance in dynamic testing was made when Kolsky (1949) developed the Hopkinson pressure bar technique for compression testing. In this technique a short compression specimen is sandwiched between two long, elastic bars which serve to transmit the loading to the specimen and, with suitable instrumentation, to monitor the transient load, displacement and velocity of the bar faces in contact with

the specimen. The load is generated by a single elastic pulse and the measurements rely only on the accuracy of elastic wave theory in long bars. Since both load and deformation are measured, the stress-strain relation is derived directly. The average strain rate in this test is controlled by the amplitude to the elastic loading pulse and the length of the test specimen. By varying these parameters it has been possible to use the technique to generate stress-strain data in the range of strain rates from approximately $10^2 s^{-1}$ to $10^4 s^{-1}$. Since its introduction, the Hopkinson pressure bar technique has been extensively studied, analyzed and modified such that today it is a generally accepted and utilized method in dynamic testing. Modifications have included its adaptation to tension, torsion, and direct shear testing as well as compression. Despite its wide use and the requirements for test data in this range, there is as yet no move toward standardization of this test method.

In the intermediate strain-rate range between conventional "static" testing and $10^2 s^{-1}$, hydraulic, ram-type, actuated test machines are now available. These machines are basically conventional type universal load frames, but with special hydraulic actuator and valving that in combination produce very high crosshead velocity. Maximum velocities reach strain rates on the order of $10^2 s^{-1}$ with small test specimens. However, at these crosshead velocities considerable attention must be paid to the effects of inertia in the total system since the accelerations are very high. The frequency response of the system and of individual components, such as the load cell and extensometer, must be accounted for if the measured forces are to provide information on the constitutive properties. This is again an area in which some move toward standardization of procedures is needed if the data are to be widely used in critical design applications.

One other type of equipment should be mentioned which has application in the intermediate strain-rate range. This is the cam-plastomer (Hockett, 1959). In this system energy is stored in a rotating mass which drives a cam having a controlled profile. By means of a cam follower mechanism the cam is coupled to the specimen and compresses it in one revolution. An advantage of this technique is that a logarithmic profile on the cam and constant rotational speed results in a constant true strain rate test. At the higher test speeds, the hydraulic machine operates with an open loop so that the strain rate is not positively controlled.

Details of these and other, less widely used, test techniques are given by Lindholm (1971). Limited work has been achieved under biaxial stress conditions and varying strain rate. This type of data will be necessary to evaluate generalized constitutive equations needed for structural analysis.

Extension of mathematical models of classical plasticity to rate- or time-dependent flow is generally based upon the concept of a yield function. In many cases such a yield function may be assumed of the form

$$F = \frac{(J_2')^{1/2}}{c} - 1 \qquad \text{(IV-10)}$$

where J_2' is the second invariant of the stress deviator and c is the low rate or "static" yield stress in shear. The plastic strain rate, $\dot{\epsilon}_{ij}^{p}$, is then assumed to be proportional to the magnitude of F (where F is a measure of the difference between a scalar measure of the instantaneous stress state, $(J_2')^{1/2}$ in Equation (IV-10), and the yield surface, $(J_2')^{1/2} = c$) for positive values of F. This stress difference is often called 'overstress'. In a general formulation for one dimensional problems of viscoplastic wave propagation in the x, direction, Malvern (1951) introduced the functional dependence

$$\dot{\epsilon}_{11} = \lambda \dot{\sigma}_{11} + \Psi(\sigma_{11}, \epsilon_{11}) \qquad \begin{matrix} \Psi(\sigma_{11}, \epsilon_{11}) = 0 & \text{for} & \sigma_{11} \leqslant f(\epsilon_{11}) \\ \Psi(\sigma_{11}, \epsilon_{11}) \neq 0 & \text{for} & \sigma_{11} > f(\epsilon_{11}). \end{matrix} \qquad \text{(IV-11)}$$

Malvern, however, retained the overstress dependence in that the plastic component of the strain rate ψ, is finite only when the stress is greater than the static stress-strain c rve, $\epsilon_{11} = f(\epsilon_{11})$. Perzyna (1963) extended the Malvern formulation to generalize stress states as follows:

$$\dot{\epsilon}_{ij}' = \lambda \dot{\sigma}_{ij}' + \gamma \Phi(F) \frac{\sigma_{ij}'}{(J_2')^{1/2}} \qquad \begin{matrix} \Phi(F) = 0 & \text{for} & (J_2')^{1/2} \leqslant c \\ \Phi(F) \neq 0 & \text{for} & (J_2')^{1/2} > c. \end{matrix} \qquad \text{(IV-12)}$$

In the above, λ and γ are appropriate elastic and viscous material constants and ϵ_{ij} and σ_{ij}' are the deviatoric strain and stress tensors, respectively. These continuum formulations for dynamic plasticity rely on macroscopic

measurements of plastic flow to provide the arbitrary constants and the form of the material functions (e.g., $\Phi(F)$).

Concurrently, there has been a significant effort to describe macroscopic flow in terms of the controlling microscopic mechanisms, predominantly slip produced by the motion of dislocations, as discussed in the preceding section. In this approach we noted that the plastic strain rate is a product of the dislocation density and the mean dislocation velocity. By assuming a variety of functional dependencies of dislocation density and velocity on stress and the deformation state, qualitative and often quantitative description of macroscopic behavior can be obtained.

This dislocation dynamics approach is difficult to apply because the relevant paramenters, dislocation density and dislocation velocity, are not easily measured under transient conditions. Also, since they occur as a product, their independent contribution to the total plastic strain rate is difficult to define. Nevertheless, a very significant increase in understanding of metal plasticity has resulted from this approach. Somewhat recent work, the most notably by S. R. Bodner (1968), combines the results of dislocation dynamics into the framework of continuum plasticity theory. As a generalization, Bodner proposes that the second invariant of the plastic deformation rate deviator is a function of the corresponding stress invariant, or

$$D_2^p = f(J_2'). \qquad \text{(IV-13)}$$

He then develops incremental forms of the flow equations. A significant difference in this approach and the classical plasticity approach is the absence of an explicit yield function. From dislocation dynamics, plastic flow may occur at any value of finite stress and temperature. This eliminates the need for partitioning of the stress space into elastic and plastic domains, with the attendant bookkeeping problems in associated computational procedures. Yield phenomena can still be adequately described by a proper choice of functions representing dislocation multiplication or annihilation. This approach also eliminates the reliance on a 'static' stress-strain curve or yield surface, which has no real physical significance other than a reference. The 'overstress hypothesis' is not needed.

Another current approach is to rely heavily on the concepts of irreversible thermodynamics (e.g., Schapery, 1968 and Valanis, 1972). This approach brings appropriate attention to the need to formulate the problem in terms of true state variables. These theories introduce internal variables which characterize the deformed state of the material and enable the formulation of constitutive equations that account for complex strain-history and temperature effects. For further discussions of the thermodynamic approach as well as detailed reviews of other constitutive equations see Stricklin and Saczalski (1976) and Valanis (1976).

These approaches have all been developed in the attempt to describe the same phenomena, attacking the problem from different conceptual bases. At present, the amount of experimental data available concerning rate-dependent materials under combined stresses and time varying strains and nonproportional strain histories and temperature is not sufficient to assess the validity of any generalized theory. The number of independent variables can become very large when testing in multiaxial stress states. Some guidance from theory is needed in the design of critical experiments which can differentiate between alternate models of the plastic deformation process.

4. Dynamic Fracture Analysis and Tests

a. Introduction

The discussion given in this section of the report is based on the point of view of fracture mechanics. This requires adoption of the premise that a flaw in the form of a crack exists in a given structure at the time that a specified high rate of loading is applied. The distinction between fracture mechanics and a "failure mechanics" approach is illustrated for an idealized situation in Figure IV-27. In failure mechanics, a dominant flaw does not exist

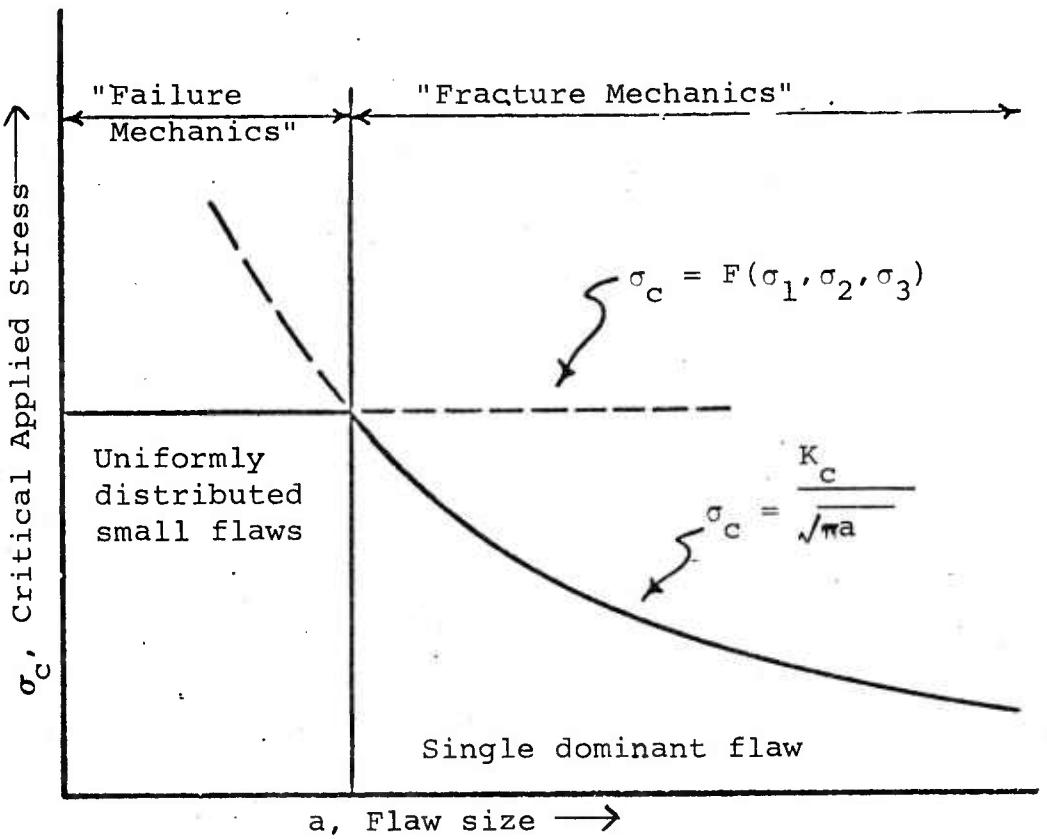

FIGURE IV-27 Distinction Between Failure Mechanics and Fracture Mechanics Viewpoints

and the material is considered to be completely homogeneous. Then it is often appropriate to develop a failure surface that is a function of the principal stresses at each point in a body, not unlike the Tresca and von Mises criteria in the theory of plasticity. In fracture mechanics, in contrast, attention is focused on the conditions at the tip of the dominant crack-like flaw. The dimensions of the crack are explicitly included in a criterion for failure through the growth of this flaw which also depends upon the "fracture toughness" of the material; e.g., the parameter K_c in Figure IV-27.

All materials, of course, contain flaws. These may arise from inherent defects in the material or from defects introduced by processing and manufacturing operations. In either instance, it is likely that a more or less uniform distribution of small defects exists in every material at the beginning of its service life. When subjected to loads while in service, these flaws may become enlarged and grow in a stable fashion by creep or fatigue mechanisms. This growth may be aided by an aggressive environment. Because of the presence of stress concentrations or high localized loads, some flaws will grow more than others. When at least one well-defined crack exists, a fracture mechanics point of view becomes appropriate. More definitely, fracture mechanics is the discipline concerned with failure by the initiation and subsequent propagation of a flaw in its most deleterious condition: a sharp crack.

Note that the term fracture mechanics is used here in a broad sense. It includes the growth initiation, stable growth, and/or the unstable propagation of a crack in a body without regard to the constitutive relation obeyed by the material and the environmental and loading conditions to which it is subjected. This definition should be distinguished from linear elastic fracture mechanisms (LEFM) which is a special case, albeit the most widely known, of the general methodology; by definition, LEFM is concerned with the fracture of media which are linearly elastic except for a relatively small zone of damage or plastic deformation at the crack tip.

Just as for any fracture problem, the characterization of crack propagation initiated by high rates of loading involves three distinct, but highly interrelated components: dynamic analysis, dynamic material properties, and a dynamic crack growth criterion. This report is primarily aimed at

delineating the material properties necessary to cope with high strain rate loadings. However, presentation of such data by themselves is meaningless. Equal prominence must be given to the theoretical basis by which the data are first extracted from a laboratory experiment and subsequently applied to evaluate a structure. Accordingly, the discussion in this section contains an integrated description of all three aspects of the problem.

While some background material is provided, the discussion primarily describes the extensions and generalizations of ordinary fracture mechanics treatments that are required in high strain rate loading problems. This is in accord with the general approach taken in this report which is to emphasize the theoretical concepts and material properties beyond those of the corresponding static problem. An exhaustive review of the literature has not been attempted. Instead, the intent was to focus on a few key results, emphasizing reports and journal articles that have appeared fairly recently in the literature, in an attempt to provide an up-to-date perspective on the subject. The primary goal is to provide a basis for defining the directions that subsequent research on the mechanics of dynamic deformation and failure under high strain rates must take.

b. Background Discussion, Definitions and Terminology of Fracture Mechanics

The words "failure" and "strength" are often used but seldom defined in a precise manner. Consider first the term failure. There are many different ways that a structure can become unable to adequately perform its primary function. In each such instance, failure can be considered to have occurred. As noted in the introduction to Section IV, the possible failure modes range from simple loss of structural stiffness due to gross inelastic deformation; e.g., yielding to the complete loss of load-carrying capacity by gross macroscopic deformation and separation; e.g., fracture. As an intermediate situation, failure may involve a reduction in load-carrying capacity due to localized damage; e.g., spallation. Thus, failure can be gradual or rapid, may or may not be readily detectable, and need not be catastrophic in nature.

The term strength is conventionally associated with the load level at which a failure occurs by some means in a standard test specimen. Clearly, the strength will depend upon the failure mode under consideration and may be a function of many different parameters in the test program, such as specimen size. It may also depend upon the assumptions in an analysis technique that is introduced to equate the numbers actually measured in the experiment to the desired strength parameter. Consequently, even for a given failure, the strength parameter may not be a true material property at all, but will depend upon the geometry and other details of the test specimen used to measure it. Hence, the "strength" of a material determined in a laboratory test is often not directly applicable to the same material when it is used differently in service.

In view of the foregoing remarks, it is clear that an analysis procedure that correctly extracts a material property from a standard test procedure which is applicable to engineering applications involving different geometries and loads is absolutely necessary. Only in this way can reliable estimates of the service failure loads be made using strengths determined in small-scale laboratory tests. But, even though substantial experimental work has been performed to date, this capability does not seem to exist for materials subjected to high strain rate loading. It is likely that the least progress has been made in the most critical problem area--when crack-like defects exist in the material. To treat this subject, it is appropriate to briefly review the subject of fracture mechanics. Accordingly, the basis of existing fracture mechanics techniques for quasi-static problems (i.e., inertia due to straining is neglected) will be given next as a prelude to a more thorough examination of the fracture mechanics of structural materials under high rates of loading.

Consider that a sharp planar crack exists in a linear elastic material subjected to in-plane symmetric loading remote from the crack. Consider further that the crack lies along the x axis and will extend in a self-similar manner. Then, in the close proximity of the tip of a crack, the component of stress which acts in the y direction (i.e., the direction normal to the crack plane) can be written as

$$\sigma_y\ (r,\theta) = \frac{K_I}{\sqrt{2\pi r}} \cos\frac{\theta}{2}\left[1 + \sin\frac{\theta}{2}\sin\frac{3\theta}{2}\right] + \ldots \quad \text{(IV-14)}$$

where $\theta = 0$ coincides with the prolongation of the crack, $\theta = \pi$ coincides with the crack face, and r is the distance from the crack tip.* Similarly, the displacement normal to the crack plane is, for local plane strain conditions,

$$v(r,\theta) = \frac{K_I}{\mu}\sqrt{\frac{r}{2\pi}}\sin\frac{\theta}{2}\left[2(1-\nu) - \cos^2\frac{\theta}{2}\right] + \ldots \quad \text{(IV-15)}$$

where μ is the shear modulus and ν is Poisson's ratio. In equations IV-14 and IV-15, K_I is a parameter called the stress-intensity factor.** It depends upon the applied loads, the crack length, the geometry and, in some cases, the elastic properties of the components. In fact, one major element of the LEFM approach is that these parameters influence the stress field close to the crack tip only via the stress-intensity factor.

As illustrative examples, consider that a uniform tensile loading in the y direction, $\sigma_y(\infty) = \sigma_0$, acts on a large body. Then $K_I = \sigma_0\sqrt{\pi a}$ for a single isolated crack of length 2a on the x-axis. For an infinite periodic sequence of cracks on the x axis with midpoints a distance 2b apart, $K_I = \sigma_0\sqrt{2b}\tan^{1/2}(\frac{\pi a}{2b})$. And, for a central crack in a long strip of width 2w, $K_I \simeq \sigma_0\sqrt{\pi a}\sec^{1/2}(\frac{\pi a}{2w})$.

The second major element of LEFM is the connection between the local crack tip quantity--the parameter K_I--and a global energy balance related parameter G. This arises as follows. Consider a virtual extension Δa of the crack. Then, under conditions where LEFM applies, G is defined as

---

* Several standard formulas are given in this background discussion withoug citing publications; they can be found in recent books on fracture (Hertzberg, 1976 and Rolfe and Barson, 1977).

** Conventionally, the subscript I is used in order to distinguish between this mode of loading, the so-called opening mode, and K_{II} and K_{III} which correspond to in-plane and out-of-plane shear loadings (i.e., the skew-symmetric and antiplane shear modes, respectively).

$$G = \frac{1}{b} \frac{dW}{da} - \frac{dU}{da} \qquad \text{(IV-16)}$$

where W denotes the work done by the applied tractions, U denotes the elastic strain energy in the body, and b is the length of the advancing crack front; the quantity G is observed to be the excess energy dW - dU divided by the area of crack extension, dba. Therefore, assuming inelastic behavior is limited essentially to the crack plane, and neglecting heat flow and kinetic energy, G must be the work done by the traction σ (r,o) on separating the material at the crack tip (per unit of new surface). For a linear elastic body this work is

$$G = 2 \lim_{\Delta a \to o} \frac{1}{\Delta a} \int_o^{\Delta a} \frac{1}{2} \sigma_y (r,o)\ v(\Delta a - r, \pi)\, dr \qquad \text{(IV-17)}$$

Upon substituting from Equation IV-14 and IV-15, performing the integration, and taking the limit, it is found that

$$G = \frac{1-\nu^2}{E} K_I^2 \qquad \text{(IV-18)}$$

Now, it may be taken as a basic principle of LEFM that the crack will extend when, and only when, G exceeds a critical value of energy G_c. Then, in view of Equation IV-18, it is exactly equivalent to consider that crack extension takes place when K_I exceeds a critical value. Denoting this latter parameter by K_{Ic}, we can write

$$K_{Ic}^2 = \frac{E}{1-\nu^2} G_c \qquad \text{(IV-19)}$$

The energy G_c is a material property and thus K_{Ic} is also a material property. The latter quantity is called the plane-strain fracture toughness*

In essence, LEFM provides a criterion for fracture by crack extension by equating a function of the applied loads and the geometry of a structural component--the stress-intensity factor--to a material property--the fracture toughness. To illustrate the application of this idea, the stress-intensity factors quoted above can be used to express the fracture stress σ_f for materials with given toughnesses and geometries. These are obtained by simply replacing K_I by K_{Ic} and taking the applied stress equal to σ_f. The results are

$$\sigma_f = K_{Ic} (\pi a)^{-1/2}, \quad \text{isolated crack} \qquad \text{(IV-20a)}$$

$$\sigma_f = K_{Ic} \left(2b \tan \frac{\pi a}{2b}\right)^{-1/2}, \quad \text{colinear cracks} \qquad \text{(IV-20b)}$$

$$\sigma_f = K_{Ic} \left(\pi a \sec \frac{\pi a}{2w}\right)^{-1/2} \quad \text{finite width strip} \qquad \text{(IV-20c)}$$

In an ideal, completely elastic body for which the material separates along a single plane, one writes $G_c=2\gamma$ where γ is now the so-called surface energy. Hence, from Equations IV-19 and IV-20a,

$$\sigma_f = \sqrt{\frac{2E\gamma}{\pi a(1-\nu^2)}} \qquad \text{(IV-21)}$$

* According to ASTM E399, plane strain conditions are achieved near the tip of a through-the-thickness crack when the plate thickness $B \leq 2.5 (K_{Ic}/\sigma_Y)^2$, where σ_Y is the yield stress. A similar expression has been used for fast running cracks where σ_Y is interpreted as the dynamic yield stress corresponding to a strain rate within or adjacent to the plastic zone.

which is the familiar Griffith equation except for the factor $1-\upsilon^2$; this factor accounts for the fact that the crack tip is in a state of plane strain, rather than plane stress. In metals, however, it is generally true that $G_c >> 2\gamma$ because of the complex failure processes that occur at the crack tip when crack extension initiates. In situations where the loads are not applied symmetrically with respect to the crack plane, more than one type of stress intensity factor prevails; indeed, in some cases all three factors, K_I, K_{II}, and K_{III} may be needed. The use of the strain energy density factor S associated with an element ahead of the crack has been proposed as a criterion of fracture for static and dynamic problems (Sih, 1977). Crack instability is taken to coincide with the failure of this element when the stored energy reaches a critical value of S, denoted as S_c, which is assumed to be a characteristic property of the material. For the case of an angle crack of length 2a subjected to uniaxial dynamic loading, the fracture stress may be expressed as

$$\sigma_f = \sqrt{\frac{S_c}{\pi a F(\beta, t, \theta_o)}} \qquad \text{(IV-22)}$$

in which F is an analytically determined function that depends on time as well as the geometrical parameters (cf. Section IV.B.4.e). In Equation IV-22, B is the angle between the crack plane and the axis of loading, while θ_o is the direction of crack initiation determined from the condition of minimum strain energy density. As discussed in Section IV.B.4.e other criteria have also been proposed for mixed mode problems.

One of the basic considerations in LEFM is that the amount of plastic deformation surrounding the crack tip must be small enough that the perturbation of the linear elastic stress and displacement fields can be neglected when calculating energy release rate G. While this is essentially true for brittle materials, it will not be a good assumption for ductile materials. In the latter case, however, a plasticity correction to crack length known as the Dugdale or strip yielding model has been usefully employed. In this model, plastic deformation without strain hardening is considered to occur in a thin strip which is, in effect,

an extension of the crack. Then, the plastic zone length ℓ for an isolated, through-the-thickness crack in a body under uniform tension is given by

$$\frac{\ell}{a} = \sec\left(\frac{\pi}{2}\frac{\sigma_0}{\sigma_Y}\right) - 1 \qquad \text{(IV-23a)}$$

where σ_0 is the applied tensile stress and σ_Y is the yield stress of the material. If ℓ is large compared to sheet thickness, plane stress theory is employed to compute the crack opening displacement at the tip,

$$\delta_t = \frac{8}{\pi}\frac{\sigma_Y a}{E}\log\sec\left(\frac{\pi}{2}\frac{\sigma_0}{\sigma_Y}\right) \qquad \text{(IV-23b)}$$

A critical value of the crack-opening displacement δ_t is sometimes offered as an alternative fracture criterion. But when $\ell/a \ll 1$, it is found from Equation IV-23b and IV-20a that $\delta = K_I^2/E\sigma_Y$, which shows that a critical crack-opening displacement criterion is equivalent to a criterion on the stress intensity factor when the amount of plastic deformation is small. Hence, there is no basic contradiction between these two approaches.

We should add that a strip-like yield zone is certainly not universally observed and, in fact, does not even represent the most usual case in metals; it appears to be limited to thin sheets of moderate or low strain-hardening material. When this is not the case, the plastic zone has a two or three-dimensional character, and a very involved mathematical treatment may be required.

An even more useful and general approach to characterizing the critical condition for fracture initiation in the presence of large-scale plasticity is based on the so-called J-integral (Rice, 1968; see also Rolfe and Barsom, (1977)). Initiation is assumed to occur when J reaches a critical value J_{Ic}; for small-scale yielding, $J_{Ic} = G_c$, and therefore this criterion is consistent with LEFM. It should be noted that the use of J for the opening mode is limited to plane strain or generalized plane stress problems, and to situations where the deformation theory of plasticity is a realistic approximation of the elastic-plastic behavior. It is of interest here to evaluate the J-integral for the

case of a body in which material separation occurs entirely within a thin layer or strip ahead of the crack tip, and outside of this layer the material is either elastic, or the deformation theory applies. The J-integral becomes (Rice, 1968)

$$J = \int_0^{\delta_t} \sigma_y \frac{d\delta}{dx} dx \qquad \text{(IV-24a)}$$

where σ_y is the reaction of the separating material on the intact (elastic or plastic) material and δ is the separation between the edges of the intact material; δ_t is the value of δ at the tip. If $\sigma_y = \sigma_y(\delta)$, then Equation IV-24a becomes

$$J = \int_0^{\delta_t} \sigma_y (\delta) d\delta \qquad \text{(IV-24b)}$$

which is the work done in pulling to failure a ligament of material in the thin layer at the crack tip; note that the J-value does not include the work of plastic deformation of material outside of the thin strip. If we further assume σ_y= constant $\equiv (\sigma_Y)$then $J = \sigma_Y \delta_t$, which implies a J_c criterion is equivalent to a crack opening displacement criterion. This fact that J equals the work done in separating the material at the tip, and not the work of large-scale plastic deformation, may be the reason for the success of the J_{Ic} criterion.

A substantial portion of current fracture testing work is focused on the recommendations of the Pressure Vessel Research Committee (PVRC) and the requirements of Sections III and XI of the ASME Boiler and Pressure Vessel Code. These are based largely on the concepts and methodology of LEFM. More specifically, the PVRC recommendations and the ASME Code criteria represent the fracture toughness of pertinent steels by K_{IR}, the so-called "reference value" of the critical stress-intensity factor for unstable crack propagation. The curve of K_{IR} as a function of the temperature relative to the drop-weight nil ductility temperature (NDT) test (see Section IV.B.4.C.(2)(6) as derived in the PVRC recommendations is shown in Figure IV-28. As can be seen from Figure IV-28, K_{IR} is simply a lower bound to the available fracture toughness values for nuclear pressure vessel steels. The most important contributions to this data

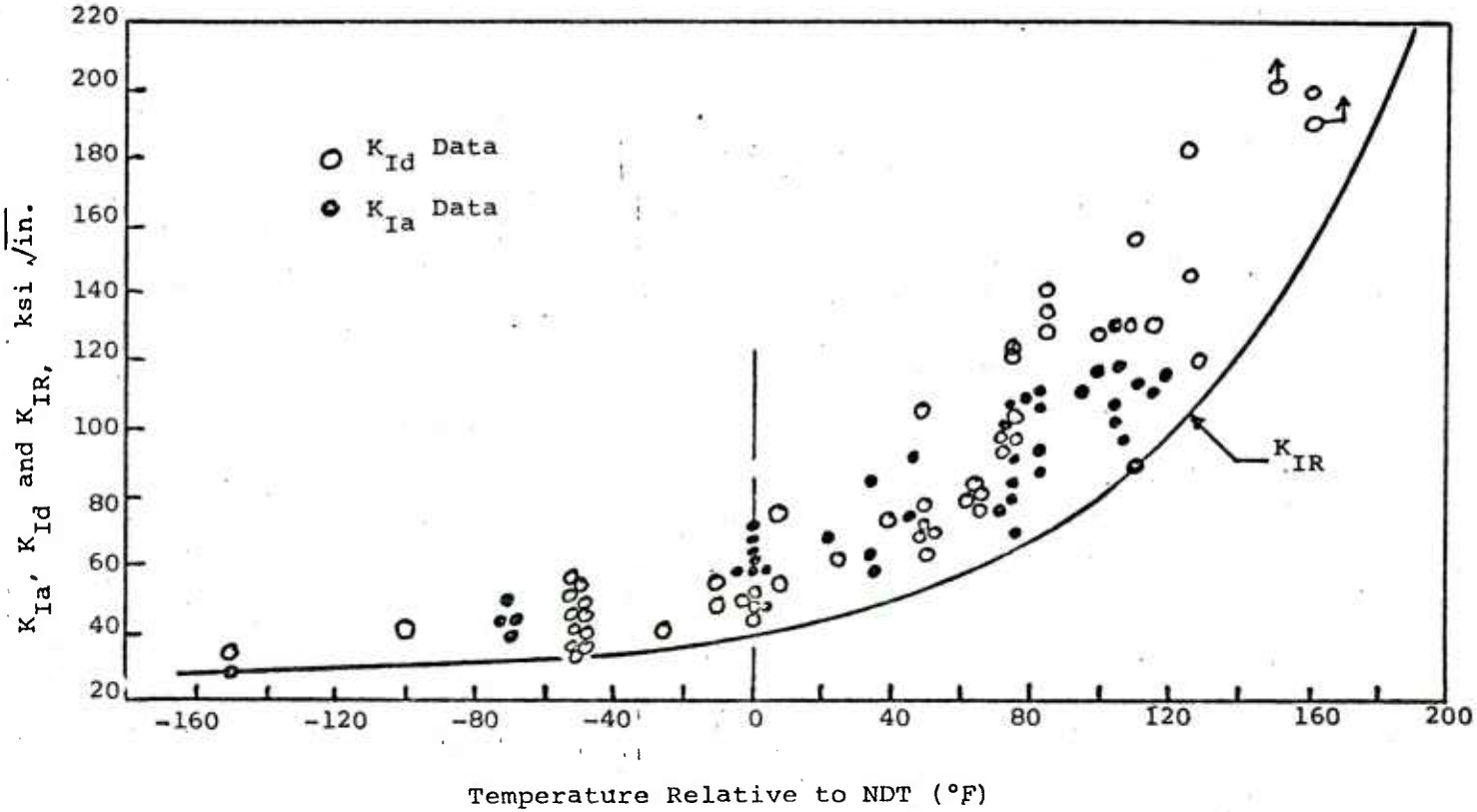

FIGURE IV-28 The Reference Fracture Toughness Values for A533, Grade B, Class 1 and A508, Class 2 Steel

SOURCE: Rolfe and Barsom, 1977, Figure 15

base are the parameters K_{Id} and K_{Ia}, where K_{Id} is the value of the stress intensity factor for crack growth initiation under dynamic loading, and K_{Ia}, is an approximation to the value at the arrest of a rapidly propagating crack.

In view of the practical importance of the results given in Figure IV-28, the basis for determining K_{Id} and K_{Ia} values is quite important. Both values are purported to be material properties. As noted above, K_{Id} is the toughness value measured by rapid (dynamic) loading of a specimen with a stationary (nonmoving) precrack. K_{Ia} is the toughness value measured on a specimen immediately after the arrest of a propagating crack. In both cases, static analyses have been used to obtain the values of stress intensity factors. In view of the role of these values in defining the K_{IR} curve, their origin in a static analysis when, in fact, the experiments in which they are determined are highly dynamic is a point of some concern. In contrast, the parameter K_{Id}, the dynamic toughness of a rapidly propagating crack, is entirely based on dynamic (i.e., inertia forces included) analysis procedures.

c. Crack Growth Initiation Under High Loading Rates

(1) Dynamic Fracture Concepts. At present, both crack initiation and crack arrest studies are analyzed predominately in a manner mathematically identical to a crack initiation analysis using LEFM. Thus, it is supposed that crack arrest is the reverse, in time, of crack growth initiation. The arrested crack is treated as a stationary crack whose stress-intensity factor is derived from a static analysis. The crack arrest toughness K_{Ia} is interpreted in a way that is analogous to K_{Ic}. Similarly, in analyzing crack growth initiation under high loading rates, crack-tip inertia effects are neglected; this leads to the high loading rate crack growth initiation toughness K_{Id}, which is analogous to K_{Ic}.

The use of K_{Ia} as a material property is based on the assumption that it is uniquely related to the minimum value of fracture toughness as a function of crack speed. This assumption is supported in the K_{Ia} measurements that have been reported by Crosley and Ripling (1975). But, because inertia effects are neglected, Hahn, et al. (1975-76) have argued that K_{Ia} cannot be a true material property

and will instead be a function of the stress-intensity factor at the onset of rapid crack propagation and of the test piece geometry.

A more correct viewpoint for crack arrest is based on an extension of LEFM to the dynamic case. This delineates the role of a fundamental dynamic toughness parameter K_{Id}; there is evidence that $K_{Id} = K_{Id}(\dot{a})$ where $\dot{a}$ denotes the instantageous crack propagation speed.

The emphasis in this section is on the measurements and analyses associated with the K_{Id} parameter. Such measurements are made with impact tests of various kinds. It is interesting that impact tests traditionally have been used only in a qualitative fashion for the acceptance of materials to preclude fracture under various design codes. But, because such design procedures (based on tensile strength with large factors of safety) do not always suffice when flaws are present and, in addition, do not allow any flexibility to scale up the fracture resistance, they have begun to give way to quantitative procedures based on LEFM. In support of a fracture mechanics approach, more precise information has been required from impact testing.

The applicability of fracture resistance data generated by the high strain rates in impact tests may be questioned for statically loaded structures. Stress-intensity rates from 3×10^4 to 1×10^6 MN·m $^{3/2}$/s (3×10^4 to 1×10^6 ksi$\sqrt{\text{in.}}$/s), causing fracture to occur in 1 to 0.1 ms, are common in specimens under conventional impact loading rates. These relatively high rates may be several orders of magnitude higher than those encountered in engineering structures. However, catastrophic fractures of large welded structures are related to the dynamic, high-strain-rate properties of the materials. This is a consequence of the steep strain gradient that exists ahead of a sharp crack which subjects the material ahead of a running crack to quick high strain rates even at relatively moderate applied loading rates.

(2) Dynamic Fracture Initiation Testing Methods. In this subsection, the more prominent of the testing techniques used to extract dynamic crack growth initiation data on engineering materials will be briefly described. Attention will be primarily addressed to K_{Id} determination methods; but, because of the correlations that exist between the

several different parameters determined in impact tests, attention will not be limited exclusively to these. Thus, in the following, the Charpy test, the drop weight tear test, and the dynamic tear test will be discussed. The brief treatment given here is based in large part upon the extensive exposition given by Lange (1976). (See also Hertzberg, 1976.)

(a) Charpy V-Notch Test. The Charpy test is the oldest standardized impact test in general use (ASTME23-33T). The C_V energy criterion provided the first correlation between the results of a laboratory fracture test and the service performance of the material in a structure; this energy was correlated with the initiation, propagation, and arrest of fracture in the World War II Liberty ships and T-2 tankers. Fractures initiated from small flaws when the C_V energy was less than 14 J (10 ft-lb), and arrested cracks were found only when the C_V energy was more than 27 J (20 ft-lb). These correlations have been used to justify the use of a 20 J (15 ft-lb) criterion to preclude brittle fracture in all types of welded steel structures. Unfortunately, while the 20 J (15 ft-lb) criterion was found to be valid for ship steels, it is not generally useful.

Although there are several specimen designs, the most commonly used specimen today is shown in Figure IV-29; it is a 10-mm-square specimen with a notch 2-mm deep having a 0.25-mm root radius. The relatively dull notch in the standard C_V specimen is one reason the transition of a C_V energy-temperature relation is not indicative of structural performance. To improve this feature of the C_V specimen, much recent research has been conducted with fatigue-cracked C_V specimens. Fatigue cracking the C_V specimen tends to steepen the transition region and shift it to a higher temperature. But, the plane-strain measuring capability of a 10-mm section remains at $2.0\sqrt{\text{mm}}$ $(0.4\sqrt{\text{in.}}) = K_{Id}/\sigma_{Yd}$. This limitation in plane-strain measurement can be an important restriction to the characterization of the transition region of certain steels.

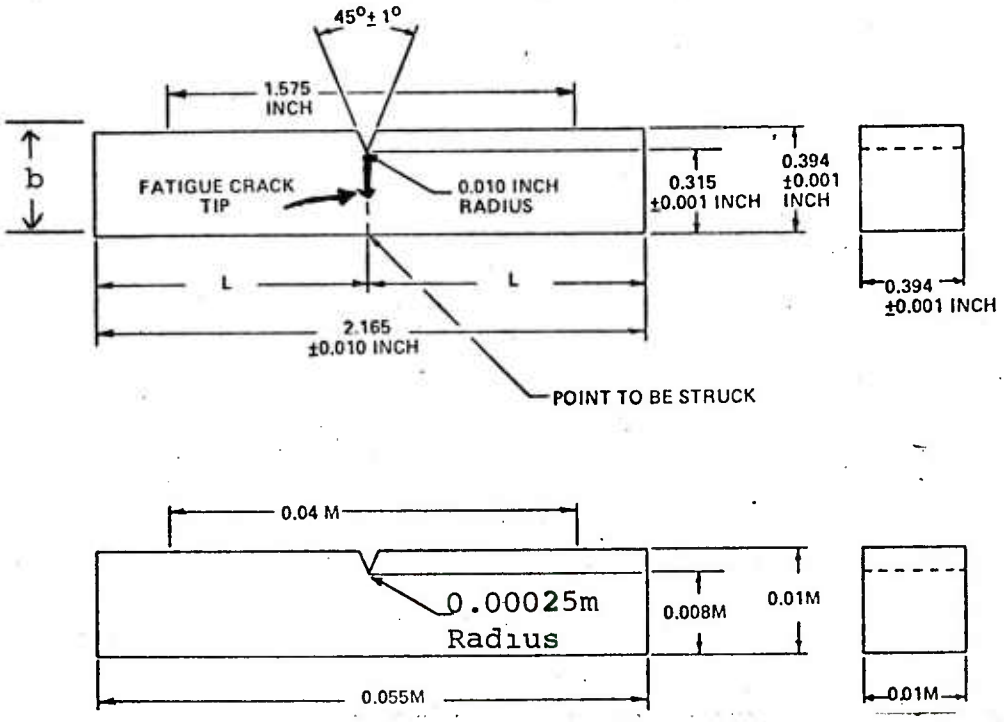

FIGURE IV-29 Geometry of Precracked Charpy Specimen

SOURCE: Ayres, 1976

The instrumented precracked Charpy test employs a Charpy V-notch specimen with a fatigue crack grown to approximately the center of the specimen. The tup or striker is instrumented so that the force on the tup is recorded as a function of time. A typical load versus time curve for a test in the brittle-ductile transition region is shown in Figure IV-30. The curve is used to determine the fracture toughness K_{Id} via the static elastic three-point bend beam relation for the static stress-intensity factor given by

$$K = \frac{6P_M}{b^2} (2\pi a)^{\frac{1}{2}} \qquad \text{(IV-25)}$$

where P_M is the maximum load recorded, b is the width of the specimen, and the crack depth a is b/2. The curve is also used to compute the elastic-plastic toughness K_{IJ} via the J-intergral by the equation (Rolfe and Barson, 1977)

$$J_{Ic} = \frac{2}{Bb}\int_{0}^{\delta \text{ fracture}} Pd\delta$$

$$K_{IJ} \equiv \left(\frac{J_{Ic}E}{1-\nu^2}\right)^{\frac{1}{2}} \qquad \text{(IV-26)}$$

where P is the load at any time, δ is the load point displacement, b is the uncracked ligament area, B is the specimen thickness, and E is the dynamic modulus of elasticity.

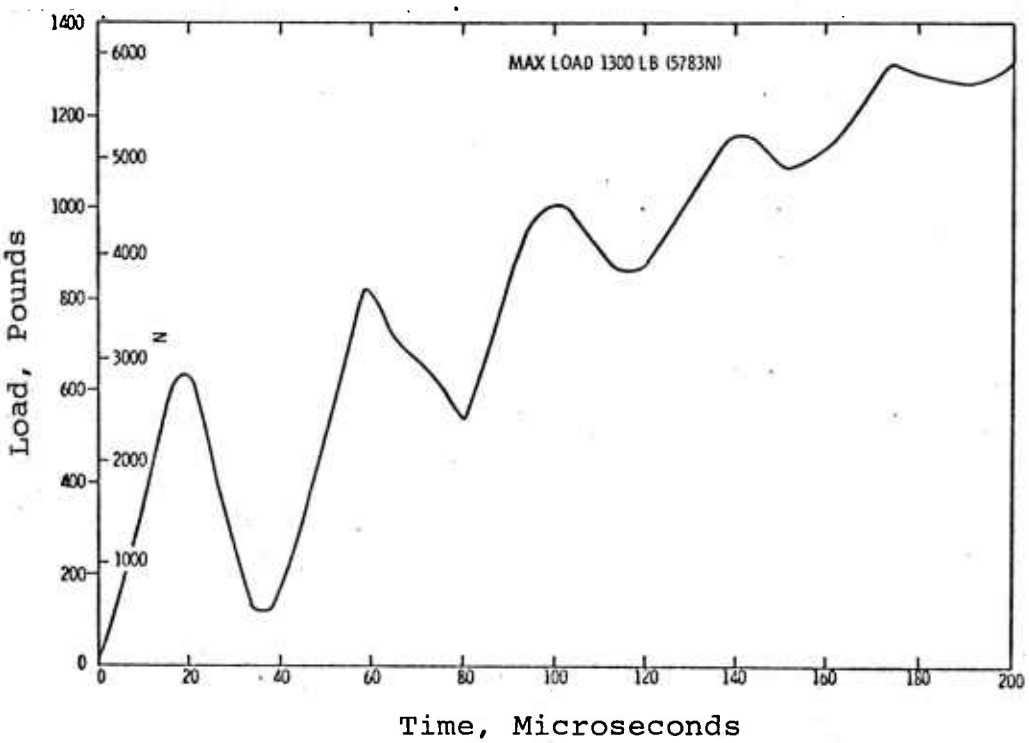

FIGURE IV-30 Load Time Curve Measured By Instrumented Precracked Charpy Test

(b) Drop Weight-Nil Ductility Transition Temperature (NDT) test. The Drop Weight-Nil Ductility Transition (NDT) Temperature Test was devised at the Naval Research Laboratory in the early 1950's (Lange, 1976). This test, currently covered by ASTM E208, was the first test to be called a Drop Weight test. The test can be used to determine the temperature at which a steel sample can plastically deform under a dynamic load in the presence of a small crack, or it can be used as a pop-in test.

The pop-in crack of the DWT-NDT specimen is formed when a brittle weld bead fractures as the specimen is loaded in a drop-weight machine. The crack from the weld bead is either arrested, or it continues to propagate across to the top surface of the specimen. If the crack does not propagate to one of the top corners of the specimen before the surface strain approaches 2 percent, the deformation is stopped by an arrestor block on the anvil and the test result is called a "no break". Specimens are subsequently tested at lower temperatures until a "break" occurs. This defines the NDT. The DWT-NDT test is, therefore, a "go--no-go" appearance test.

Another important function of the DWT-NDT test is to determine the plane-strain fracture limit for sections 16 mm (5/8-inch) thick. Because an NDT performance translates to brittle fracture initiating from a small flaw, this level of fracture resistance is $K_{Id}/\sigma_{Yd} = 2.5\sqrt{mm}$ $(0.5\sqrt{inch})$. Service experience has shown that when the steel in a welded structure has a fracture resistance less than this critical value, catastrophic fractures can be expected.

(c) Drop Weight Tear Test. The Drop-Weight Tear Test (DWTT), which employs an oversized Charpy specimen, is used to define the temperature transition region for ferritic steels in sections from 3.18 to 19.1 mm (0.125 to 0.75 inch). (The samples in the DWTT, and those in the DT test discussed below, are broken using pendulum or dropweight machines.) Its primary application has been to determine the temperature at which shear-type fractures occur in steel for linepipe. For many pipes, the propagation of cracks that can be initiated from a number of accidental sources will run for extended distances unless the appearance of the fracture is more than 80 percent shear. Although this criterion indicates the performance of some line pipes, the test and its

fracture appearance criterion do have general application for establishing the transition region for many steels in thin sections. A correlation between Charpy energies and DWTT energies for these materials, obtained by Wilkowski and reported by Popelar, et al. (1977), is shown in Figure IV-31.

When a conventional steel having a yield strength under 827 MPa (120 ksi) is used in sections less than 16 mm (5/8-inch) thick, the transition in fracture resistance tends to be restricted to a narrower range of temperatures than when the same steel is rolled to a thicker gage. Therefore, for many structural applications, a fracture appearance criterion is all that is needed to predict a brittle or ductile performance.

Fracture resistance rises so sharply in thin sections that a 50 percent shear temperature criterion is a very readily determined and unambiguous parameter for predicting service performance when a full-section specimen is used.

The DWTT is not a test for generalized use. It cannot be used to establish fracture resistance quantitatively at upper shelf temperatures or to elevate transitions for steels that do not undergo a sharp transition in fracture appearance. Energy measurements from the DWTT are not meaningful when the small notch causes the ligament to deform plastically prior to fracture even when the fracture is brittle. Although the test has its limitations, it is useful for determining the temperature transition region for plain carbon and low-alloy steels in sections thinner than 19 mm (3/4-inch).

(d) Dynamic Tear Test. The Dynamic Tear Test (DT) also uses an oversized Charpy specimen; the notch is deeper than in the DWTT and is embedded within a titanium embrittled electron beam weld. It was developed to fill the need for a practical test that could precisely measure fracture resistance over a broad range, including that encountered in the transition region of the ferritic steels. For practical reasons, the specimen is not instrumented, and the total energy used to fracture a specimen is the criterion of fracture resistance. This empirical value of fracture resistance, DT energy, is translated into structural parameters by correlation with an analytical parameter or with specific structural performance.

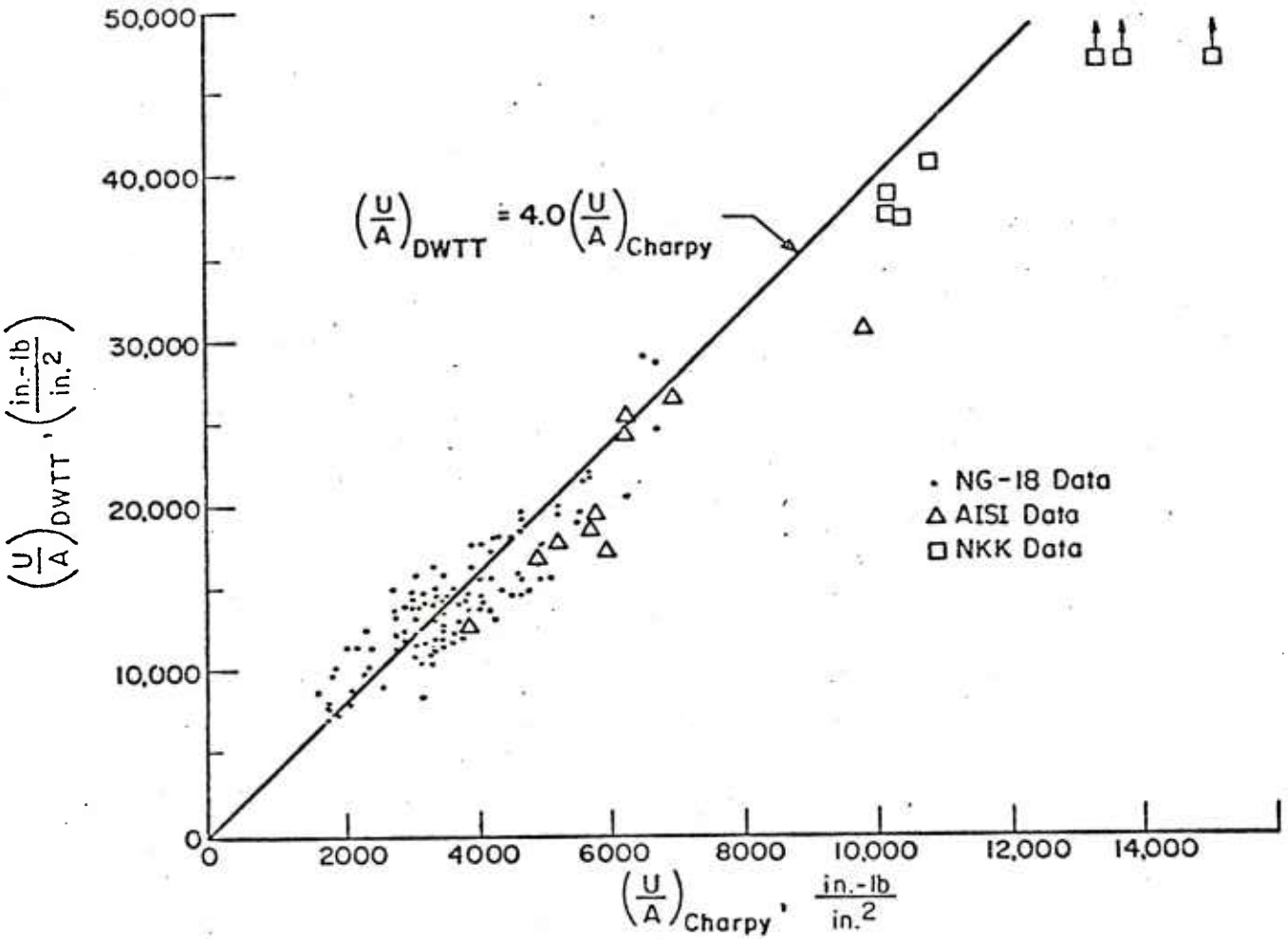

FIGURE IV-31 Correlation Between Absorbed Energy in the Drop-Weight Tear Test and the Charpy Upper Shelf Energy for Pipeline Steels

SOURCE: From Wilkowski as reported by Popelar et al, 1977

The primary intent in developing the DT test was not to develop an inexpensive K_{Ic} or K_{Id} test, but to provide a sensitive and reliable fracture-resistance criterion for the elastic-plastic and plastic regimes. Although the DT energy criterion is empirical, it has correlated very well with K_{Ic} values for various steels, titanium, and aluminum alloys. The correlations cover a sufficiently broad range of alloys in each base metal to justify the development of generalized diagrams for structural analysis. The diagrams are called Ratio Analysis Diagrams where, by a simple graphical procedure, a DT energy value can be translated into a K_{Ic}/σ_Y value or a critical flaw size.

When practical, the DT test uses a full-thickness specimen so that the crack tip constraint in the specimen is the same as that in the structural element of interest. Obviously, this is not very practical when thick sections are involved. So, extensive studies have been conducted to establish procedures to compensate for the effect of specimen size. These studies have included tests on 12-inch-thick sections, and have led to methods for extrapolating DT energy values obtained with a subsize specimen to full-section structural performance.

A correlation between K_{Id} and DT energy for the conventional structural steels remains in the developmental stage. These materials are strain-rate sensitive, and this characteristic has always complicated attempts to measure their fracture resistance properties in terms of K_{Id}. If conditions are such that fracture initiates by clevage, then the fracture resistance is low; if the fracture initiates by microvoid coalescence, then the fracture resistance is high. Therefore, the fracture mode must be consistent for the two test methods or correlation cannot be developed. In addition, the strain rates associated with impact testing are sufficient to cause complex bending waves in the specimen, which makes the analysis of K_{Id} tests quite difficult. Until more direct K_{Id} determinations are made, correlations between K_{Id} and DT energy will be of limited significance.

A correlation between K_{Ic} and DT energy was developed with high-strength steels that were not sensitive to strain rate. The initial relationship, which was developed with wrought products, was later substantiated by data using high-strength cast steels. The data from the study on cast

steels are shown plotted on the original relationship developed with wrought steels in Figure IV-32. The correlation extends to a K_{Ic} value of 110 MPa $\sqrt{m}$ (100 ksi $\sqrt{inch}$), where the 16-mm (5/8-inch) DT specimen becomes substantially plastic and the DT energy increases at a more rapid rate than does the plane-strain parameter for fracture toughness.

(e) Precracked Tension Bar. A test method has been developed by Costin et al. (1977) for accurately establishing the dynamic fracture initiation properties of structural metals at extremely high loading rates. (Although this method is new, it is included here because of its potential usefulness.) The apparatus, which is shown in Figure IV-33, is an adaptation of the Kolsky pressure bar (split-Hopkinson bar) in which a one-inch diameter round bar specimen with a pre-fatigued circumferential notch is loaded to failure by the rapidly rising tensile pulse resulting from an explosive detonation. Using the standard Kolsky technique, the average stress at the fracture site is measured as a function of time. Crack opening displacement is measured by optical

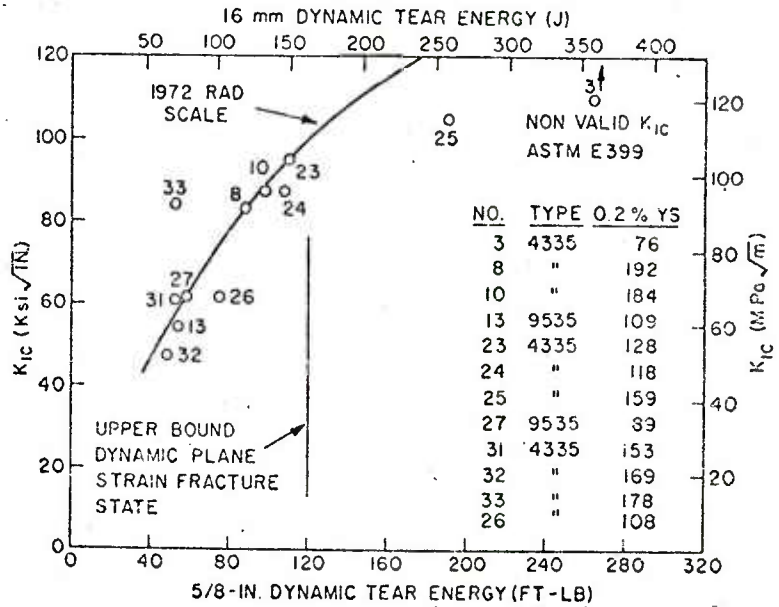

FIGURE IV-32 Correlation Between K_{Ic} and 5/8 DT Energy for High-Strength Wrought and Cast Steels

SOURCE: Lange, 1976

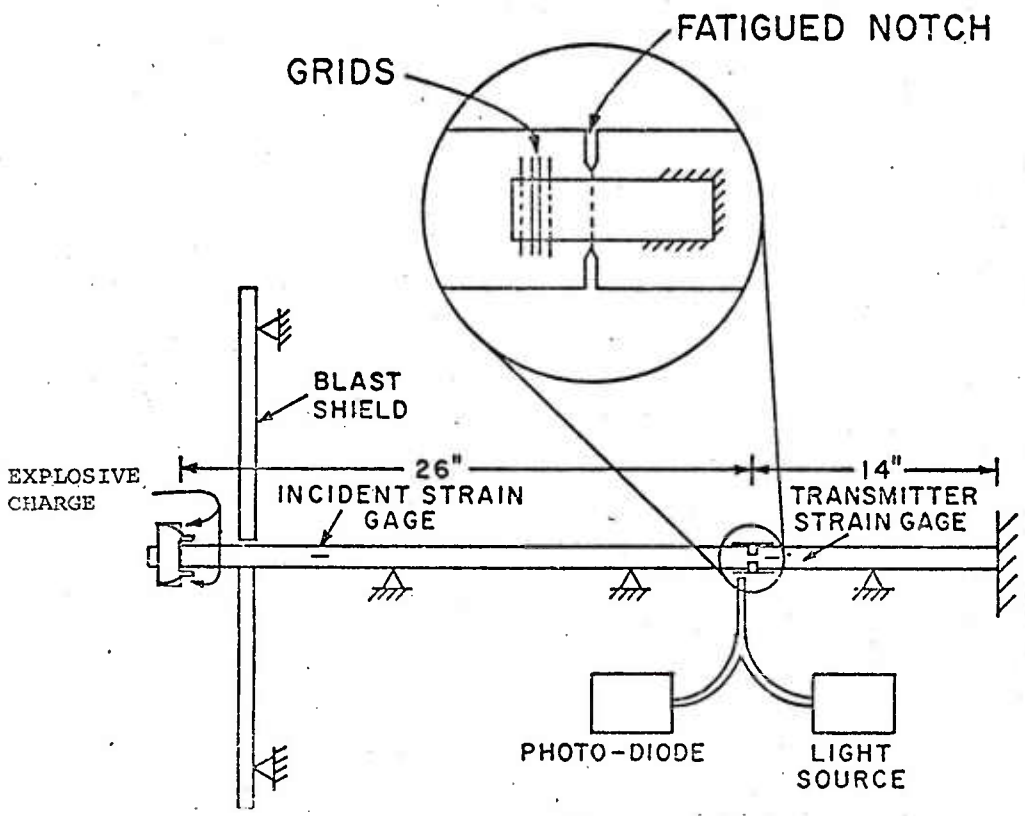

FIGURE IV-33 Schematic Diagram of Apparatus

SOURCE: Costin et al, 1977

means, as a function of time, thus yielding a complete load-displacement record for each test. From the data the critical value of the crack tip stress intensity factor, K_{Id}, at loading rates, $\dot{K}_I$, in excess of 10^6 MPa$\sqrt{m}$ /s (10^6 ksi$\sqrt{in}$/s) may be obtained. This is nearly two orders of magnitude faster than has been achieved by other standard techniques.

Analysis of the apparatus indicates that when the pulse length is long compared to the notch width, the loading of the notched section may be viewed as quasi-static. Thus, determination of fracture parameters may be accomplished by using the local load-displacement record in conjunction with existing formulas. Costin et al. (1977) employ the standard static relation

$$K_I = \frac{P}{\pi R^2} \sqrt{\pi R}\ F \qquad \text{(IV-27)}$$

when the plastic zone is very small; in Equation IV-27, P = load, R = radius of remaining circular ligament, F = function of R/D, where D is the outside diameter of the bar. They use the J-integral when the yield zone is not small compared to R.

(3) Effect of Specimen Inertia on Dynamic Fracture Initiation. Dynamic analysis of the initiation of crack growth under impact loadings generally requires the use of numerical methods. The finite element method, discussed in Section B.6, is currently being used by several investigators. The power and flexibility of the finite-element method can be economically and effectively increased by the development of special crack-tip elements with an embedded characteristic crack-tip stress singularity. Such elements are now popularly called cracked finite elements.

Results obtained with a model of an instrumented precracked Charpy specimen by Anderson, et al. (1975) are shown in Figure IV-34. Most investigators have assumed failure of the specimen occurs when the peak load develops. The peak load is then used in a static analysis of a three-point bending specimen to estimate the value of K_I at which the crack begins to grow; as an example, this value is shown as K_I (static) in Figure IV-34. In some cases the static

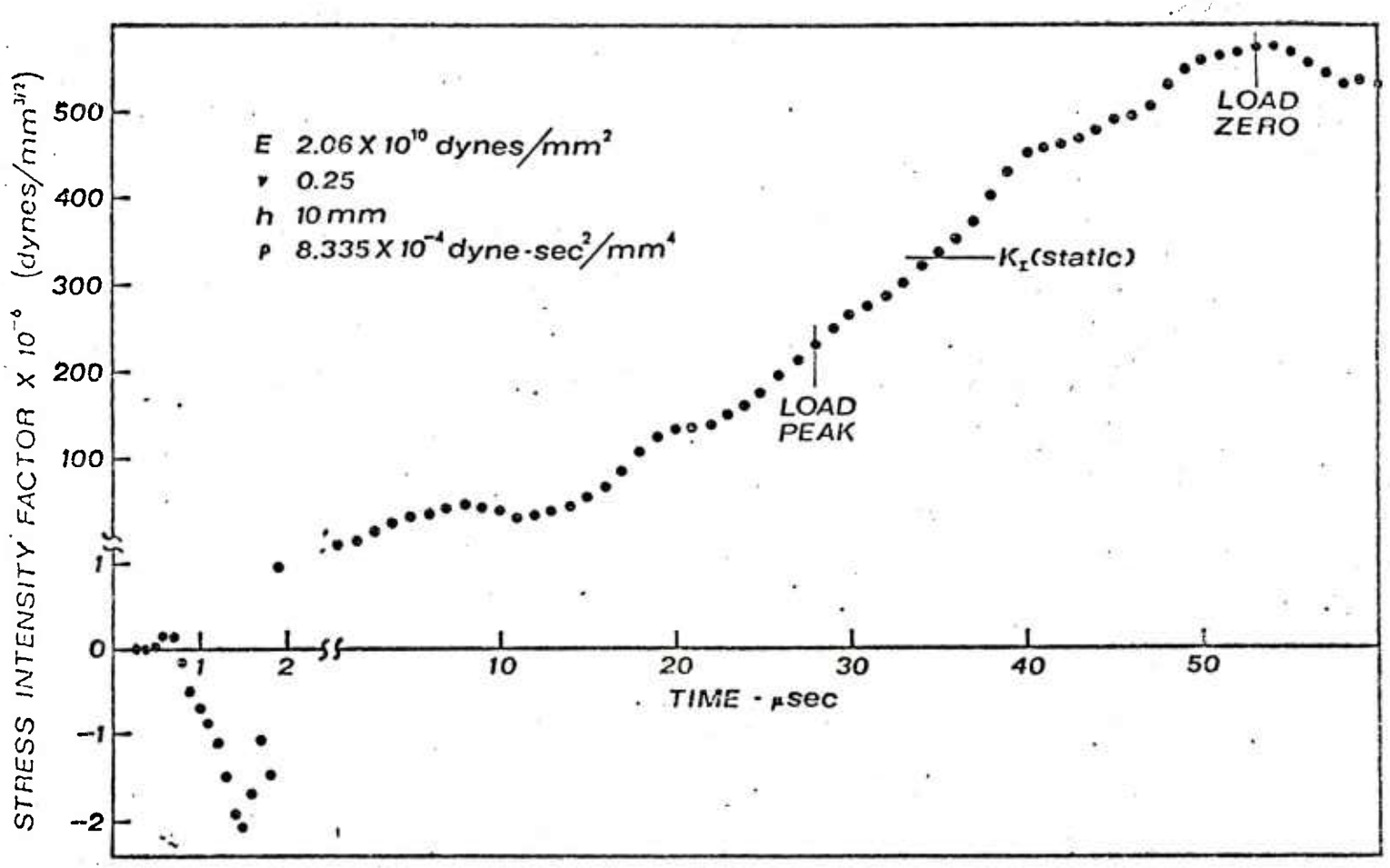

FIGURE IV-34 Calculated Stress-Intensity Factor Values in a Charpy Specimen

SOURCE: Anderson et al, 1975

value turns out to be twice the true critical stress-intensity factor K_{Ic} for static loading, and this leads to the erroneous conclusion that the material has a dynamic toughness about twice as great as the static toughness. Figure IV-34 shows that this is very likely not the case. At the time that the load peaks (less 3μ seconds for signal travel time). K is about 180 x 10^6 dynes/$mm^{3/2}$ which is not twice the static toughness for mild steel, but it is nominally about equal to it. This rather dramatically points out the significance of inertia effects in fracture specimens when the loads are applied suddenly. The initial dive to negative values of K_I just after impact, which is exhibited in Figure IV-34, is an indication of just how sensitive the dynamic cracked element is to wave phenomena. Until the compressive wave passes through the thickness and is reflected off the back side, the tendency of the crack will be to close.

(4) Material Property Data for Dynamic Crack Growth Initiation. Krafft, et al. (1970) calculated the K_{Id} values shown in Figure IV-35 from unnotched tensile properties measured at high strain rates using a theoretical relation between K_{Id} and yield stress. Since then, direct measurements of K_{Id} have been reported for a number of steels for loading rates, $\dot{K}$, up to about 10^5 to 10^6 MPa$\sqrt{m}$/s. These rates are the upper limits of the experiments and the analyses that have been used in the Krafft, et al. studies. It is of interest to note that a different test method has been suggested by Shockey and Curran (1973) which might be able to provide K_{Id} data at $\dot{K}$ of 10^8 to 10^9 MPa$\sqrt{m}$/s.

K_{Id} data for several low to medium strength steels have been obtained by Shoemaker and Rolfe (1971). K_{Id} values for an A533B steel (HSST Plate 02) have been measured by Shabbits (1970) at a series of temperatures and loading rates. Crosley and Ripling (1975) also obtained K_{Id} values on this same material during the course of their crack arrest testing. In addition, K_{Ic} values are also available for this material from the work of Shabbits (1970) and from J-integral and equivalent energy tests. All of these data for this heat of A533B steel are summarized in Figure IV-36. It indicates a rather small rate effect at low temperatures, but a fairly large effect at higher temperatures.

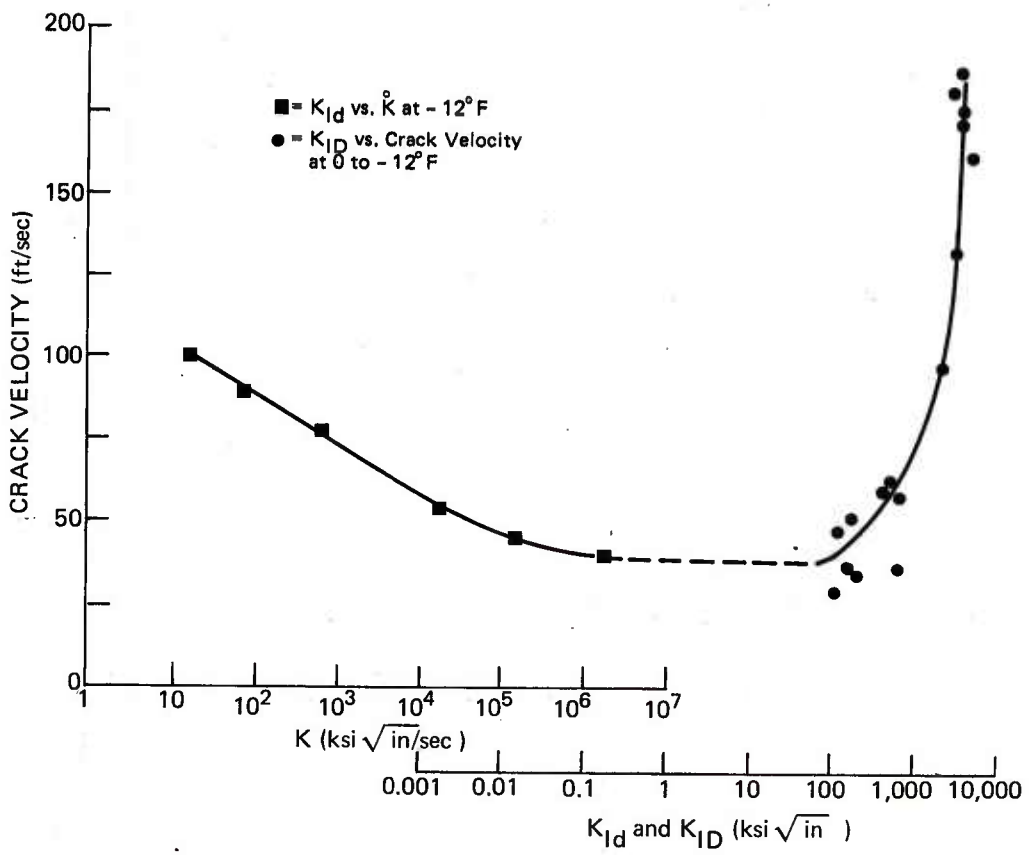

FIGURE IV-35 K_{Id} Versus Loading Rate, K, and K_{ID} Versus Crack Velocity for a C-Mn Steel Derived by Eftis and Krafft (1965). (Note positioning of horizontal scale is based only on a highly approximate model relating K and crack velocities.)

The trend observed from these investigations is a generally inverse relationship between sensitivity to loading rate effects and room temperature yield strength in ferritic steels; i.e., as noted in Section B.2, the effects are most pronounced in low strength steels. Barsom (1975), for example, concludes that the sensitivity essentially disappears in steels with room temperature yield strength above 140 ksi.

The fracture toughness of nuclear pressure vessel steels is observed to be loading rate sensitive in the region where valid LEFM toughness values have been measured.

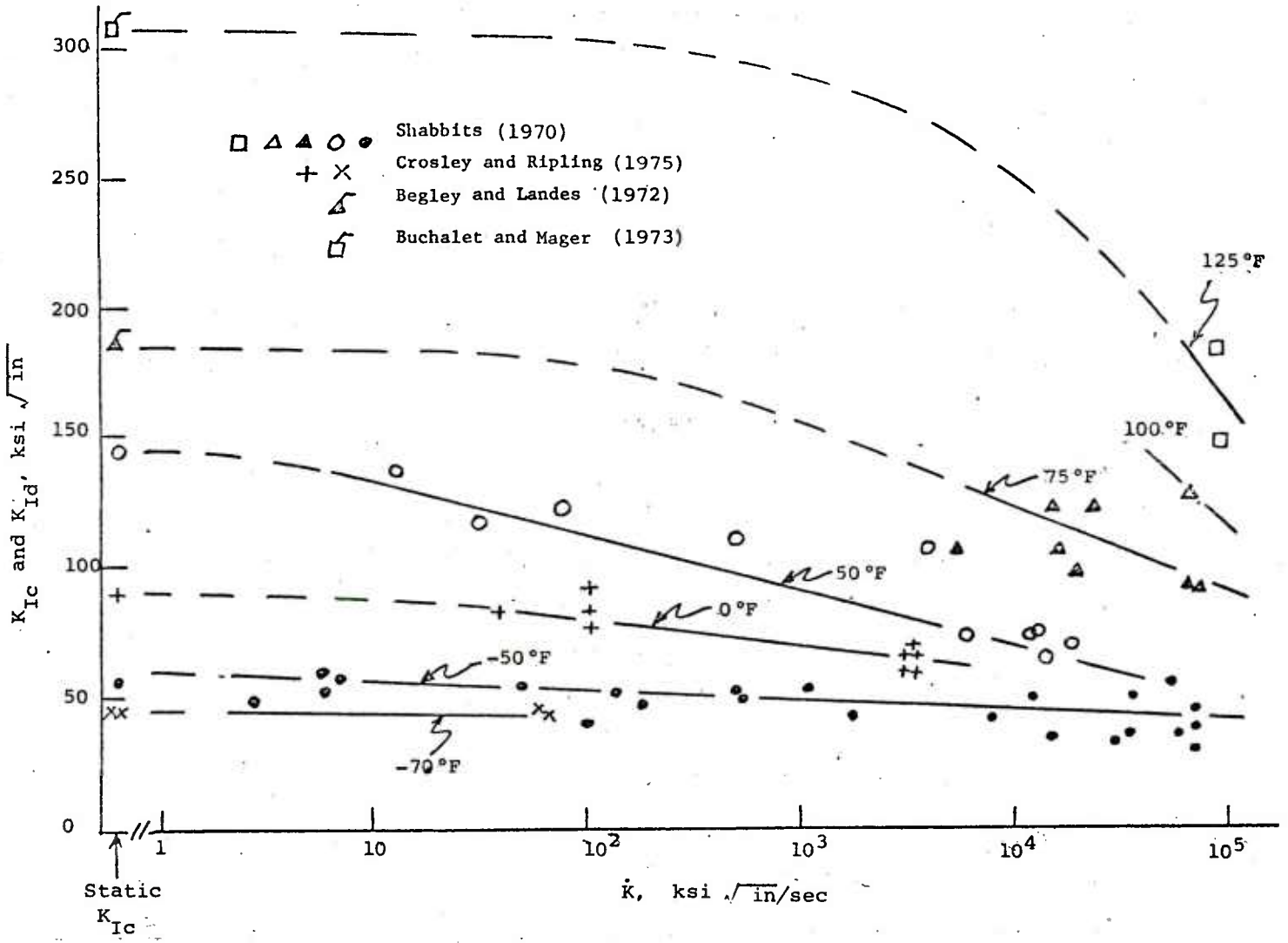

FIGURE IV-36 Influence of Loading Rate, $\dot{K}$, on the Initiation Toughness, K_{Id}, of A533B Steel. K_{Ic} is also shown

Experimentally, this has meant that, below the upper shelf temperature range, the toughness, K_{Id}, of a rapidly loaded specimen containing a stationary crack is less than the toughness, K_{Ic}, exhibited by the same specimen loaded statically. While the value of K_{Id} appears to initially decrease with increasing loading rate, $\dot{K}$, the presence of a minimum in the K_{Id} versus $\dot{K}$ curve has not yet been firmly established. The rising branch of the curve for high loading rates (cf. Figure IV-35) is based on calculated values of K_{Id} for propagating cracks, using an assumed relation between crack velocity $\dot{a}$ and loading rate, $\dot{K}$. The possibility does exist that K_{Id} achieves, and remains at, a minimum value for high loading rates.

There is some evidence, based on a comparison of Charpy V-notch slow bend and impact energy curves, that the dynamic and static fracture toughness curves, for loading rate sensitive materials, may cross in the upper shelf temperature range. (An example of this behavior, for total energy absorbed with A302B steel, is shown in Figure IV-37.) If such is the case, then the propagation resistance of loading rate sensitive materials may increase monotonically with crack speed in the upper shelf temperature range, thus initially favoring slow stable crack growth instead of rapid crack propagation, at these higher temperatures.

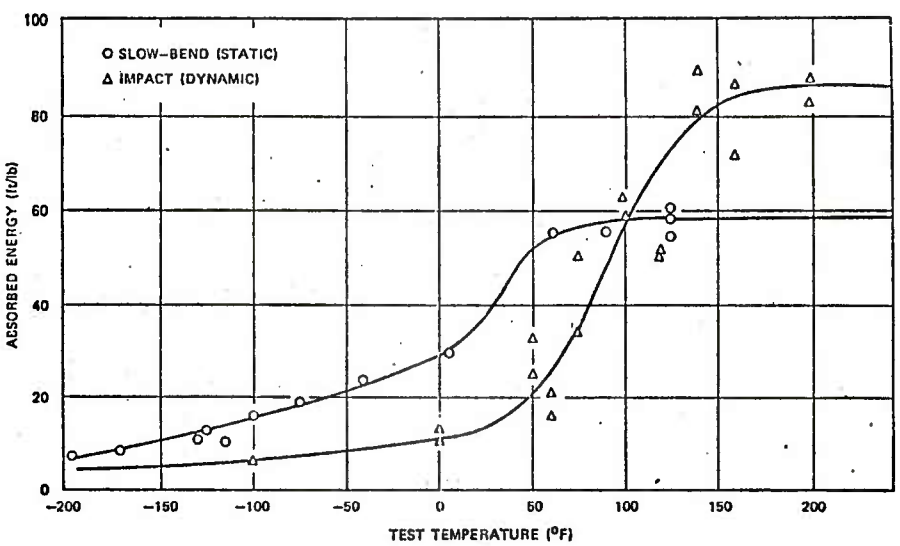

FIGURE IV-37 Slow-Bend and Impact Charpy V-Notch Test Results for A302B Steel

SOURCE: Rolfe and Barsom, 1977

Since an experimental technique is not available for detecting the onset of crack growth initiation in most dynamic tests, it is generally assumed that it occurs at maximum load. Thus, to calculate energy-based parameters, the energy to maximum load is used. It is recognized that, if the crack initiates before maximum load, the elastic-plastic values generated in this way will exceed the actual K_{Id} values for the material and, therefore, they must be accepted cautiously.

d. Rapid Unstable Crack Propagation and Crack Arrest

(1) Dynamic LEFM Concepts. The problem of determining the crack length-time response of a rapidly propagating crack is of great concern in several different kinds of engineering structures. These structures have in common the feature that unchecked unstable crack growth would have catastrophic consequences. They include aircraft, nuclear pressure vessels, bridges, gas transmission pipelines, and ship hulls, to cite only a few of those for which research has been specifically addressed.

Although many actual problems may require more complicated elastic-plastic treatments, the process of rapid unstable crack propagation and arrest in structures currently can be discussed only in terms of linear elastic fracture mechanics concepts and parameters. A dynamic extension of LEFM recognizes four energy categories: elastic strain energy, kinetic energy, work done by applied forces, and the energy dissipated by crack tip flow and fracture processes. The first three of these depend on elastic properties, the crack length, the applied loads, and the geometry of the body containing the crack. The net change in these three components, per unit area of crack extension, is called the dynamic energy-release rate, or, equivalently, the driving force for crack extension. Giving this the symbol G, then

$$G = \frac{1}{b}\left\{\frac{dW}{dt} - \frac{dU}{dt} - \frac{dT}{dt}\right\}\left(\frac{da}{dt}\right)^{-1} \qquad \text{(IV-28)}$$

where U is the strain energy, T the kinetic energy, W the

work done on the structure by external loads, a is the crack length, and b is the plate thickness.

Two differences exist between the evaluation of G in the static case, (cf. Equation IV-16), and for a fast propagating or arresting crack. First, a kinetic energy term is present. Second, U, T, and W must be evaluated from fully dynamic analyses; i.e, inertia forces explicitly included in the equations of motion for the structure.

The energy dissipated per unit area of fracture is called the fracture energy R. This expresses the resistance to cracking. The fracture energy is a material property essentially independent of the geometry and applied loads. It is, in fact, a basic postulate of LEFM that all inelastic irreversible energy dissipation processes that accompany crack extension can be included in a single material property that is possibly a function of the instantaneous crack speed, but is independent of the crack length, the applied loads, and the external geometry of the body. The extent to which this is true really determines the applicability of LEFM.

A crack extension criterion follows from the principle of energy conservation. That is, the energy-release rate must be balanced by the fracture energy for the crack to propagate. This statement means that the initiation of growth of a stationary crack and the continued propagation of a moving crack are only possible when $G = R$. Conversely, initiation of crack growth is precluded--and, for a propagating crack, arrest must take place--when $G < R$ for all values of R.

Note that the condition where G exceeds R is not possible because it would violate the energy balance principle. The stationary crack inequality does not violate the energy balance because the basic energy balance is actually Equation IV-28 multiplied by $\dot{a}$. Note also that in LEFM the fracture energy for the extension of a stationary crack due to slowly applied loads, designated as G_c, corresponds to a critical value of the static energy-release rate.

The arrest of a rapidly propagating crack in a structure under load can be considered on several different levels of complexity. Starting from the simplest (and least accurate) and continuing with more complicated and more accurate approaches, the various types can be classified as either a:

- Static or quasi-static analysis

- Infinite medium dynamic analysis
- Fully dynamic analysis

The primary distinction that differentiates between static and dynamic approaches is that specimen inertia terms and the contribution of kinetic energy to the crack-driving force equation are excluded in the former. Physically, this means that static or quasi-static theories are limited to situations where (1) the loading is static or applied slowly, (2) the crack propagates slowly and it (3) changes speed only gradually. As the extensive work done at Battelle (Hahn, et al., 1975-1976) and other facilities has shown, the arrest of rapid crack propagation tends to occur rather abruptly. This alone indicates that statically based treatments must be applied to crack arrest with due caution. Quantitative results reinforcing this idea have also been produced.

The distinction between the two dynamic analysis procedures lies in the particular specialization that is involved for simplification. By considering the structure to be an infinite elastic medium, the effect of stress waves reflected back to the propagating crack tip from the boundaries of the structure and/or from internal load points and discontinuities (e.g., welded-on stiffeners) are neglected. These effects are taken into account in a fully dynamic analysis, albeit for practical reasons at the expense of specializing the structural geometry under consideration.

(2) Dynamic Crack Propagation Analysis Methods.

(a) Basis of Dynamic Crack Propagation Analyses. There is currently no universally accepted theoretically-based design approach to ensure crack arrest. A static approach (or, what amounts to the same thing, the "arrest toughness", K_{Ia}, approach) is not generally valid. This statement is based upon a body of experimental results together with a rigorous energy-based method of anlaysis that has shown that crack arrest is a dynamic process that must be treated within the context of a dynamic fracture mechanics theory. This work includes the generalizations of the static approach discussed above.

One purpose of this subsection of the report is to demonstrate that statically based analyses can dangerously

overestimate the capacity of a structure to arrest a rapidly propagating crack. It will be further shown that even analyses taking full account of the essential aspects of dynamic fracture mechanics can still be inadequate for predicting crack arrest when other vital features of the problem are neglected. In particular, the otherwise admirable analyses of Freund (1972, a, b) cannot cope with stress waves reflected back to the propagating crack tip from the specimen boundaries. This feature is not only important for experimental work carried out using small laboratory size test specimens, but might also be important in analyzing other mechanical crack arrest devices.

It is a fact that the arrest point determined from either a static, a quasi-static, or an infinite medium dynamic treatment will always be closely related and, in some cases, will be exactly the same. Consequently, for the purpose of this report, it will suffice to describe the most accurate of these with a view toward contrasting its crack arrest predictions with those of a fully dynamic calculation.

(b) Crack Propagation in an Infinite Medium. A very elegant analysis of the propagation of a semi-infinite crack in an infinite medium is that given by Freund (1972, a,b; see also Freund (1976)). Using a Laplace transform in conjunction with the Wiener-Hopf Technique, Freund has solved the equations of motion for a half-plane crack propagating in an unbounded medium for a fairly unrestricted class of crack motion. A key result of the analysis relates the dynamic stress intensity factor K, which is a function of instantaneous crack length a and speed $\dot{a}$ to the product of the static intensity factor K_s and a universal function $k(\dot{\alpha})$ of instantaneous crack speed relative to the elastic wave speeds according to

$$K(a,\dot{a}) = k(\dot{a})\ K_s(a) \qquad \text{(IV-29)}$$

The function k decreases monotonically from unity at zero crack speed to zero at the Rayleigh wave speed. The quantity K_s is a "static" factor in that it corresponds to zero crack speed; however, K_s may result from dynamic loading of the type described by Freund (1976).

A second key result obtained by Freund is one that relates the dynamic energy-release rate to the opening-mode dynamic stress-intensity factor. For plane strain conditions, this is

$$G(a,\dot{a}) = \frac{1-\nu^2}{E} B(\dot{a}) K^2(a,\dot{a}) , \qquad \text{(IV-30)}$$

where B is also a geometry independent universal function of the crack speed relative to the elastic wave speeds. In contrast to k, it is a monotonically increasing function which is unity at zero speed and becomes unbounded at the Rayleigh speed.

It is important to recognize that Equation IV-30 is valid for arbitrary geometries and time-variation of crack speed (Freund, 1976). As a result, it is possible to use the idea of dynamic fracture toughness $K_D = K_D(\dot{a})$ interchangeably with an intrinsic material energy dissipation rate, $R(\dot{a})$, (also called "specific fracture energy" or simply "fracture energy"). That is, let us define $K_D(\dot{a})$ through the equation

$$R(\dot{a}) = \frac{1-\nu^2}{E} K_D^2(\dot{a}) . \qquad \text{(IV-31)}$$

Then, by equating R and G there results

$$BK^2(a,\dot{a}) = K_D^2(\dot{a}) , \qquad \text{(IV-32)}$$

which serves as the crack propagation criterion; i.e., as an equation for predicting a and $\dot{a}$. It is also found from Equations IV-29 and IV-32 that

$$K_s^2(a) = K_D^2(\dot{a})/g(\dot{a}) , \qquad \text{(IV-33)}$$

where $g \equiv Bk^2$ is also a universal function of instantaneous crack speed. The function $g = g(\dot{a})$ can be interpreted as

the ratio of the dynamic to the static energy release rates.

In order to apply Equation IV-33 to investigate crack arrest, an explicit relation for the function $g(\dot{a})$ is needed. In Freund's analysis, a numerical integration was used to determine this function. His prediction reveals that the function $g = g(\dot{a})$ is more than adequately expressed by the simple relation

$$g(\dot{a}) = 1 - \frac{\dot{a}}{C_R} \qquad \text{(IV-34)}$$

where C_R denotes the Rayleigh wave speed. Then, by substituting Equation IV-34 into Equation IV-33, the equation of motion for the crack tip becomes

$$K_s(a) = K_D(\dot{a}) \left[1 - \frac{\dot{a}}{C_R}\right]^{-\frac{1}{2}} \qquad \text{(IV-35)}$$

The next step is to introduce a relation for K_s for the geometry of interest. Given $K_D(\dot{a})$, Equation IV-35 can then be solved iteratively for the crack speed as a function of crack length. Bu numerically integrating this result, the crack length can be obtained as a function of time for comparison with results computed with a fully dynamic approach. This comparison is made below.

A propagating crack will arrest when (and only when) Equation IV-33 can no longer be satisfied. Suppose the right-hand side of Equation IV-33 possesses one minimum point and that it occurs at the speed a_M (which may be zero). Then, the arrest occurs at the crack length a_r, as calculated from

$$K_s^2(a_r) = K_D^2(\dot{a}_M)/g(a_M) \quad . \qquad \text{(IV-36)}$$

Equation IV-35 shows that if $\dot{a}_M/C_R << 1$, crack arrest occurs at the speed for which K_D is a minimum; viz

$$K_s(a_r) = K_{D,\ min} \qquad \text{(IV-37)}$$

(c) An Analysis Procedure for the DCB Test Specimen. A laboratory test specimen that has been used effectively by Hahn, et al., (1975-1976) is the double cantilever beam (DCB) specimen (cf. Figure IV-40). A model for predicting dynamic crack propagation in the DCB specimen has been given by Kanninen (1974). The starting point for the derivation is the equations of the theory of elasticity with inertia terms included. Because the peculiar "beam-like" geometry of this specimen can be exploited, only four equations need to be explicitly considered. These are the two equations for motion along the length of the beam (the x direction) and normal to the crack plane (the z direction) and two Hooke's law equations. The two equations of motion are given by

$$\frac{\partial \sigma_x}{\partial x} + \frac{\partial \tau_{xy}}{\partial y} + \frac{\partial \tau_{xz}}{\partial z} = \frac{\partial^2 u_x}{\partial t^2} \qquad \text{(IV-38)}$$

and

$$\frac{\partial \tau_{xz}}{\partial x} + \frac{\partial \tau_{yz}}{\partial y} + \frac{\partial \sigma_z}{\partial z} = \rho \frac{\partial^2 u_z}{\partial t^2} \quad . \qquad \text{(IV-39)}$$

The two constitutive or Hooke's law equations that enter into the analysis are given by

$$E\frac{\partial u_x}{\partial x} = \sigma_x - \nu(\sigma_y + \sigma_z) \qquad \text{(IV-40)}$$

and

$$\frac{\partial u_x}{\partial z} + \frac{\partial u_z}{\partial x} = \frac{\tau_{xz}}{G} \quad . \qquad \text{(IV-41)}$$

In the above equations, E, G, ν, and ρ denote Young's

modulus, the shear modulus, Poisson's ratio, and the density, respectively; u_x and u_z are displacement components; σ_x, σ_y, σ_z, τ_{xy}, τ_{xz}, τ_{yz} are stress components; and t denotes time. The simplification that can be introduced to make the mathematical analysis more manageable is made by introducing cross-sectionally averaged dependent variables into the analysis. If A = A(x) is the area of the DCB specimen cross section at any axial position x, then these new variables can be obtained formally as follows. The deflection w = w(x) is

$$w = \frac{1}{A}\iint_A u_z \, dydz \quad . \tag{IV-42}$$

The rotation $\psi = \psi(x)$ is

$$\psi = -\frac{1}{I}\iint_A z u_x \, dydz \quad . \tag{IV-43}$$

By operating on Equations IV-38 through IV-41 by $\iint_A dydz$ and using the above definitions, the equations of motion for a rectangular DCB specimen in terms of the cross-sectionally averaged variables for the case of fixed displacement loading are found to be

$$\frac{\partial^2 w}{\partial x^2} - \frac{\partial \psi}{\partial x} + \frac{6}{h^2} H(x-a)\, w = \frac{3}{C_0^2}\frac{\partial^2 w}{\partial t^2} \tag{IV-44}$$

and

$$\frac{\partial^2 \psi}{\partial x^2} + \frac{4}{h^2}\left[\frac{\partial w}{\partial x} - \psi\right] - \frac{2}{h^2} H(x-a)\,\psi = \frac{1}{C_0^2}\frac{\partial^2 \psi}{\partial t^2} \tag{IV-45}$$

where h is the half-height of the specimen, b is the specimen thickness, and $C_0^2 = E/\rho$ is the elastic bar wave speed. The function H denotes the Heaviside step function which delineates the position of the crack tip (i.e., x=a).

Expressions for the strain energy and the kinetic energy of the system can be obtained in terms of the variables introduced above. Omitting the details, the resulting expression for the strain energy U is

$$U = \int_0^L \left\{ EI\left(\frac{\partial \psi}{\partial x}\right)^2 + kGA\left(\frac{\partial w}{\partial x} - \psi\right)^2 + F\psi^2 + H(x-a)\left[k_e w^2 + k_r \psi^2\right] \right\} dx \qquad \text{(IV-46)}$$

while the kinetic energy T is

$$T = \int_0^L \left\{ \rho A\left(\frac{\partial w}{\partial t}\right)^2 + \rho I\left(\frac{\partial \psi}{\partial t}\right)^2 \right\} dx \quad , \qquad \text{(IV-47)}$$

where L is the overall length of the specimen. The most important use of the strain and kinetic energy expressions is in determining the crack-driving force. This is done through the definition of the dynamic energy-release rate G in terms of an energy balance for the system as given by Equation IV-28. By substituting Equation IV-46 and IV-47 into IV-28, it is found that G can be interpreted in terms of "crack tip" values. That is

$$G = \frac{2E}{h}\left\{ w^2 + \frac{h^2}{12}\psi^2 \right\}_{x=a(t)} \quad , \qquad \text{(IV-48)}$$

where, as indicated, the bracketed quantity is evaluated at the axial position representing the current crack tip.

As will be explained below, tests in the DCB specimen are conducted by blunting the initial crack tip. This allows enough elastic strain energy to be stored in the specimen that the crack (which propagates as a sharp crack) can propagate at a high speed. The measure of the bluntness ks K_q, the "apparent" stress-intensity factor at the initiation of crack growth. An example set of computational results is shown in Figures IV-38 and IV-39 for the case

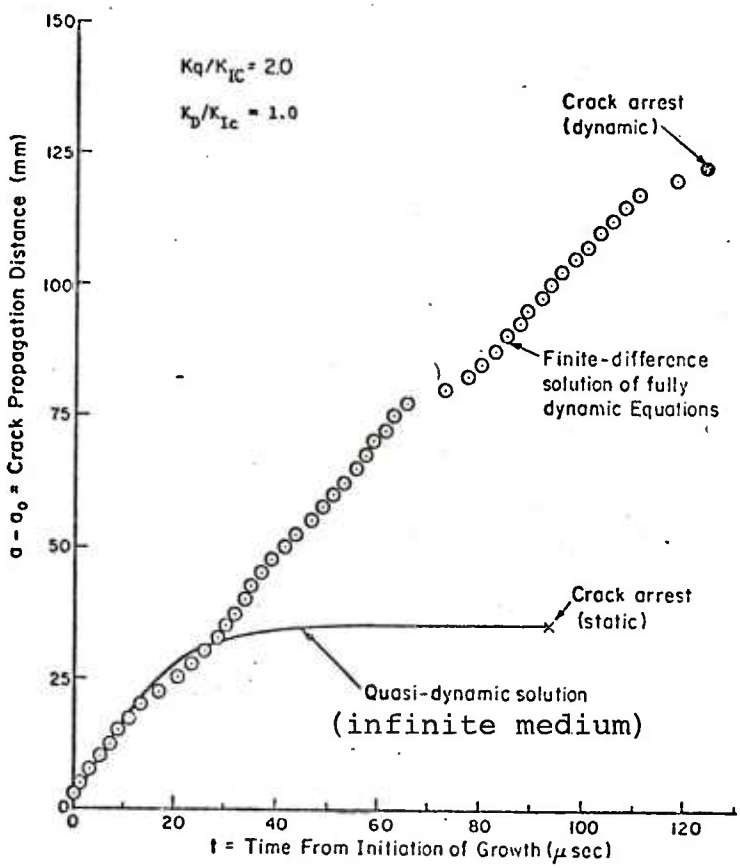

FIGURE IV-38 Comparison of Crack Arrest Points Predicted by a Fully Dynamic Analysis with that of a Quasi-Dynamic Analysis for a Standard Rectangular DCB Specimen

SOURCE: Kanninen et al, 1977

where $K_q = 2K_{Ic}$ and $K_D = K_{Ic}$.

It can be clearly seen in Figure IV-38 that the crack arrest point given by the solution for an infinite medium is considerably underestimated. That is, while the fully dynamic theory coincides with the infinite medium solution until the time of the first stress wave reflection (approximately 30 μ sec in this example), sizable differences can be seen thereafter.

Consideration of the results shown in Figure IV-39 reveals that a statically calculated arrest point (i.e., $a - a_o = 37$ mm) is reached at about the same point that kinetic energy reaches a maximum in the fully dynamic

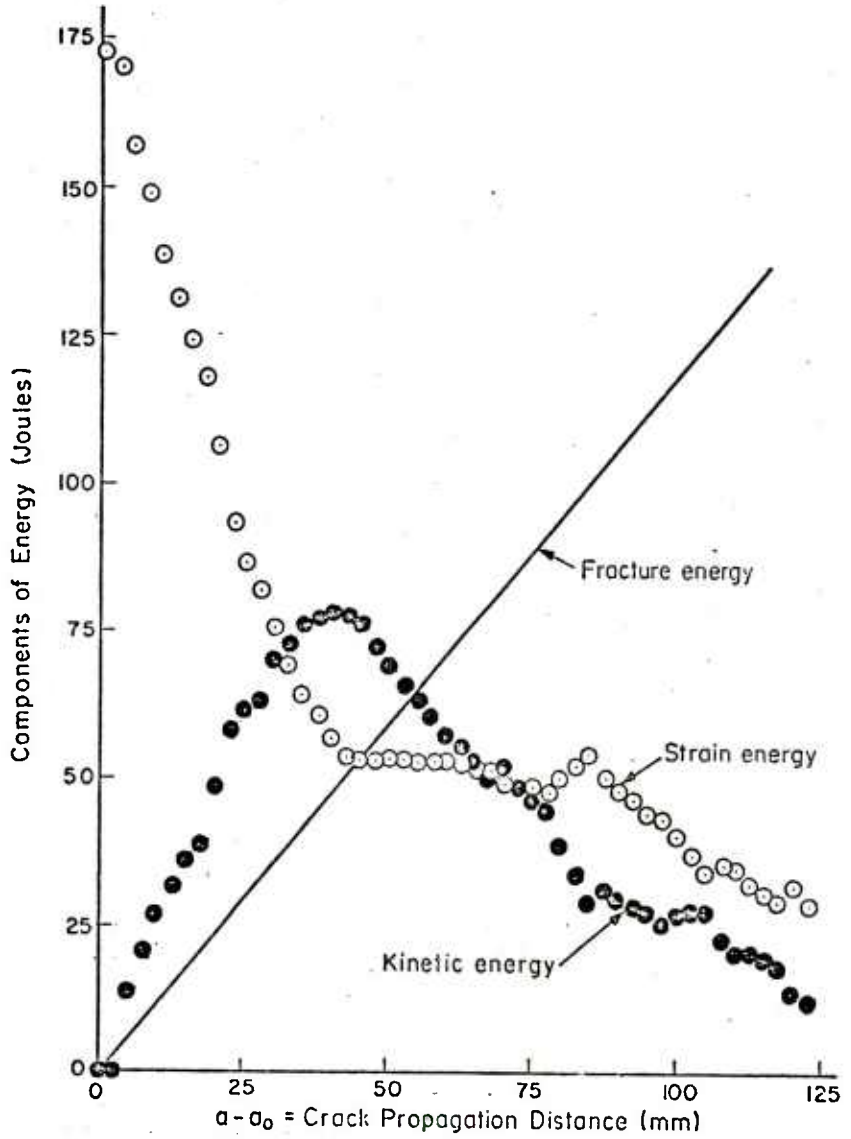

FIGURE IV-39 Distribution of Energy During Rapid Crack Propagation in a DCB Test Specimen for $K_q/K_{IC} = 2.0$ and $K_D = K_{IC}$

SOURCE: Kanninen et al, 1977

calculation. That the average rate of change of the kinetic energy is greater (negatively) than the strain energy after the maximum has been reached further shows that the kinetic energy provides the greater contribution to the crack-driving force, Equation IV-28.

In a recent analytical study by Freund (1977), the arms of the DCB specimen are assumed to deform as shear beams. This idealization yields a mathematically tractable model which predicts qualitatively correct behavior and lends itself to a simple physical interpretation of the specimen response. It is found that crack arrest occurs when the tip is overtaken by a stress wave which is set up at fracture initiation and reflects off the top end of the DCB (cf. Figure IV-40).

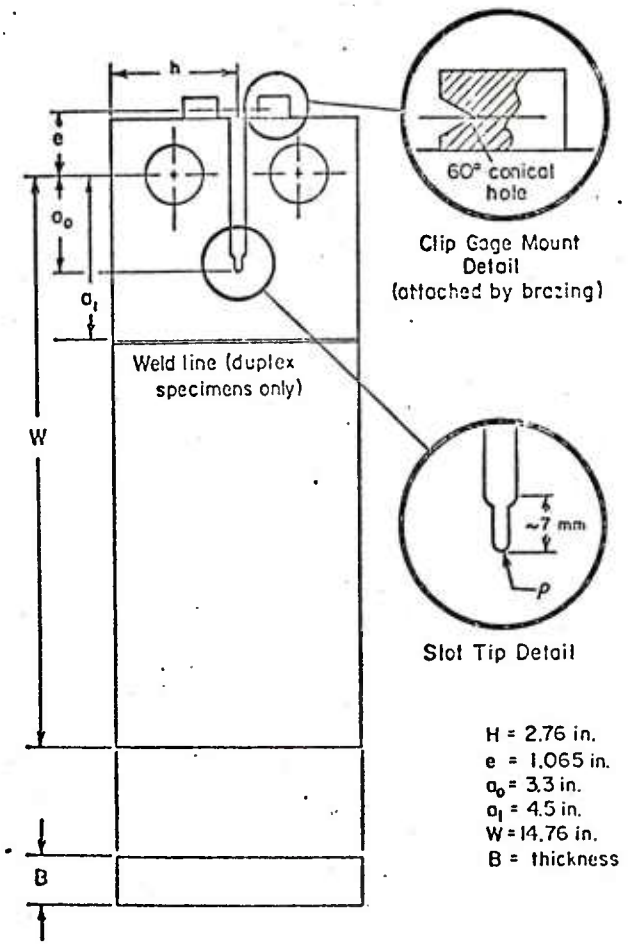

FIGURE IV-40 DCB Test Piece Configuration: Side Grooves are not Shown

SOURCE: Hahn et al, 1975-76

(3) Dynamic Crack Propagation Testing Methods. Certain problems exist in the measurement of the high levels of fracture toughness exhibited by many useful engineering materials. The reason is that the most highly developed methods for measuring fracture toughness are restricted to fractures in which plasticity is limited. Specifically, only fractures that occur under plane strain conditions or under plane stress conditions in which the plastic zone size is small relative to specimen dimensions and crack length (see ASTM-E-399-74) can be approached in this way.

As may be clear from the preceding discussion, it is necessary to distinguish among several different fracture toughness parameters. It is generally agreed that the most convenient to use in material testing work are the following:

Criterion for onset of crack extension: $K = K_c$

Criterion for continuing propagation: $K = K_D$

Criterion for crack arrest: $K < K_{D,min}$.

The plane stress values of tough materials display a modest thickness dependence, $K \sim b^n$, where b is the thickness and $0.25 < n < 1.0$. When plasticity is limited, fractures can be analyzed by the methods of LEFM to obtain plane strain fracture toughness parameters such as K_{Ic}, K_{Id}, K_{ID}, and K_{Ia}, and their plane stress counterparts with the I removed from the subscript.* However, the limited plasticity at fracture that is necessary for successful application of LEFM methods is the very antithesis of the desired behavior of tough materials where large plastic zones and significant shear lips are essential to proper performance. Accordingly, problems arise in attempting to use LEFM methods for measuring fracture toughness parameters of tough materials.

* The subscript I (i.e., G_{Ic}, K_{Ic}, G_{Ia}, K_{Ia}) is used in this subsection to distinguish energy and toughness values measured when the crack tip plastic flow is predominantly plane strain as opposed to so-called "plane stress" values which reflect significant amounts of through-the-thickness deformation.

In the following paragraphs several methods for measuring or approximating K_D values for tough steels by the methods of fracture mechanics are described.

(a) Approximating K_D Values with K_c, K_{Ic}, or J_{Ic} Measurements. When $K_{D,min}$ coincides with K_c (the K_D-value at zero velocity), static measurements of K_c can serve as a conservative estimate of K_D. The K_c-values can, in turn, be related to the plane strain K_{Ic} via a relation of the type

$$K_c = CK_{Ic} \qquad \text{(IV-49)}$$

where $1 < C < 2$. This means that K_{Ic}-values could also serve as a lower bound measure of K_D or as a way of estimating K_c provided the factor C is known. In practice, the plate size and thickness requirements for measuring K_c- and K_{Ic}-values for materials with $\frac{K_c}{\sigma_Y} > 0.2m^{\frac{1}{2}}$ are prohibitive. For example, for a steel with a yield strength $\sigma_Y = 275\ MNm^{-2}$ and $K_c = 300\ MNm^{-3/2}$, the width of a center cracked panel adequate to measure K_c is about 3m, and the thickness required to measure K_{Ic} is about 1m. More recent J_{Ic} - techniques offer the possibility of reducing the thickness requirement by an order of magnitude. Consequently, J_{Ic} - measurements may offer one practical route to the evaluation of K_D - or R values of high toughness materials. However, the path independence of the J-integral does not hold for dynamic situations. This means that the conventional interpretations may be invalid in those cases.

(b) Approximating K_D from Crack-Opening Displacement. Robinson and Tetelman (1976) have shown that K_{Ic} can be calculated from measurement of the crack-tip opening displacement δ_t (COD) at the onset of unstable fracture in relatively small specimens, using a relation that can be obtained from Equations IV-20a and IV-23b:

$$K_{Ic} = \left(\frac{\sigma_Y \cdot E \cdot \delta_t}{1-\nu^2}\right)^{\frac{1}{2}} \qquad \text{(IV-50)}$$

Methods for measuring COD are described in British Standards DD19:1972. Use of such COD techniques would then permit K_D to be approximated by this relation.

The possibility of applying COD methods to dynamic tests also exists. Actual COD measurements are difficult but, as Robinson and Tetelman have shown, COD values can be approximated reasonably well from measurements of the notch root contraction on the fractured test piece.

(c) Direct Measurement of K_{ID} or K_D with the Duplex-Double-Cantilever Beam Tests. Although several kinds of specimen geometries can be used for obtaining the data necessary to determine K_{ID} -velocity relations, the wedge-loaded DCB specimen has been predomimately utilized. (The rectangular DCB specimen and wedge-loading arrangement are illustrated in Figure IV-40.) In this specimen, the fracture is initiated with the aid of a blunt slot rather than a sharp crack. The blunted notch permits the specimen to sustain an "apparent" stress intensity factor, K_q, which is much larger than K_{Ic}. Consequently, as soon as a sharp crack emerges from the blunt notch, the crack immediately becomes unstable and propagates rapidly. The stress intensity at the onset of fast fracture can be systematically altered by varying the slot root radius. Typically, root radii of 0.02 to 0.08 inch have been used. The K-values at initiation and arrest are measured with a clip gage fixed to the end of the test piece. The velocity during propagation is measured with conducting strips deposited over a thin insulating layer of epoxy.

The specimen is slowly loaded in an ordinary testing machine by forcing a split wedge between the pins. Since the wedge loading is inherently stiff, crack propagation proceeds with essentially constant displacement at the load point. Under quasi-static conditions, the crack-driving force would decrease as the crack grows. This behavior ultimately causes a high-speed crack to arrest within the confines of the specimen, provided the test piece is long enough.

Wedge loading has two other virtues. One is that, since little energy is exchanged between the DCB specimen and the testing machine during the propagation event, the results are relatively insensitive to the character of the testing machine. The second is that the friction between the wedge and the pins introduces a modest com-

pressive stress parallel to the crack plane. This tends to stabilize the crack path. Hence, the side grooves ordinarily required to keep the crack from turning can be omitted for those materials in which the crack has some tendency to branch.

Although the experimental method outlined above has proven satisfactory for testing high strength materials, several modifications have been found necessary for testing the lower strength grades of steels. One modification is the use of a so-called "duplex" specimen where a high strength material is used for the starter section to avoid excessive plastic deformation in the loading regions of the specimen. A starter section of high strength 4340 steel welded to the test material has been successfully employed for fabricating duplex specimens. Another problem has been a tendency for crack branching in the lower strength steels. This has necessitated side grooving to maintain a straight crack plane. Currently, a 60-percent side groove depth duplex specimen is being used for tests on A533b steel.

Some typical crack length time results are shown in Figure IV-41. Of interest is the fact that these are ostensibly linear, which gives considerable credence to the use of the mathematical model described in Section B.4.d(2)(c)(cf. Figure IV-38). This linearity also facilitates the interpretation of the results since a uniform crack speed value can be associated with the results of each test. Thus, using the results of the dynamic analysis of the DCB, there are three methods of extracting K_{ID} values from the two independent quantities measured on the test specimen: the crack velocity and the crack length at arrest. These are

(1) Obtaining K_{ID} by matching the initial average velocity with calculated velocities for various K_q, $K_{ID}(\dot{a})$, and specimen parameters.

(2) Obtaining K_{ID} by matching the arrest crack length with calculated values.

(3) Evaluating an average value of K_{ID} ($\overline{K}_{ID}$) over the entire propagation event through the approximation

$$\overline{K}_{ID} = \sqrt{K_q K_{Ia}} \quad . \qquad \text{(IV-51)}$$

which is based primarily on the assumption that no kinetic energy is left in the specimen at arrest.

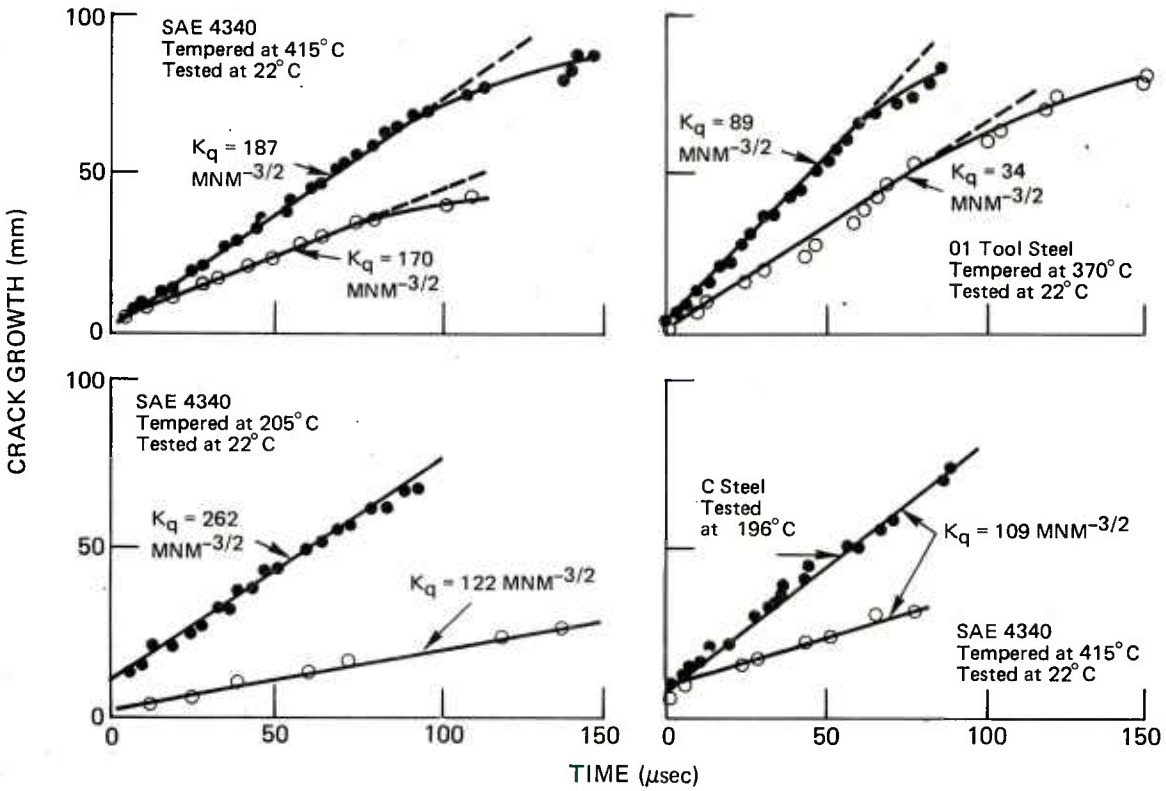

FIGURE IV-41 Assorted Crack Length-Time Measurements from Wedge-Loaded, Rectangular DCB Specimen Tests

SOURCE: Hahn et al, 1975-76

For Method 2 (and also for Method 1 to some degree) an iterative determination is necessary since the calculated values depend on K_{ID}- velocity relations which are not known beforehand for the material being tested. In the case of duplex specimens, some modifications of each of the three methods are required, but the basic principles remain the same.

There are several reasons why valid K_{ID} data can be obtained from relatively small duplex DCB specimens

of moderately tough steels. First, the high-strength/low-toughness starter section reduces the plane strain thickness requirements drastically. Second, the grooves along the fracture path develop constraints similar to those associated with increased plate thickness. Third, the propagating crack produces a very high strain rate at the crack tip. This causes the effective yield strength to be raised (perhaps twice the static yield strength), hence reducing the plastic zone size.

In principle, the duplex DCB test can be also used to obtain valid K_D data by eliminating the side grooves. However, for the specimen dimensions currently employed to measure K_{ID}, removal of the side grooves would introduce several problems, particularly for high toughness steels. The amount of strain energy that can be stored in the arms of the test piece is not sufficient to drive the crack into the tough test section for any appreciably distance, thus making analysis of the results difficult. With existing specimen dimensions and procedures, the estimated upper limit of toughness measurements is about 250 $MNm^{-3/2}$. Also, the plastic zone radius may approach or exceed the arm height of the specimen. Finally, cracks propagating into the tough test section frequently branch in the absence of side grooves; this may preclude analysis of the results.

(4) Material Property Data for Dynamic Crack Propagation. The treatment of dynamic crack propagation and arrest is complicated by the variation of the fracture energy with crack velocity and plate thickness. A schematic of velocity dependence is shown in Figure IV-42a. Eftis and Krafft (1965) have deduced K_{ID} values from wide plate, ship steel experiments. Their results reflect low energy cleavage fractures below the nil ductility temperature (NDT). These results indicate that K_{ID} first decreases with increasing velocity, becomes a minimum at a finite velocity, and then increases dramatically for crack velocities in excess of 600 ms. In contrast, recent results for low energy fibrous fractures in AISI 4340 steel are reproduced in Figure IV-42b. Here the fracture energy increases monotonically with crack velocity.

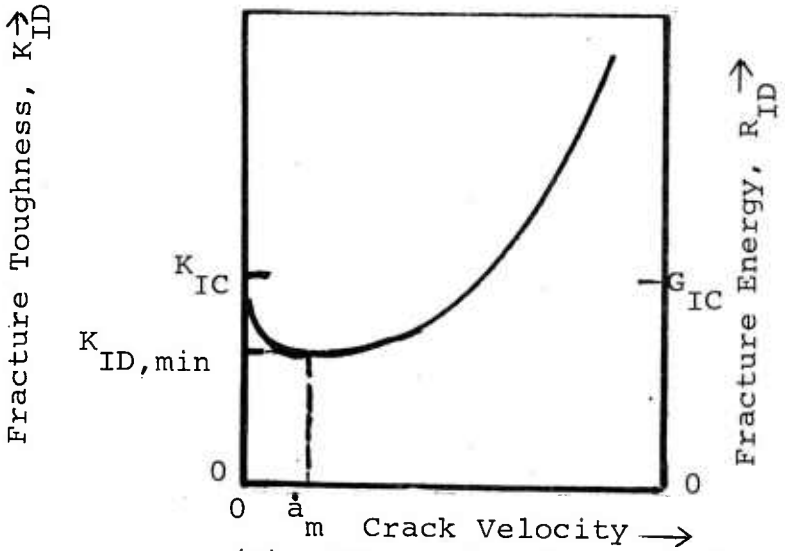

(a) Schematic of a dependence with a minimum showing $K_{D,\ min}$

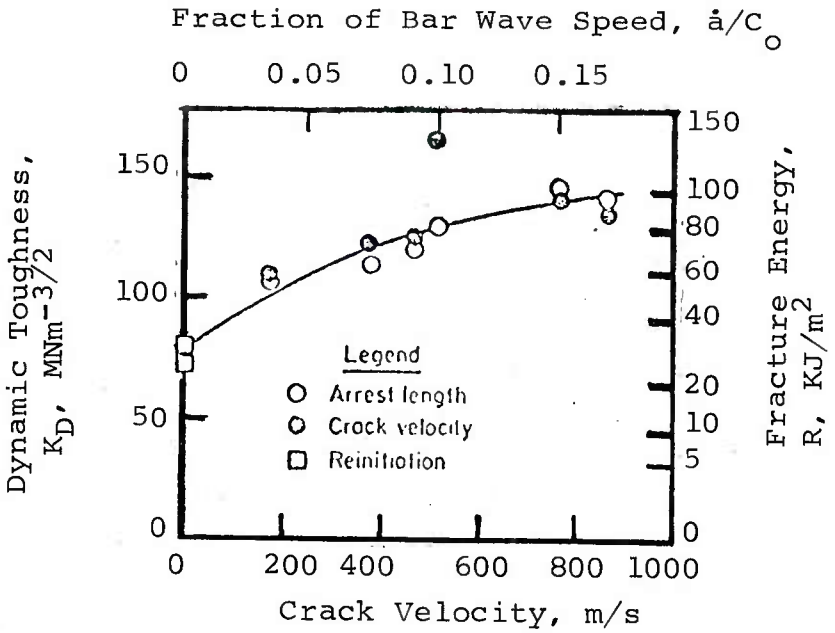

(b) Results for flat fibrous fracture of 4340 steel after Hahn, et al.

FIGURE IV-42 Examples of the Crack Velocity Dependence of the Propagating Crack Fracture Toughness

SOURCE: Hahn et al, 1975-76

Figure IV-43 shows measured values of K_{ID} obtained from duplex DCB specimens for several grades of ship steel tested near the nil ductility temperature. The behavior of these steels is interesting from several standpoints. The toughness of each of the four steels is seen to be strongly dependent on crack velocity, being greatest at small velocities. Nonetheless, K_{ID} for a propagating crack exceeds K_{Id}, the energy associated with crack initiation by impact. There is some thought that the minimum in the K_{ID}-versus-velocity curve (if a minimum exists) may approximate the K_{Id} values, but this has not yet been demonstrated.

K_{ID} values have been determined for a limited number of low to intermediate strength grades of steel. In the following discussion of these data, and the accompanying figures, K_D rather than K_{ID} is used to denote the measured fast fracture toughness since it is not certain that the measured values are fully plane-strain values.

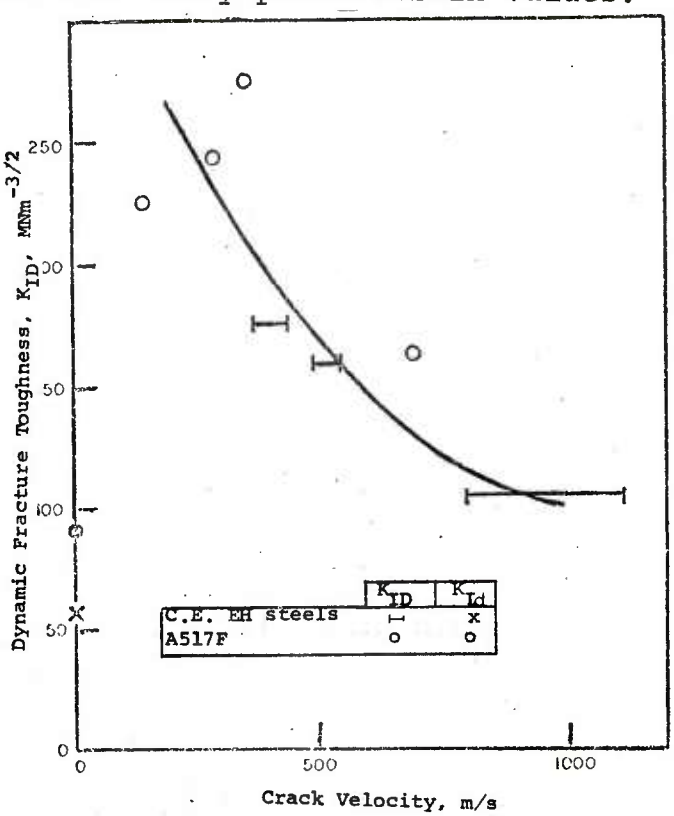

FIGURE IV-43 Relation Between Crack Velocity and Dynamic Toughness for Ship Steels Tested Near NDT

SOURCE: Kanninen et al, 1977

Figure IV-44 shows results obtained for a 9 percent Ni steel and an A517F steel at -196 C. It can be seen that the K_D values of the 9 percent Ni steel are nearly independent of crack velocity while the A517F seems to go

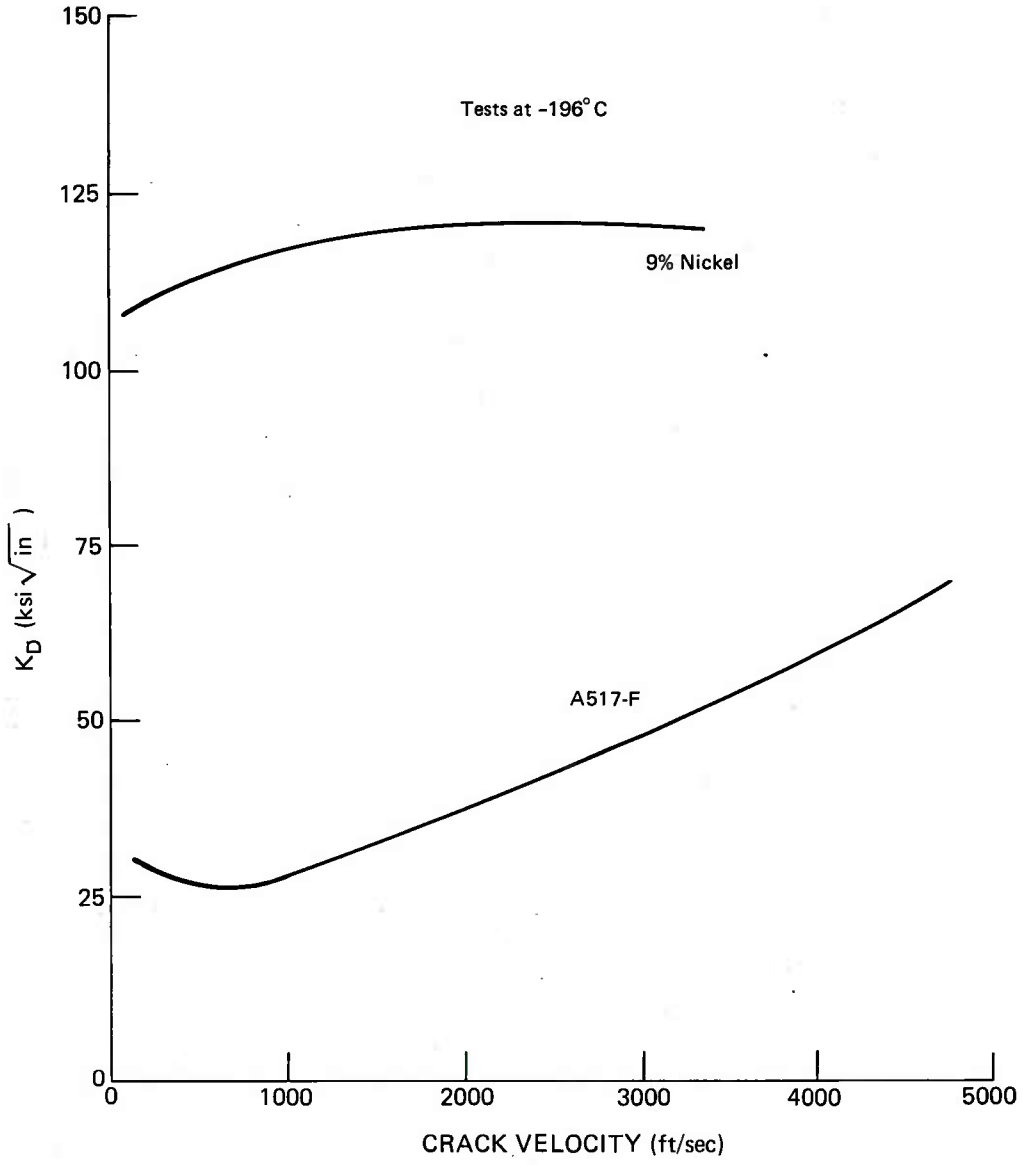

FIGURE IV-44 Fast Fracture Toughness Data for a 9 Percent Ni and an A517-F Steel

SOURCE: Battelle Columbus Laboratories, unpublished data

through a slight minimum and then an increase. At this temperature, the fracture modes are ductile dimple for the 9 percent Ni steel and cleavage for the A517F steel. Data for low carbon steels in the temperature range from -58 F to - 10 F are shown in Figure IV-45.

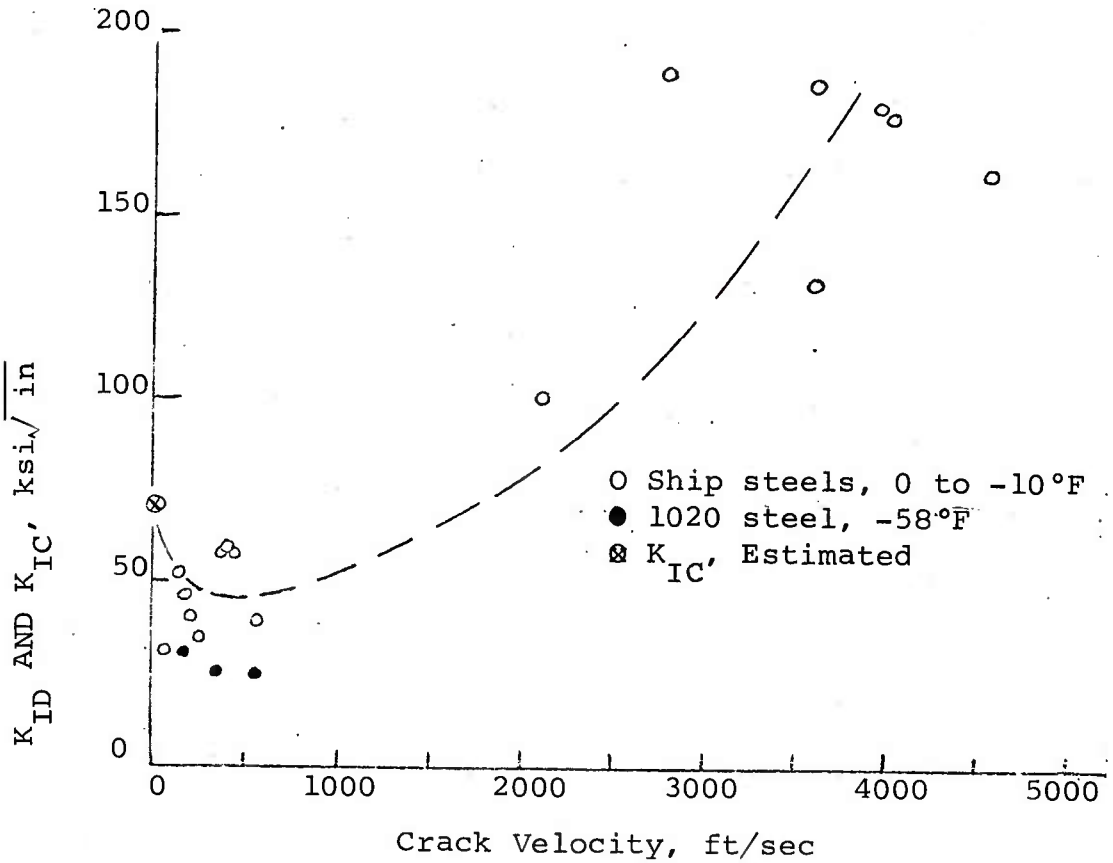

FIGURE IV-45 Fast Fracture Toughness Data for Low Carbon Steels at Low Temperatures

SOURCE: Battelle Colombus Laboratories, unpublished data

Figure IV-46 shows K_D values as a function of temperature (relative to the nil ductility temperatures, NDT) and several crack velocities for three ship-plate steels (ABS grade C, E, and EH). These are basically C-Mn steels with room temperature yield strengths in the 40 to 55 ksi range. At temperatures around and above the NDT, a rather large and continuous decrease in K_D with crack velocity is indicated for these steels. Finally, Figure IV-47

shows some preliminary K_D values for A533B steel measured in a current research program. The investigators caution that these are tentative results which may have to be corrected pending further analysis.

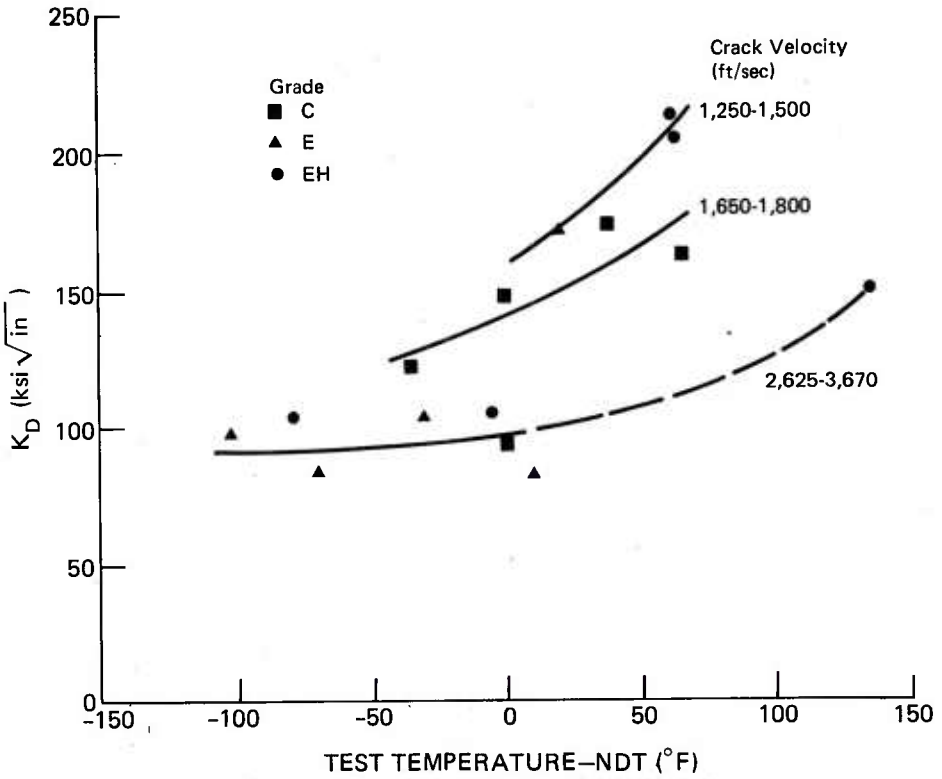

FIGURE IV-46 Fast Fracture Toughness Data for Several Grades of Ship-Plate Steels

SOURCE: Battelle Columbus Laboratories, unpublished data

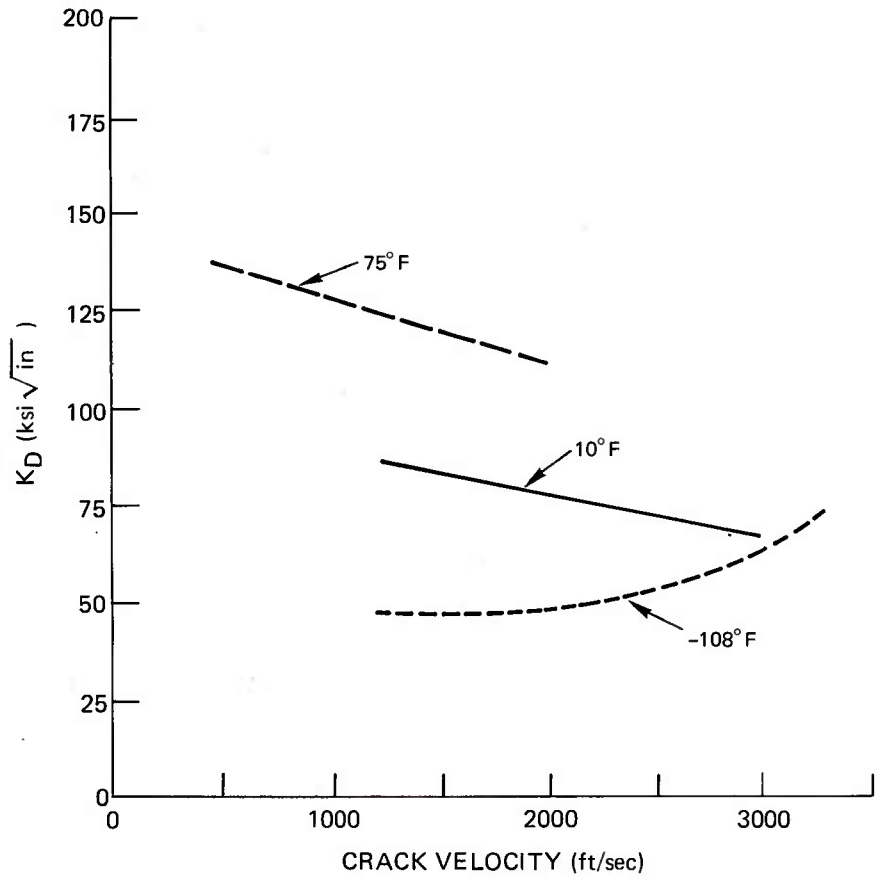

FIGURE IV-47 Preliminary K_D Data for A533B Steel

SOURCE: Battelle Columbus Laboratories, unpublished data

Another avenue proposed for evaluating large fracture toughness values is to measure the total energy absorbed in the fracture of a notched bend specimen in the dynamic tear (DT) test. The energy to fracture the specimen is provided by a pendulum whose velocity just prior to impact is approximately 5 to 10 m/s. DT, the total energy absorbed in the process of breaking the specimen, is termed the dynamic tear energy. It is observed directly by noting the height of the pendulum swing after fracture. This quantity divided by A, the cross sectional area of the test piece,

is related to the fracture energy R assuming a constant crack velocity. That is

$$R = \frac{1}{\beta} \cdot \frac{DT}{A} \quad , \qquad \text{(IV-52)}$$

where $\beta = 1$ when the energy losses in the impact test remote from the crack tip are zero and $\beta > 1$ when significant energy losses occur. The dynamic fracture toughness K_D can then be expressed as

$$K_D = \sqrt{RE} = \left(\frac{EDT}{\beta A}\right)^{\frac{1}{2}} \quad . \qquad \text{(IV-53)}$$

if plane stress is assumed. For steels, the DT versus K_{Ic} plots indicate that $\beta \approx 10$ for the 1-inch DT test and $\beta \approx 5$ for the 5/8-inch DT test if we assume $K_{Ic} = K_D$. Limited DT versus K_{ID} data suggest that β is only about 1.4, but additional data are required to confirm this.

The experimental observation that β is greater than 1.0 confirms the assumption generally made about the DT test: that the energy losses remote from the crack tip in an impact test are of a significant magnitude and, in some cases, can overwhelm the actual fracture propagation energy. Included in these losses are the crack initiation energy, the energy associated with plastic deformation at the loading points and at the specimen boundaries as the crack approaches the far side of the test bar, and the kinetic energy of the fractured specimen. The experimental data are too meager to permit estimation of reliable β values.

e. Fracture Criteria for Moving Cracks and Complex Loading.

(1) Path Independent Integral. Parameters such as K_{Ic} or J_{Ic} must be clearly distinguished from the specific surface energy quantity*, $\Gamma(t)$, frequently used in the

*This surface energy is equal to one-half the fracture energy R(á) for a propagating crack when the conditions of linear elastic fracture mechanics are met (cf. Equation IV-31).

analytical modeling of moving cracks in which $\Gamma(t)$ describes the energy dissipated in the creation of free surface as a function of time and is not necessarily associated with any point of crack instability. For a propagating crack, an energy inequality may be written in the form*

$$\int_C T_i^n \dot{u}_i ds \geq \frac{1}{2}\frac{d}{dt}\int_R \int \rho \dot{u}_i \dot{u}_i dA + \frac{d}{dt}\int_R \int \rho U dA + 2\ (t)\,\dot{a}\,\Gamma \quad \text{(IV-54)}$$

if temperature changes due to straining are neglected (except for those in a thin layer next to the new surface). The above equation states that the rate at which work is being done by tractions T_i^n acting across the contour C surrounding the crack tip (Figure IV-48) is greater than or equal to the rate of increase of stored and kinetic energies inside C plus the rate at which energy is dissipated by the moving crack. In Equation IV-54, $\dot{a}$ is the crack velocity, U is the Helmholtz free energy per unit mass, ρ is the mass density, and the dot represents the differentiation with respect to time. The components of the displacement vector are u_i.

To reiterate, the specific energy $\Gamma(t)$ in Equation IV-54 should be clearly distinguished from the fracture initiation quantity, $2\Gamma_c = J_{Ic}$, used for analyzing stationary cracks that become unstable upon a small segment of crack extension. While Γ_c can be determined from a K_{Ic} or J_{Ic} type of test and used as a fracture toughness quantity, $\Gamma(t)$ simply represents the energy dissipated in the continuous creation of new crack surface. A reliable method of determining $\Gamma(t)$ is lacking when large-scale plastic deformation exists.

The form of Equation IV-54 may be cast into a convenient form for the evaluation of $\Gamma(t)$ by imposing the following assumptions on the physical system:

(a) The crack is restricted to propagate along the x-axis (Figure IV-50) in a steady state manner; i.e., the stress and displacement distributions are assumed independent of time when referred to a coordinate system that moves with the crack tip. The tip speed $\dot{a}$ is assumed constant.

---

* The summation convention is followed whereby repeated indices are to be summed over their range (i,j=1,2,3).

(b) The material is assumed to be purely elastic with a strain energy function

$$W = \int_{o}^{e_{ij}} \sigma_{ij} \, de_{ij} \qquad \text{(IV-55)}$$

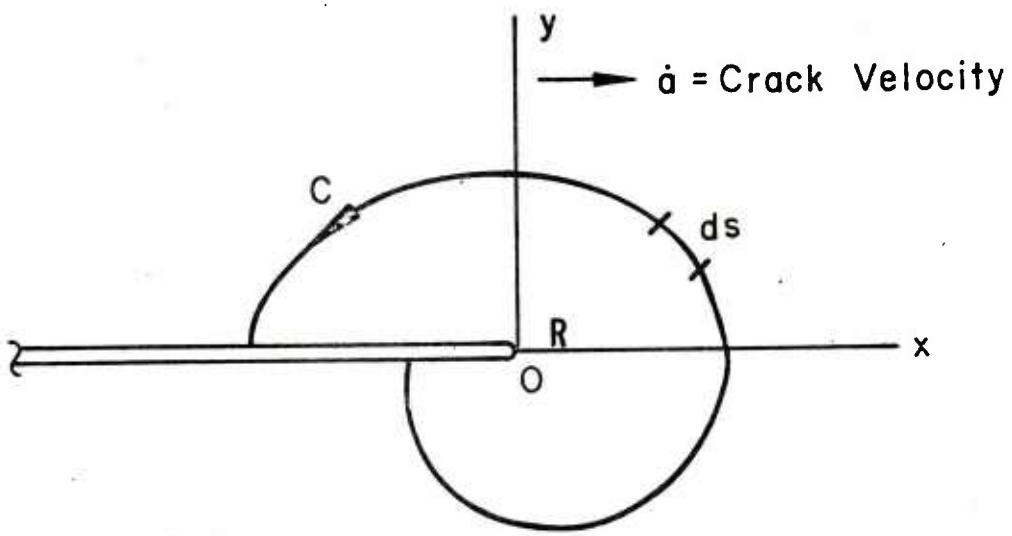

FIGURE IV-48 Contour Around a Moving Crack Tip

The quantities σ_{ij} and e_{ij} are components of the stress and strain tensors and may be related nonlinearly. The material, however, must deform in a reversible manner.

Under these assumptions, Sih (1970) has reduced Equation IV-54 to the form

$$R(\dot{a}) = \int_{C} \left(W + \frac{1}{2} \rho \dot{a}^2 \frac{\partial u_i}{\partial x} \frac{\partial u_i}{\partial x}\right) dy - T_i^n \frac{\partial u_i}{\partial x} \, ds \; . \qquad \text{(IV-56)}$$

As a direct consequence of assumption (b), the value of the integral in Equation IV-54 is independent of the path of integration. In other words, the result obtained from any two arbitrary contours surrounding the moving crack tip will be the same.

For stationary cracks ($\dot{a}=0$), Equation IV-56 reduces to the J-integral by Rice (1968). Furthermore, if the material is linear with $W = \frac{1}{2} \sigma_{ij} e_{ij}$, it has been shown by Sih (1970) that Equation IV-56 further simplifies to

$$R = \int_c \left(\frac{1}{2} u_i \frac{\partial T_i^n}{\partial x} - \frac{1}{2} T_i^n \frac{\partial u_i}{\partial x} \right) ds \qquad \text{(IV-57)}$$

It should be clearly pointed out that the contour integrals in Equations IV-56 and IV-57 are valid only if assumption (a) is observed. In situations where the speed changes or the crack changes its direction of propagation for the dynamic crack problem containing both stress intensity factors k_1 and k_2, no path independent integrals have been found;* refer to Eshelby (1974).

(2) Strain Energy Density Criterion. A fracture criterion that is free from the restrictions mentioned in subsection e.(1) is based on the strain energy density factor S which has been suggested as a parameter for predicting unstable crack initiation and growth under static (Sih, 1973) and dynamic (Sih, 1977) loads of a general nature, not necessarily symmetrical with reference to the crack plane. This factor represents the product of the radical distance, say r_o, measured from the crack tip, multiplied by the strain energy density function, dW/dV, commonly employed in the theory of elasticity; i.e., $S = r_o(dW/dV)$. The minimum value of S, S_{min}, determines the direction of crack initiation and the critical value of S_{min}, S_c, determines incipient fracture. The value S_c is assumed to be characteristic of the material and taken as the fracture toughness. It should be added that experimental verification of this criterion is currently very limited.

For the nontrivial problem of an inclined crack in Figure IV-49, the critical dynamic stress of σ_f that the plate could sustain can be obtained from S_c as

$$f = \sqrt{\frac{S_c}{aF(\beta, t, \theta_o)}} \qquad \text{(IV-58)}$$

where the function $F(\beta, t, \theta_o)$ is given by

---

* The lower case letters k_1 and K_2 are used in this subsection for stress intensity factors. For instance, k_1 differs from K_1 by a factor of $\sqrt{\pi}$; i.e., $K_1 = \sqrt{\pi} k_1$.

$$F(\beta, t, \theta_o) = (a_{11} f_1^2 \sin^2\beta + 2a_{12} f_1 f_2 \sin\beta\cos\beta + a_{22} f_2^2 \cos^2\beta)\sin^2 \quad \text{(IV-59)}$$

The angle β denotes the crack position with reference to the applied stress and the fracture angle, θ_o, corresponds to the location of S_{min} through the coefficients a_{ij} (i,j,= 1,2) depending on θ_o and the elastic constants (say, shear modulus μ and Poisson's ratio ν). To be emphasized is that the same S_c value is assumed for both static and dynamic loads. The time dependent functions f_1 and f_2 (Sih, 1977) in Equation IV-59 are associated with the stress intensity factors

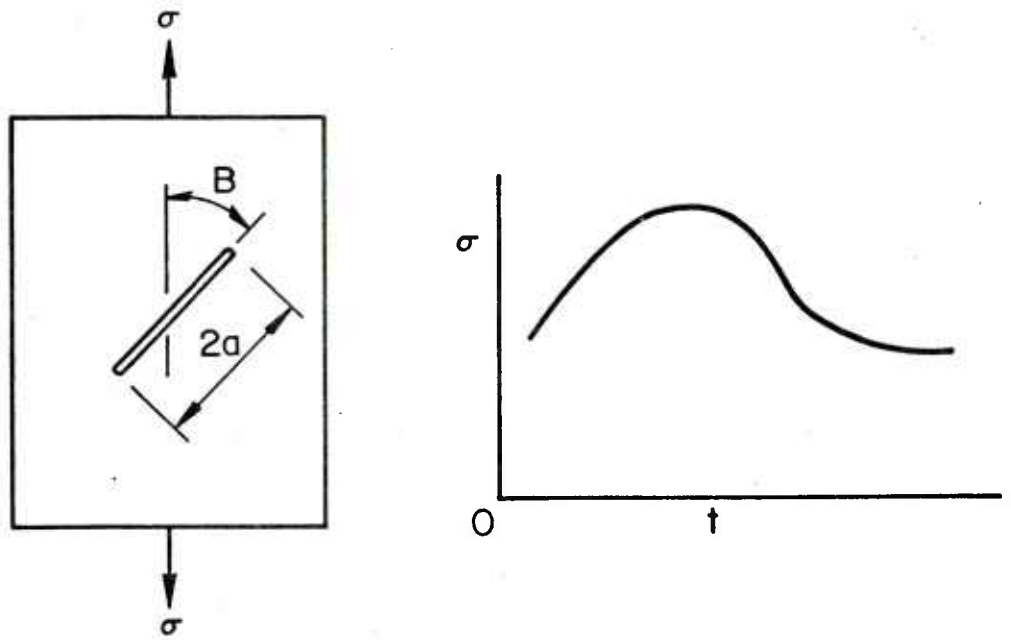

FIGURE IV-49 Time Dependent Loading on an Inclined Crack

$$k_1 = f_1(t)\sigma\sqrt{a}\,\sin^2\beta,\quad k_2 = f_2(t)\sigma\sqrt{a}\,\sin\beta\cos\beta \quad \text{(IV-60)}$$

and are unity for static loading. It is important to know that under dynamic loading, k_1 and k_2 do not necessarily

attain their maximum values at the same time. The way in which the combination of k_1 and k_2 affects the critical stress, σ_f, can be found from the strain energy density factor:

$$S = \sigma^2 a \sin^2\beta [a_{11} f_1^2 \sin^2\beta + 2a_{12} f_1 f_2 \sin\beta\cos\beta + a_{22} f_2^2 \cos^2\beta] \quad \text{(IV-61)}$$

First, the fracture angle θ_0 in Equation IV-58 is found from the condition $\partial S/\partial\theta = 0$ such that S is a minimum. Hence, a plot of $16\mu S_{min}/\sigma^2 a$ versus $c_2 t/a$ is established as illustrated in Figure IV-50 for steel with $\nu = 0.29$. In the

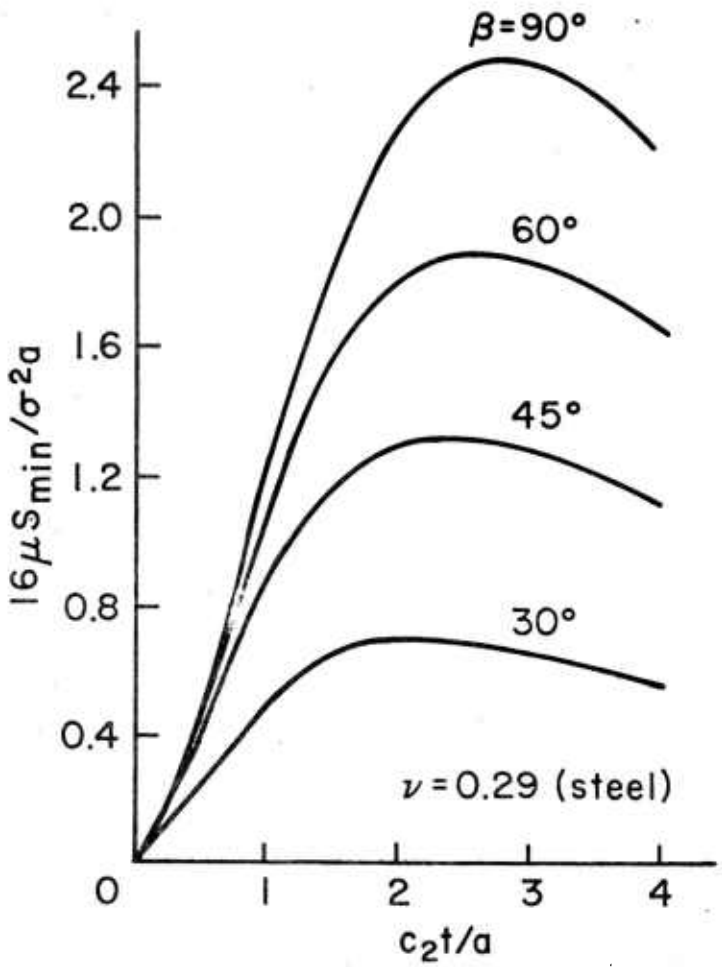

FIGURE IV-50 Variations of Strain Energy Density Factor With Time

SOURCE: (Sih 1977)

S-theory, the crack is assumed to extend in the direction θ_o when S_{min} reaches the critical value S_c of a given material. Depending on the angle β and the amplitude of the dynamic load, S_{min} may be equal to S_c on any part of the curve in Figure IV-50, or never reach S_c. Since the objective of any dynamic analysis is to predict the applied failure stress, it is convenient to compare the ratio of the dynamic failure stress, σ_f, to that of the static failure stress, σ_s, which may be obtained from Equation IV-61 as $16\mu S_c = 4(1-2\nu)\sigma_s^2 a$. Keeping the fracture toughness value, S_c, constant, the ratio σ_f/σ_s may be written as

$$\frac{\sigma_f}{\sigma_s} = \sqrt{\frac{4(1-2\nu)}{N}} \qquad \text{(IV-62)}$$

The quantity N stands for $16\mu S_{min}/\sigma^2\sqrt{a}$ which may be obtained from Figure IV-50 with σ_f in Equation IV-62 corresponding to S_{min} reaching S_c.

A plot of σ_s versus $c_2 t/a$ is given in Figure IV-51. Each curve passes through a minimum in the

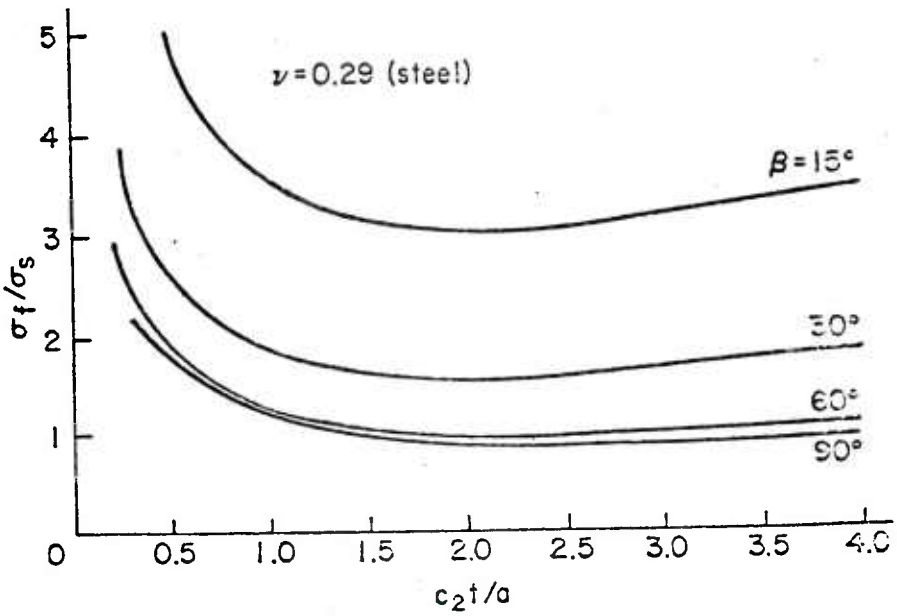

FIGURE IV-51 Dynamic Load Amplification

SOURCE: (Sih 1977)

neighborhood of $c_2t/a = 2$. For $\beta = 15°$, this minimum is at the smallest value of c_2t/a, corresponding to the smallest value of σ_f to cause fracture.

Examples on application of the S-Criterion to the running crack problem can be found in Sih (1977-b).

(3) Maximum Normal Stress. The maximum normal stress criterion assumes that fracture occurs when the maximum principal stress local to the crack tip reaches a critical value. The plane along which crack growth takes place is assumed to be normal to this stress. This criterion is widely used for quasi-static problems and has received considerable experimental verification. In a two-dimensional situation, crack initiates in a radial direction and hence the stress component under consideration is a circumferential direction given by

$$\sigma_\theta = \frac{k_1}{4\sqrt{2r}}\left[\cos\frac{3\theta}{2} + 3\cos\frac{\theta}{2}\right] - \frac{3k_2}{4\sqrt{2r}}\left[\sin\frac{3\theta}{2} + \sin\frac{\theta}{2}\right] \quad \text{(IV-63)}$$

where r and θ are local polar coordinates shown in Figure IV-52. The direction θ_o along which the crack initiates can

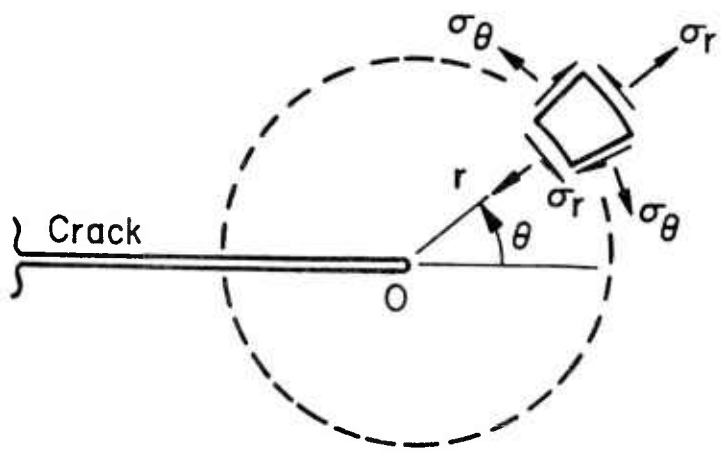

FIGURE IV-52 Stress Components Near a Stationary Crack Tip

be found from the condition $\partial\sigma_\theta/\partial\theta = 0$ such that $\sigma\theta$ is a maximum. Equation IV-63 has been applied to study the mixed mode fracture under static loads by Erdogan and Sih (1963) and is potentially applicable to stationary cracks subjected to dynamic loads.

The presence of biaxiality or triaxiality, on an element ahead of the crack, however, causes limitations on the maximum principal stress criterion. For instance, the stress state ahead of a crack under symmetric loading is hydrostatic in that both principal stresses are equal and hence there is no maximum. Generally speaking, this criterion is effective only when the magnitude of one of the normal stress components is much larger than the others.

Conceptual difficulties also arise when applying the maximum normal stress criterion to the running crack in Figure IV-53. Sih (1968) has shown that this ratio is

$$\frac{\sigma_x}{\sigma_y} = \frac{(1+s_2^2)(2s_1^2+1-s_2^2)-4s_1s_2}{4s_1s_2-(1+s_2^2)} \qquad \text{(IV-64)}$$

is always greater than unity. In Equation IV-64

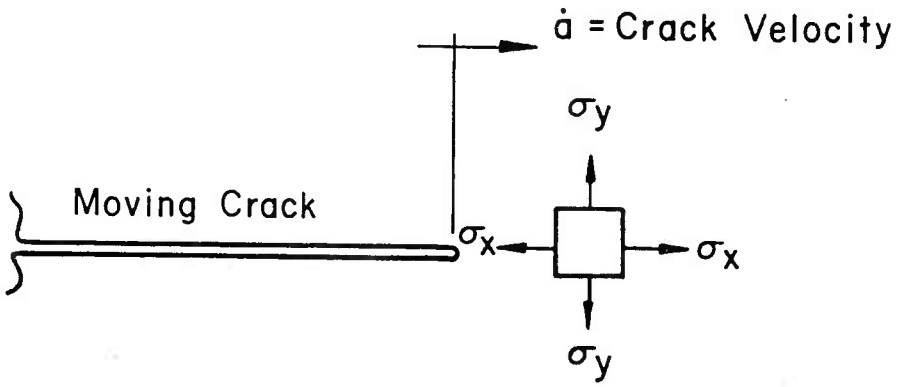

FIGURE IV-53 Running Crack

$$s_j = [1 - (\dot{a}/c_j)^2]^{\frac{1}{2}}, \quad j = 1,2 \qquad \text{(IV-65)}$$

depends on the crack speed $\dot{a}$ and the wave speeds.

$$c_1 = \sqrt{(\lambda+2\mu)/\rho}, \quad c_2 = \sqrt{\mu/\rho} \qquad \text{(IV-66)}$$

The constants λ and μ are the Lamé coefficients and ρ is the mass density. Equation IV-64 with $\sigma_x > \sigma_y$ implies that crack runs in a direction parallel to the maximum stress rather than normal to it, a condition that contradicts the original assumption.

(4) Maximum Energy Release Rate. The amount of energy released by a crack traveling in an elastic material that undergoes no plastic deformation can be computed from Equation IV-56 since $R = G_1$. The subscript 1 means that the relation applies only for Mode I; i.e., symmetrical loading. Depending on the boundary-value problem, the dynamic G_1 may be related to its corresponding static value G_{1S} (Sih, 1970) as

$$\frac{G_1}{G_{1S}} = \frac{s_1(1-s_2^2)}{1-\nu}\,[4s_1s_2 - (1+s_2^2)^2]\,F_1^2(s_1,s_2) \qquad \text{(IV-67)}$$

for plane strain; see also Freund (1976). The quantities s_j have already been defined in Equation IV-65 and $F_1^j(s_1,s_2)$ depends on the geometric and loading conditions. In the limit as the crack velocity goes to zero, $\dot{a}\to 0$, G reduces to G_{1S}, the static value:

$$\lim_{\dot{a}\to 0} G_1 \to G_{1S} = \frac{\pi(1-\nu^2)k_1^2}{E} \qquad \text{(IV-68)}$$

For cracks that turn or propagate without symmetry, the maximum energy release rate concept can be used to predict both the condition for propagation and the direction of growth; however, it is difficult to apply in a rigorous fashion. Analytically, the corner singularity in addition to that at the crack tip poses a uniqueness problem on the value of G in the limit as the branched or angled portion of the main crack tends to zero. Also, the numerical evaluation of G for a bent crack tends to smooth out stress peaks and singularities and also presents difficulties that cannot be easily resolved. Nevertheless, work is continuing on refining this physically appealing criterion (Palinswamy and Knauss, 1977).

f. Conclusions

One of the oldest ideas in fracture control is the certification of materials for service by testing under high rates of loading. As discussed above, impact tests such as the Charpy test, the drop-weight tear test, and the dynamic tear test have been (and continue to be) widely used. These tests were originally intended to give qualitative information only; e.g., a temperature transition. Recently, however, it has become widely realized that useful quantitative information can also be extracted from the results of these tests. What is not yet generally recognized is that the conventional analytical interpretation of such tests via a completely static point of view can be substantially in error. The recent research work using dynamic (i.e., inertia forces included) analyses described in this report have clearly shown this for precracked Charpy specimens and for the drop-weigh tear test.

The certification of materials for service is presently evolving from a loose qualitative approach into a much more quantitative procedure, as illustrated by the Air Force's fracture tolerance guidelines adopted for the B-1 bomber. Other Department of Defense concerns with high loading rate applications are cited elsewhere in this report. Hence, there is a strong need for dynamic analyses to accompany high strain rate testing in order that material properties appropriate for engineering structural design can be correctly extracted from such tests.

The work reviewed in this section reveals that there are two main approaches in dynamic fracture analysis and

testing. Some investigators have considered the dynamic propagation of a crack initiated under quasi-static loading conditions. Other investigators have confined themselves to considering the conditions prior to the initiation of growth under dynamic loading. Obviously, both aspects are involved in a proper analysis of the problem. In our judgment, the key contribution that needs to be made in this field is the development of an analysis capability that considers both dynamic crack initiation and propagation. Only with such a tool can meaningful, dynamic fracture data be extracted from high loading rate experiments.

It is not difficult to conclude that the existing theories are not sufficient for a general treatment of material response to high strain rate loading, particularly in handling the effects of specimen size and the range of operating temperatures. From the fracture mechanics point of view, many of the proposed fracture toughness parameters are still sensitive to the operating conditions, and undergo sharp variations, normally referred to as the brittle-ductile transition behavior, Figure IV-54. In principle, a material parameter should remain invariant with respect to changes in specimen size, and it is very desirable if this invariance exists for temperature and loading rate changes as well.

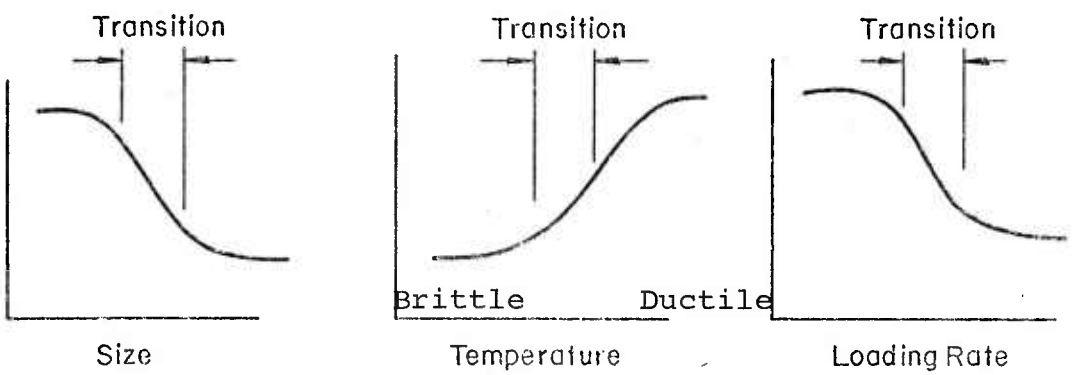

FIGURE IV-54 Transition Behavior

If a material exhibits a distinct point of instability on the load-deformation curve regardless of whether it is linear (Figure IV-55) or nonlinear (Figure IV-56), the fracture toughness value (if interpreted as $(\Delta W/\Delta a)_c$ at instability, where ΔW_c is the local energy needed to cause instability, should be the same for both cases provided that the material behavior within which Δa is created remains unchanged. It is believed important to adopt a local view of the fracture process in the failure analysis of structural components where predictions on allowable load and/or net section size must be made; such a view is used in Section B.5.c. in which three-dimensional crack growth predictions are discussed. As noted previously, the critical value of J may be interpreted as a local fracture initiation criterion (cf. Equation IV-24), and therefore the great success achieved with this criterion supports this point of view. However, ductile fracture for static and dynamic conditions is a subject which is still little understood and requires extensive future research.

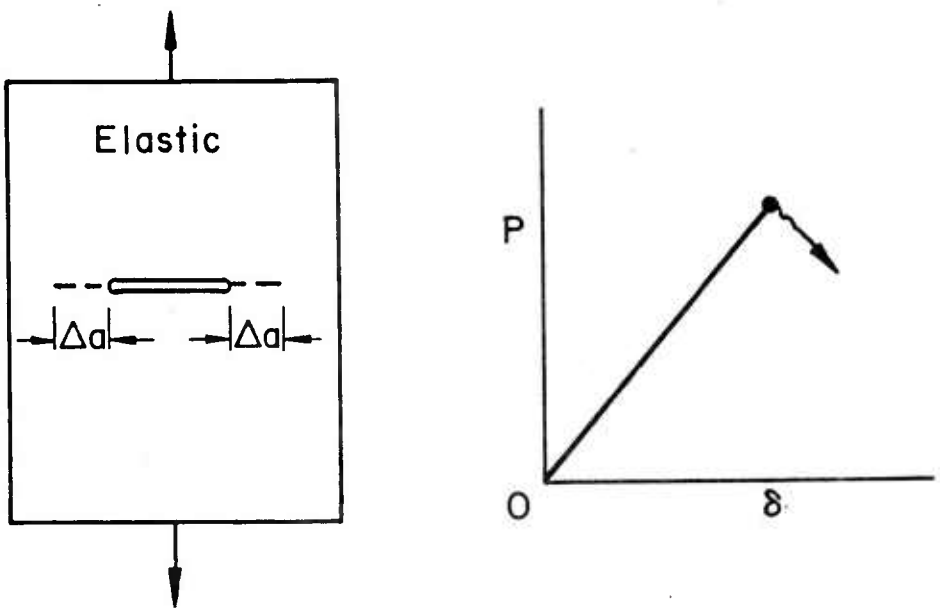

FIGURE IV-55 Linear (Brittle) Behavior

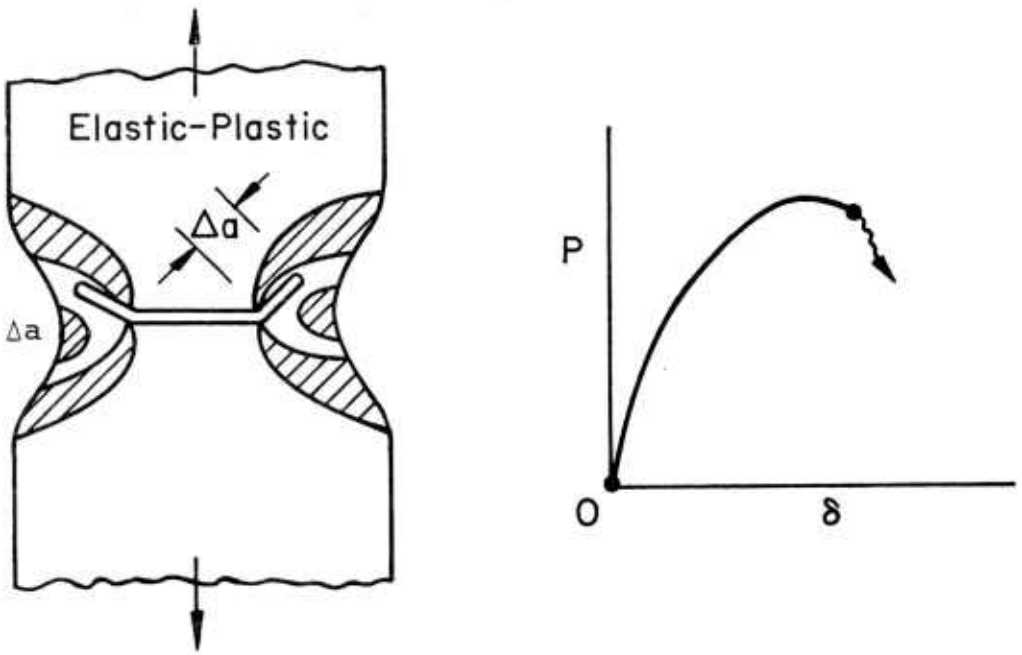

FIGURE IV-56 Nonlinear (Ductile) Behavior

5. Three-Dimensional Elastic-Plastic Fracture Considerations.

a. Introduction

With the advent of fracture mechanics, it is now possible to design structures using the concept of fracture toughness in addition to the traditional practice of using strength and structural buckling instability criteria. One of the major shortcomings of the strength and toughness approach lies in the inability of the analyst to translate small specimen laboratory data to the design of large size structures made of tough materials. This lack of understanding of fracture size effect cannot be resolved by testing alone.

A realistic modeling of ductile fracture* is a prerequisite for resolving the effect of size on the brittle-ductile transition.** The basic features of ductile fracture can be observed from macrofractography and involve three distinct stages (Sih, 1976) which should be included in an elastic-plastic crack analysis. Fracture first originates in a region subjected to nearly hydrostatic tension. It then changes from slow or stable growth to rapid or unstable crack propagation. Final separation of the material occurs when the crack turns away from the normal to the free surface of the solid. This slanted fracture surface is referred to usually as the shear lip or cup-and-cone. The transition from slow to rapid fracture occurs so quickly that it is difficult to observe the load-deformation curve. The last ligament of material separation, however, does coincide with a sharp drop in load. Because the fracturing process is seldom symmetrical, the shear lip or cup-and-cone appears only on one half of the broken specimen.

b. Ductile Fracture

Preliminary analysis of a tensile bar with a crack shows that plastic zones are formed on both sides of the macrocrack as it moves through the material, Figure IV-57a. Initial instability corresponds to essentially brittle fracture where the fracture path is almost flat. If the crack is allowed to approach the boundary, the bar begins

* Elastic-plastic stress analyses of two-dimensional crack models are found to be inadequate as they do not account for necking and the slanted fracture terminating at the free surface. This is a basic feature of ductile fracture and is a three-dimensional phenomenon.

** It should be noted, however, that data obtained for various structural steels demonstrate that a true plane-strain fracture toughness transition exists which is independent of specimen thickness. Fractographic analyses show that this transition temperature is associated with the onset of change in the microscopic fracture initiation mode at the crack tip; the mode changes continuously from cleavage at the low temperature end to ductile tear at the upper end (Rolfe and Barsom, 1977).

to neck until the plastic zones intersect the free boundary. An additional island of yielded material has been found (Sih, 1977-a), leaving a forked region of elastic material. Should the bar fail unstably at this point, a possible path of fracture is through the forked elastic region as shown in Figure IV-57b. For the more ductile material, the bar may neck further until the entire ligament between the crack and outer specimen surface is yielded, Figure IV-57c.

Further loading suggests a further distinction of zones of distortion from dilatation. This is illustrated in Figure IV-57d where the zones of distortion are marked as second degree yielding. A possible path of fracture is again suggested to take place on a slant in which the material is distorted to a lesser degree than that in the cross-hatched region.

To reiterate, Figures IV-57a through d illustrate the various degrees of yielding that correspond to materials with different degrees of ductility and different loads of instability on the load deformation curve. The mechanics problem of ductile fracture is to predict the fracture path and load in terms of the continuum material parameters such as yield strength, strain hardening exponent, etc., as well as the fracture toughness associated with the local behavior of the material at the crack tip.

Similar phenomena are observed in the fracture of moderately thick plate specimens with a through crack such that the combinations of material properties and plate geometry would not satify the ASTM requirements (ASTM Special Technical Publication No. 410, 1966) for plane strain where the smallest geometric length parameter must be greater than or equal to 2.5 $(K_{Ic}/\sigma_Y)^2$. Here, as before, K_{Ic} is the valid critical Mode I stress intensity factor and σ_Y is the uniaxial yield strength of the material. Figure IV-58 shows that the critical stress intensity factor K_c* becomes K_{Ic} or geometry independent only when the plate is sufficiently thick. The fracture surface appearance as

*Strictly speaking K_c should not be referred to as the plane stress fracture toughness value because the mode of fracture for this specimen is in no way related to the plane stress plasticity crack solution.

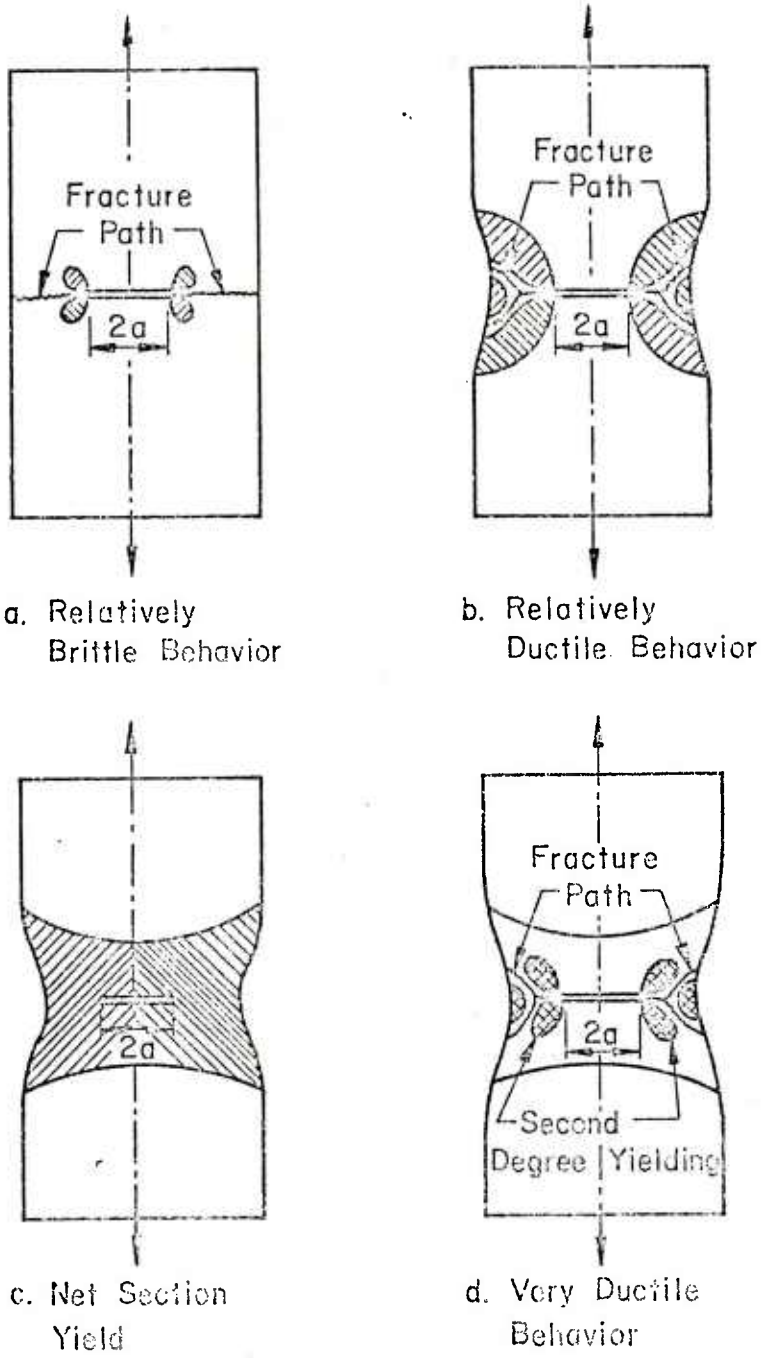

FIGURE IV-57 Brittle and Ductile Fracture Models

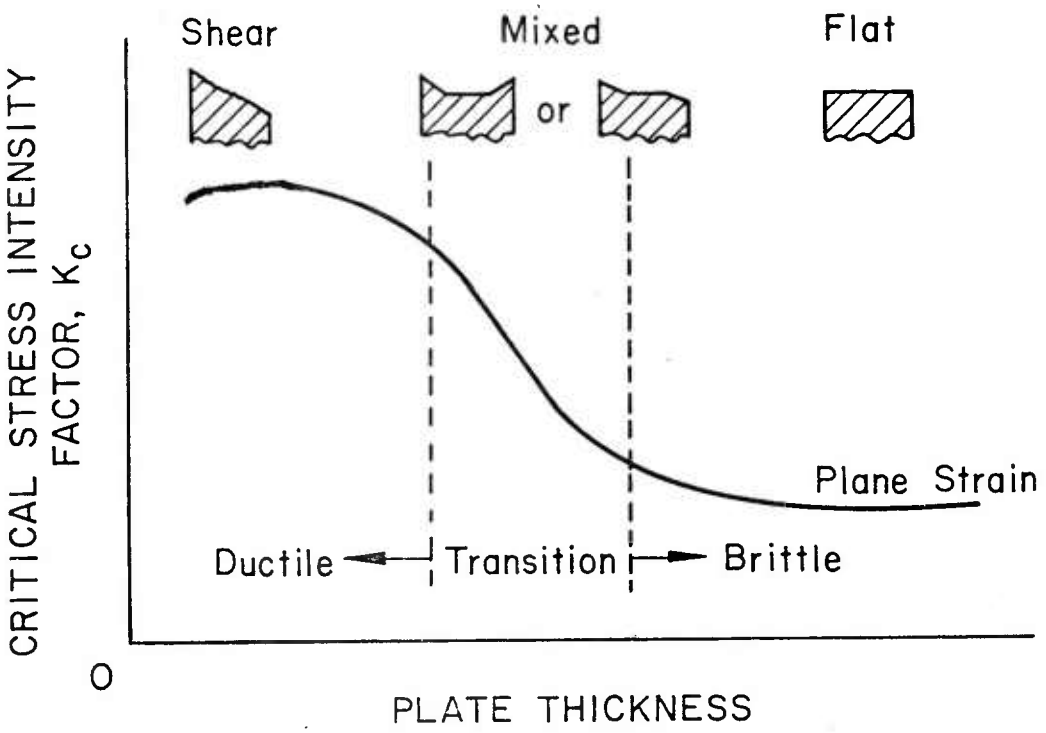

FIGURE IV-58 Variation of K_c with Plate Thickness

shown in Figure IV-59a is almost all flat; i.e., the through crack grows in its initial plane normal to the applied load. As the plate thickness is decreased, the crack will initially tunnel and then deviate from its own plane near the plate surfaces forming "shear lips." The crack growth is stable at first, advancing from its initial configuration in a planar fashion marked by the dotted area in Figure IV-59b with a curved front. Upon reaching the point of instability, the curved crack breaks through the plate. This can be traced on the loading history curve. Again, local conditions will determine whether the shear lip will form on one crack surface or the other. Further reduction in plate thickness leads to the decrease of flat surface, Figure IV-59c, and a slanted fracture pattern is finally observed.

c. Three-Dimensional Slow Crack Growth Predictions

In order to predict the aforementioned ductile fracture phenomenon, it is necessary to perform a three-dimensional elastic-plastic stress analysis and to have a fracture criterion that is amenable to analyzing crack

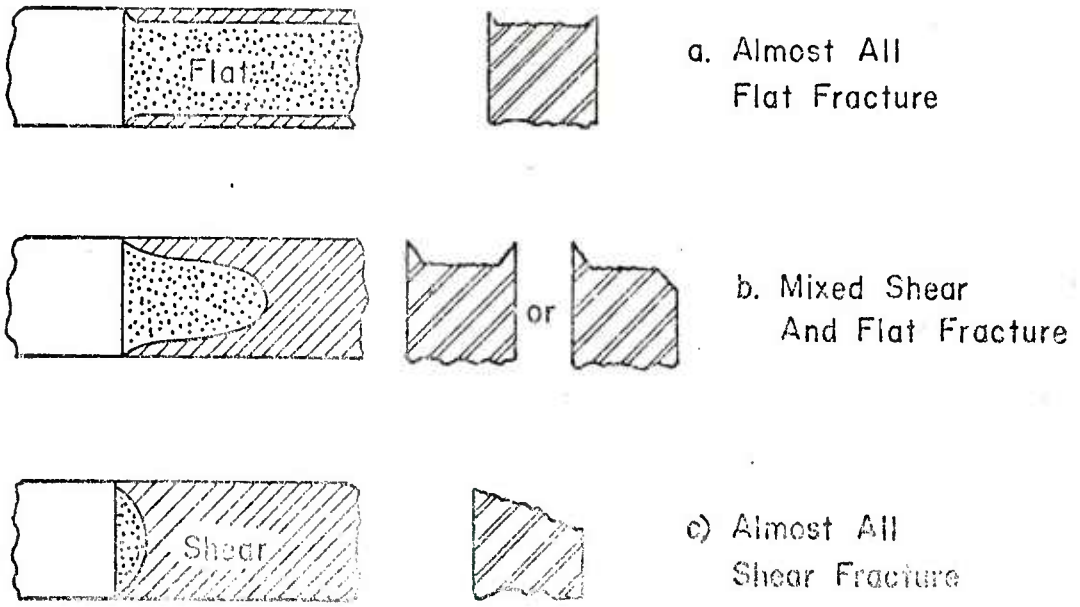

FIGURE IV-59 Appearance of Fracture Surfaces

tunneling and mixed mode crack extension of the type described earlier. It is desirable to analyze the stable growth process of a tunnel crack in a plate of ductile material. The influence of crack front curvature can be examined with the aid of a three-dimensional elastic finite element analysis in conjunction with a local growth criterion to predict increments of crack growth and corresponding changes in crack front shape. In general, both the direction and magnitude of local crack growth from the current crack front are expected to vary with position along that front. As a possible crack growth criterion, the strain-energy-density theory may be used (Sih, 1973). This criterion assumes that the path of growth from each point along the crack edge will follow the minimum strain energy density path emanating from that point. Further, growth at points along the current crack front will initiate when the strain energy density at a "core" distance r_0 along the minimum path reaches a prescribed value $(dW/dV)_c$.

Hence, growth of the crack front is approximated by discrete increments of growth. The amount of growth at a point along the crack front in an increment is taken to be the distance along the minimum strain energy density path, $(dW/dV)_{min}$, to the point where $(dW/dV)_{min}$ reaches a preset value, $(dW/dV)_c$, which depends on the material. (This value of $(dW/dV)_c$, assumed constant, is to be determined experimentally for a particular material.) Figure IV-60 gives a descriptive plot of strain energy density $(dW/dV)_{min}$ against the radial distance r in a plane normal to the applied load from the associated points A,B,---,F on the crack front. The new crack profile is determined from the various values of r and z/h on the graph where intersected by $(dW/dV)_c$. The selected value of $(dW/dV)_c$ will obviously affect the magnitude of growth and shape of the subsequent crack fronts. In Figure IV-60, z is the thickness coordinate measured from the mid-plane such that z/h = 0.5 locates the plate surface. This process can be repeated and the crack front geometry with each of growth can be

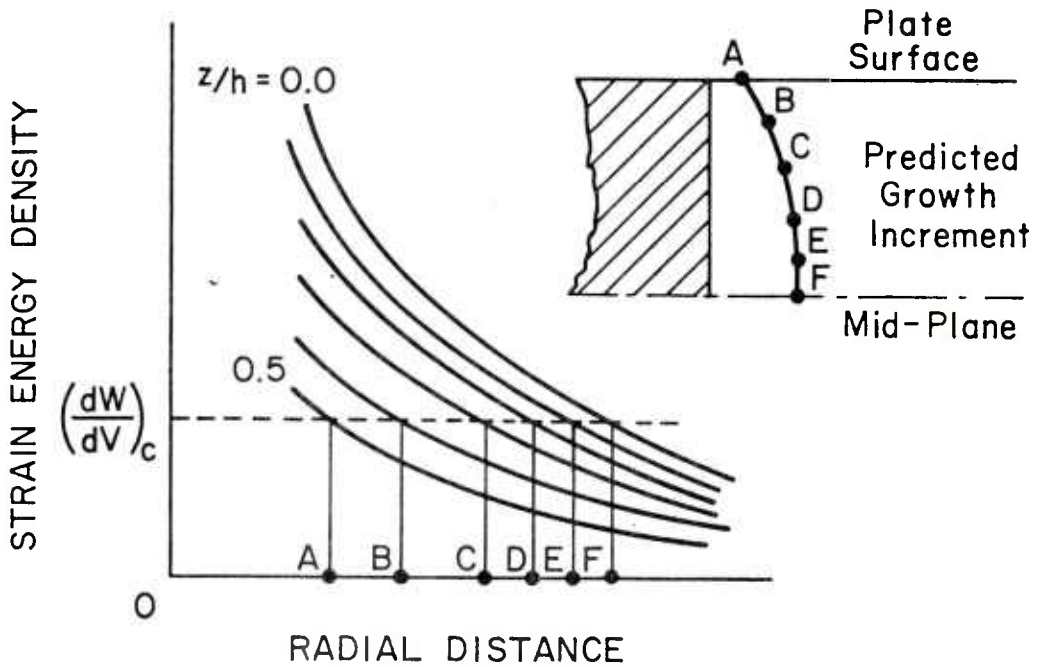

FIGURE IV-60 Crack Growth Predictions Based on Strain Energy Density

predicted as displayed in Figure IV-61. Crack tunneling will be a stable process as long as there is sufficient constraint from the necking of the plate surfaces. As this process continues, there will be a point on the load-deformation diagram at which the crack begins to grow rapidly; that is, when the specimen loses its structural integrity. It is expected that once the phenomenon of ductile fracture is analyzed and the shape and size of these tunneling cracks are calculated for a variety of situations, simple engineering formulas for design applications can be established.

6. Methods of Dynamic Failure Analysis

a. Introduction

For the types of loading described in Section III, dynamic (rather than static) stress analyses are normally required in assessing structural integrity. Similarly, as emphasized earlier in Section IV,B, dynamic analysis of test

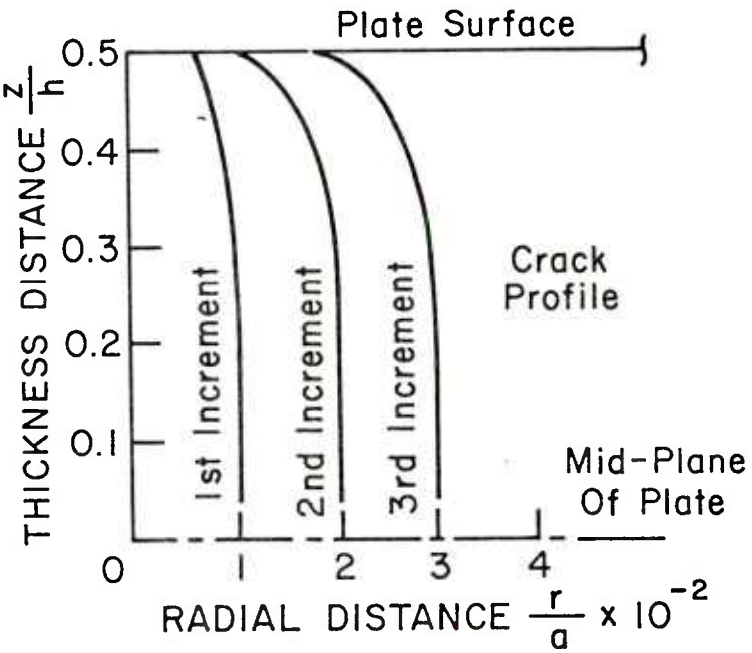

FIGURE IV -61 Predicted Increments of Crack Growth

specimens must be made in most cases if basic material and fracture parameters are to be properly extracted from test data. In this section, a brief review will be made of dynamic analysis techniques. The area of numerical methods of fracture analysis will be emphasized because significant advances have been made very recently, and it is believed these methods, when combined with general structural analysis computer codes, will provide the engineer with powerful, cost-effective tools that will aid greatly the design and evaluation of complex structures.

Dynamic buckling represents another mode of failure; it may lead to the total collapse of a structure and/or fracture, or at least excessive deformations. Furthermore, it is often true that dynamic buckling loads are less than the corresponding quasi-static critical loads, depending on the loading duration. In view of the importance of the problem of dynamic buckling of shells, with or without stiffeners, this area will also be discussed. Buckling is covered first, and it is followed by a more extensive review of dynamic fracture.

b. Dynamic Deformation and Buckling of Shells and Rings.

Numerical methods exist that are suitable for the analysis of a great many dynamic structural shell problems, with or without buckling action; e.g., see Pilkey et al. (1974), Almroth et al. (1976), Stricklin et al. (1974), and Yeung and Welch, (1977). There are, however, certain types of problems for which existing techniques are inadequate. In particular, very little progress has been made with respect to (1) the prediction of large deflections and rotations (as opposed to small or moderate values), (2) interactions with a surrounding medium, and (3) inclusion of realistic inelastic constitutive equations (especially if unloading and reloading effects are needed in the prediction of failure). Furthermore, the problem of asymetric dynamic buckling of shells is so complicated that the criteria for buckling are not even reasonably well understood; Akkaş, 1976, however, has made some recent progress in this area for spherical shells.

It should be pointed out that there has not always been complete agreement on a useful definition of dynamic buckling, whether symmetric or asymmetric. Currently, the most generally accepted criterion is based on that proposed

by Budiansky and Roth (1962): the peak in time history of a deflection is predicted as a function of the amplitude of the applied pressure or load; the amplitude for which this peak value undergoes a rapid increase is the buckling load or pressure. Unfortunately, to establish a dynamic buckling load according to this criterion requires a greater effort than that involved in the determination of all details of the response to a given loading history; the critical amplitude can only be determined after a number of transient response analyses have been performed. Nevertheless, the concept of a dynamic buckling load or pressure has the advantage of making possible the construction of design charts for at least relatively simple structures.

If one simplifies the material response to a rigid-plastic material with linear strain hardening, it is often possible to predict analytically the dynamic buckling of rings and shells (Jones and Okawa, 1976). Incorporation of rate-dependence of material behavior through the simple method of using a yield stress evaluated at the initial strain rate is found to be quite accurate in some problems (Perrone, 1965). Agreement between analytical predictions and experimental results for average permanent radial deformation of rings due to impulsive external pressure loading is quite good; similarly, experimental verification exists for the theoretical threshold value of impulse which produces significant wrinkles (Jones and Okawa, 1976).

c. A Review of Some Recent Literature on Dynamic Fracture Analysis.

Much of the work in the area of dynamic fracture analysis has been done on simple geometries, often two-dimensional. The use of such analytical studies is three-fold: (1) analytical solution using simple shapes is relatively expedient (indeed, often at the time, treatment of more complex shapes is not feasible); (2) comparison of the dynamic analysis results with static results for some geometries provides a simple means of understanding the dynamic effects; and finally, (3) results of the analysis can be checked against experimental results, thus not only providing a means of validating the analysis procedure but also helping one to understand the experiment more thoroughly.

The methods of dynamic fracture anlaysis can be broadly classified into three categories:

Classical, finite difference, finite element

Classical Methods - Classical Methods (i.e., analytical methods of solution) have been in vogue for the longest period of time. These methods have been successfully applied to many simple geometries. For example, Sih and Embley (1972) applied the integral transforms method coupled with the technique of Cagniard to the solution of impact response of a finite crack. The Laplace transform technique was applied by Freund and Rice (1974) to the elastodynamic crack tip stress field. More recently, influence of specimen boundaries on the dynamic stress intensity factor was studied by Chen and Sih (1974) by means of Laplace and Fourier transforms.

Problems of running cracks have also been analyzed by the classical methods. Rapid extension of a penny-shaped crack under torsion was studied by Kennedy and Achenbach (1972), using the Green's function technique. Achenbach (1975) analytically studied the elastodynamic bifurcation of running crack in antiplane strain. Chen and Sih (1975) studied the problem of scattering of plane waves by a propagating crack using the Fourier transform. The effect of crack speed and other related phenomena in the dynamic ductile fracture of a central crack were analyzed by Tsai (1976) with the help of the integral transform method.

It must be stated here that most of the applications above are phenomena oriented. To study a problem or gain understanding of certain phenomena, the researcher develops his field equations and solves those equations by a method most attractive to him for various reasons. That the results obtained from various such studies are useful cannot be disputed. On the other hand, these methods cannot solve a general geometric shape and are otherwise limited in scope. Therefore, whereas individual researchers will continue to use these methods, at the present time the classical methods do not qualify as a general purpose engineering analysis tool.

Finite Difference Method - The finite difference method is a powerful numerical tool for solving a complex boundary value problem. The method itself is widely illustrated in the literature and therefore will not be discussed here. We present instead some of the recent applications of the method to the fracture problems.

A two-dimensional dynamic fracture experiment was simulated using the finite difference method by Stöckl and Auer (1976). They solved two problems. In the first problem, they studied the constant velocity propagation of a brittle tensile crack in finite plane-strain model under uniaxial tension. In the second problem, the model was modified to allow for a specified variable crack propagation velocity in a nonhomogeneous prestress field. The authors advocate the use of a transition zone at the crack tip between the stress-free surfaces and the uncracked state. They point out that if a transition zone is not used, the "cracking node" is released suddenly and the energy stored at the crack tip is converted into large oscillations. In solving the first problem through 250 time steps with a 110 x 110 grid, it took 3.5 min on UNIVAC 1108 computer.

Shmuely and Peretz (1976) modeled the static and dynamic DCB tests using the finite difference method. The authors use the stress σ_{θ} normal to the crack plane at one-half the finite difference grid length ahead of the crack tip as the criterion for predicting speed. When this stress reaches a specified constant value, the crack length is extended one grid length. They found that for any one value σ_{θ}, the crack propagation speed remains approximately constant. However, it should be noted that the criterion employed is purely an assumed one, and therefore is not necessarily the proper one.

HEMP and HEMP 3D (Chen and Wilkins, Aug 1976 and Nov 1976) are the well-known finite difference programs. These programs were originally designed and developed for solving dynamic problems in continuum mechanics - and have been extended to analyze the stress field around cracks in a two or three-dimensional solid with finite geometry subjected to dynamic loads. These codes employ an explicit time integration of the Lagrangian formulation of the equations of continuum mechanics in which the calculation grid moves with the material. A special extrapolation scheme to simulate the singularity near the crack tip has been introduced in the program. There are two methods employed for modeling the separation of surfaces during crack propagation. In one method the grid is actually split with the help of sliding interface logic; in the other case the effects of the free surface boundary conditions are introduced without actually splitting the grid. A smoothing procedure is used to avoid spurious oscillations during a

sudden split in the grid. The relevant constitutive properties can be rate-dependent. The material model can be elastic, plastic, etc. A discussion on crack propagation criteria is given in Chen and Wilkins (1977).

Figure IV-62 shows the Lagrange grid used in calculations of the effect of a semielliptical surface crack and an imbedded (internal) elliptical crack for a specimen which is subjected to a constant, suddenly applied symmetrical tension loading. Figures IV-63 and IV-64 illustrate

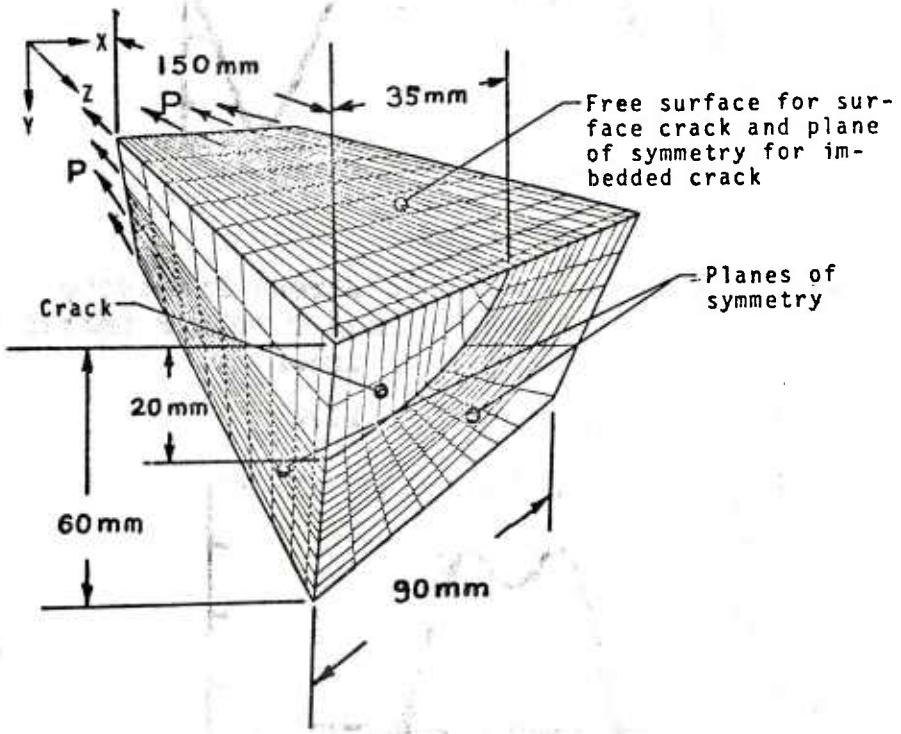

FIGURE IV-62 Lagrange Grid Used in Calculations of a Semielliptic Surface Crack and an Imbedded Elliptical Crack.

SOURCE: Chen and Wilkins, November 1976

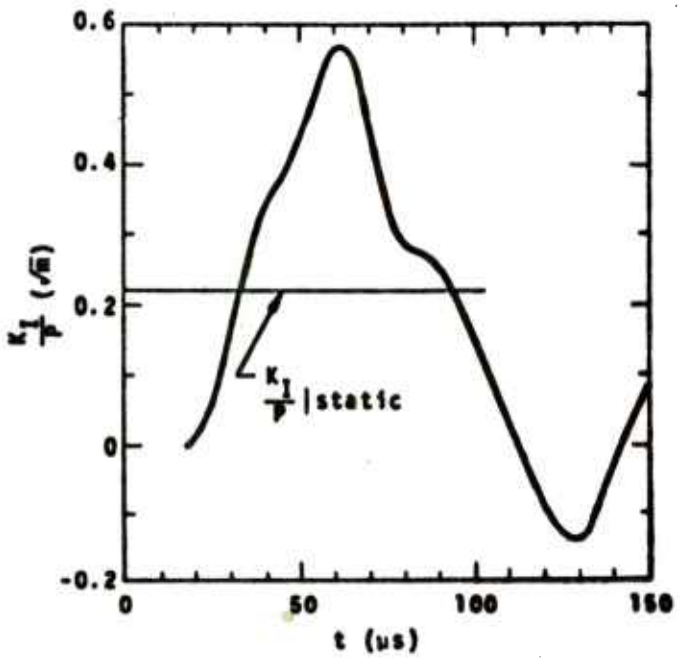

FIGURE IV-63 Normalized Stress Intensity Factor versus Time for Imbedded Elliptical Crack

SOURCE: Chen and Wilkins, November 1976

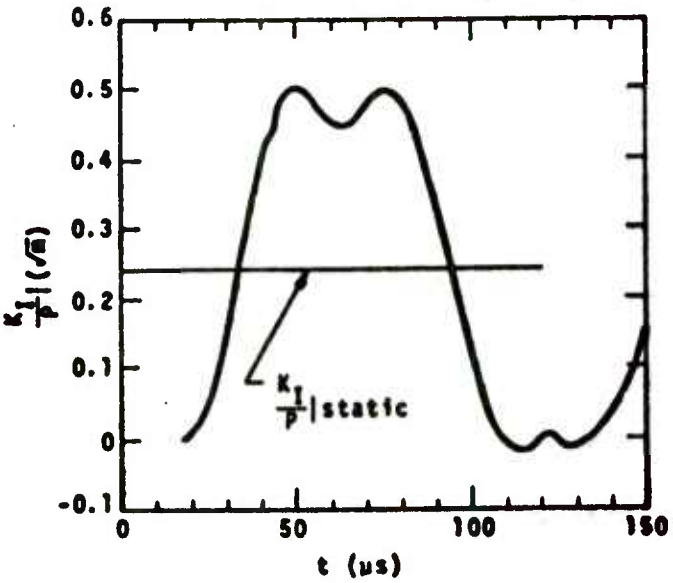

FIGURE IV-64 Normalized Stress Intensity Factor versus Time for Semielliptic Surface Crack

SOURCE: Chen and Wilkins, November 1976

the variation in the stress intensity factor with time for these two cases. The geometry of axial and circumferential cracks in the wall of a cylindrical pipe is shown in Figure IV-65; stress intensity factors due to a constant, suddenly applied pressure for these two types of cracks are shown in Figures IV-66 and IV-67 for several time steps. More recently, Wilkins (1977) extended the HEMP codes to running cracks using an accumulated damage model. In spite of the power of these codes, severe limitations to our prediction capability still exist because of uncertainties in the material characterization and the crack initiation and growth criteria.

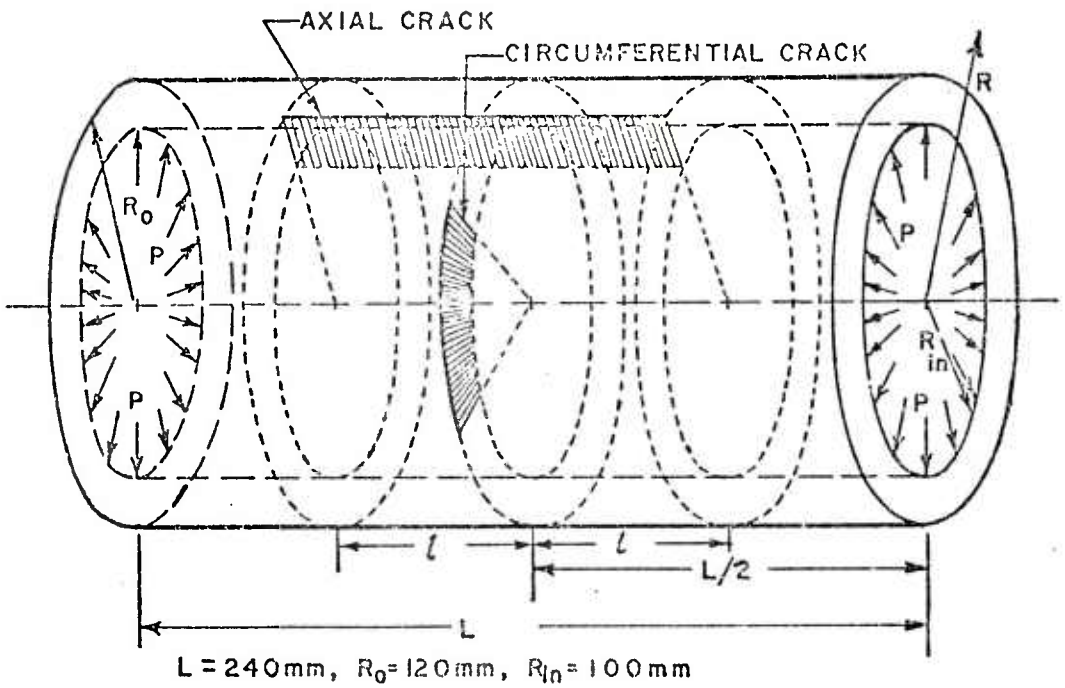

FIGURE IV-65 Geometry of the Axial and Circumferential Cracks in the Wall of a Section of Cylindrical Pipe

SOURCE: Chen and Wilkins, November 1976

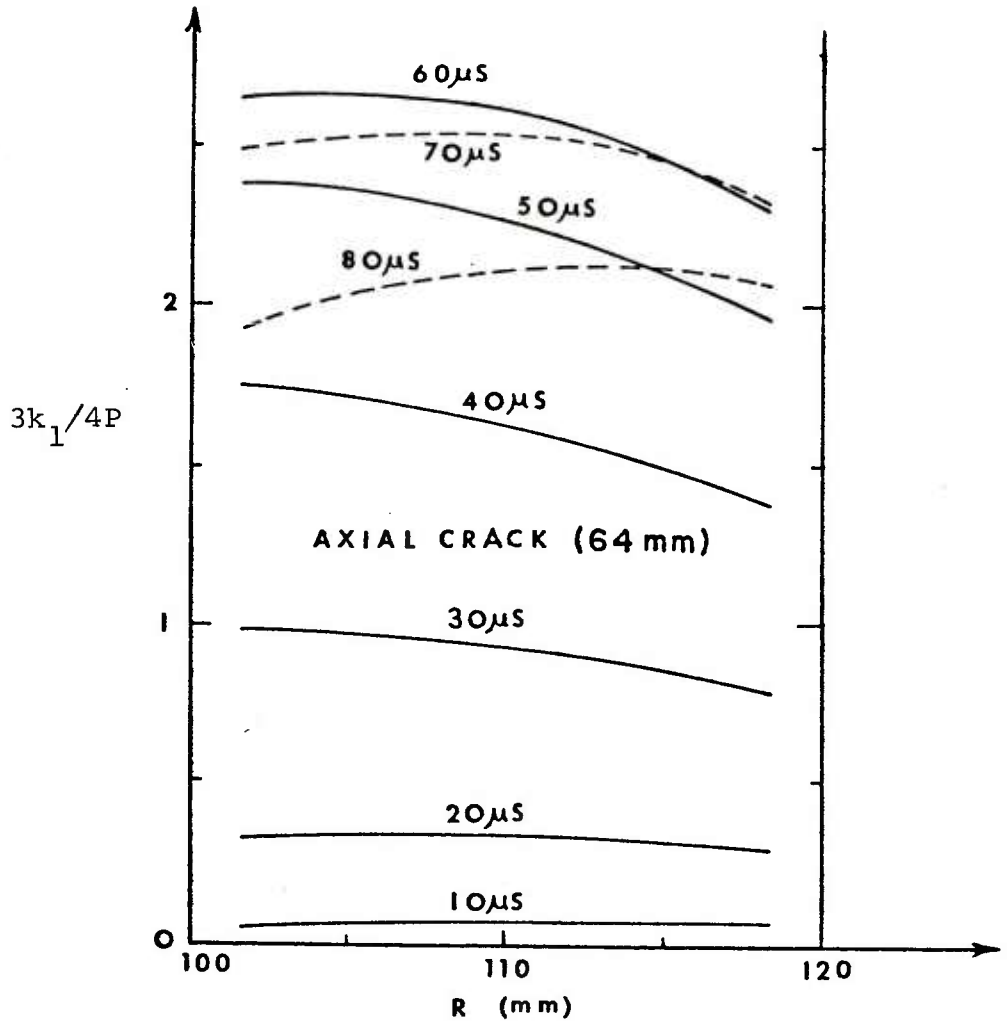

FIGURE IV-66 Normalized Stress Intensity Factor $3k_1/4P$ versus R at Several Steps for the Axial Crack

SOURCE: Chen and Wilkins, November 1976

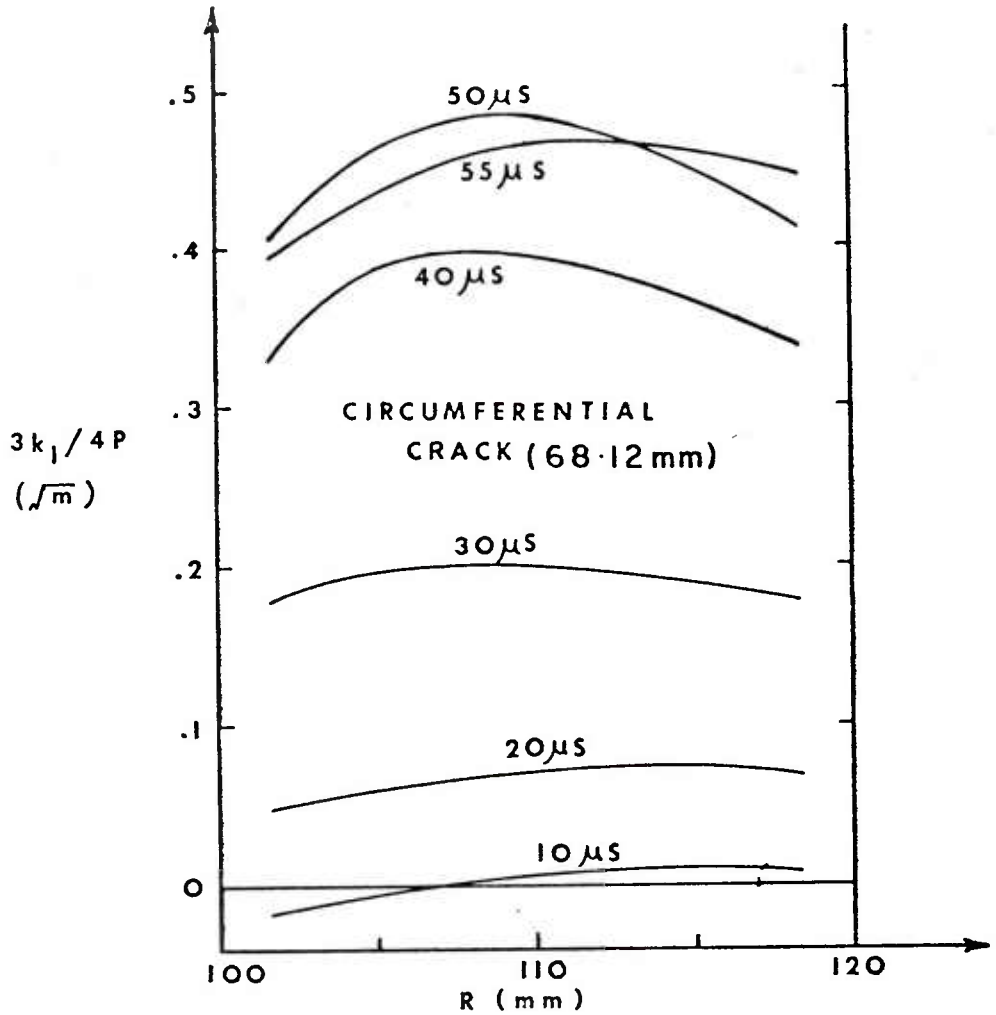

FIGURE IV-67 Normalized Stress Intensity Factor $3k_1/4P$ versus R at Several Time Steps for the Circumferential Crack

SOURCE: Chen and Wilkins, November 1976

Finite Element Method - Development of the finite difference method of solution preceded the development of the finite element method (FEM). However, the FEM is used in most stress analysis applications today. Whereas both methods are general purpose and applicable to a wide spectrum of problems, the finite element method is much more versatile and efficient in terms of adapting to almost any shape of the medium and in applying the boundary conditions. In this

section we shall review some of the recent applications of the FEM in dynamic fracture mechanics. The actual development of the method as applied to fracture problems will be discussed in the next section.

Aberson et al. (1976) applied the FEM to dynamic fracture problems. They used a computer program for two-dimensional elastic structures. It consists of rectangular elements, one for opening mode problems and one for mixed mode problems. The displacements within the elements are represented by a finite series of Williams' eigen functions. Consistent, lumped mass matrices are included in the program. Figure IV-68 shows the finite element model of a plane-strain rectangular strip which is centrally cracked. The variation in stress intensity factor with time under a suddenly applied

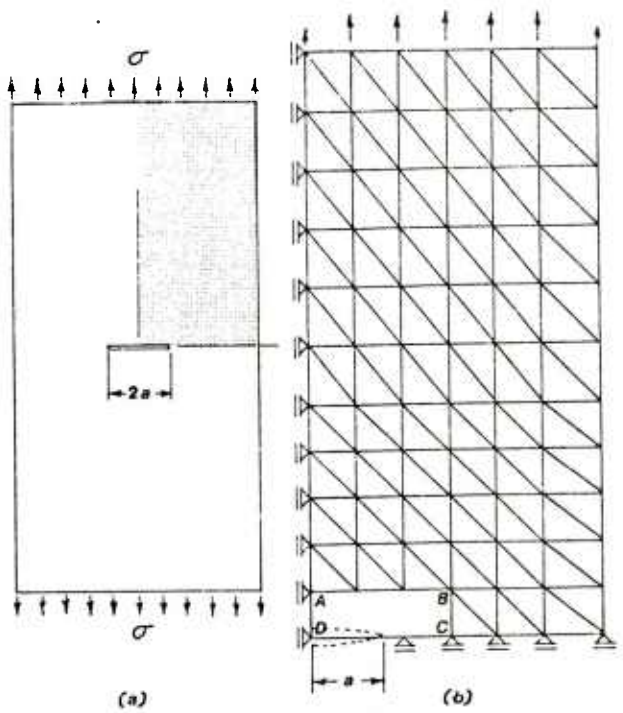

FIGURE IV-68 The Finite Element Model

SOURCE: Aberson et al, 1976

tension is shown in Figure IV-69. Figure IV-70 is a finite element model of a dynamic tear test specimen of Homalite-100, a photoelastic material. (The specimen support and loading configuration are essentially those of a Charpy test except that a translating steel hammer is used in place of a pendulum for the impact source.) The node corresponding to the impact point is assigned a mass equal to one-half of the mass M of the hammer. This node is then given an initial velocity V_0 equal to the impact velocity; all other nodes have zero initial velocity. Since the specimen is thin, plane-stress elements were used; however, it should be recognized that plane stress close to the crack tip does not

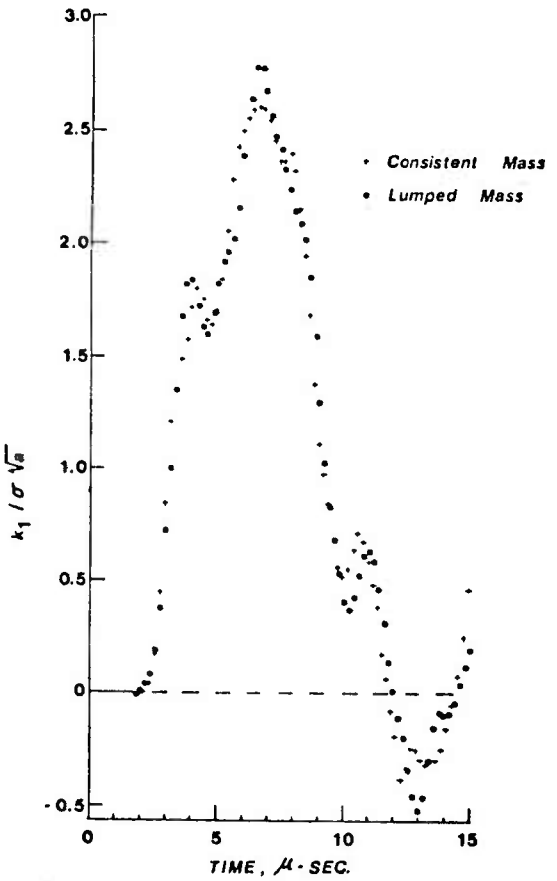

FIGURE IV-69 Stress-Intensity Factors Predicted Using Different Mass Distributions

SOURCE: Aberson et al, 1976

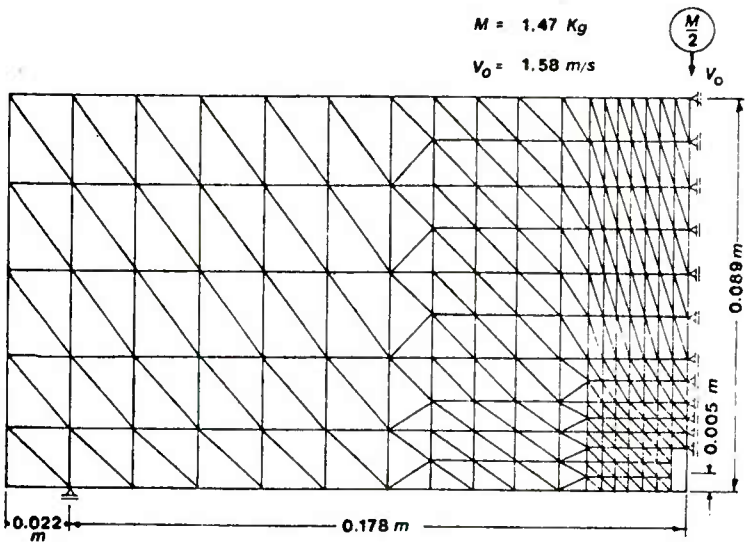

FIGURE IV-70 Finite Element Model of a Dynamic-Tear Test Specimen

SOURCE: Aberson et al, 1976

exist. The numerical results are given in Figure IV-71 for a crack of constant length of 0.005 in.

Aberson et al. (1976) have also reported a parallel study on the running cracks using the finite element method. In this case they used simple constant strain triangles. The finite element mesh is particularly refined in the vicinity of the crack path. A constant crack propagation speed is imposed. As the crack reaches a node its constraint is released. The results are preliminary in nature and need further refinement.

Ayres (1976) has performed a two-dimensional elastic-plastic finite element analysis of the precracked Charpy V notch specimen with a crack of constant length using the MARC (1976) finite element program. Figure IV-72 shows a finite element model for this specimen. The mesh at the crack tip is constructed with 8 node isoparametric quadrilaterals with midside nodes one quarter of the way from the crack tip to the element corner. The nodes of each element at the crack tip are distinct and are free to move independently in the direction of the crack. This type of modeling provides a 1/r strain singularity appropriate for plastic behavior (cf. Section d).

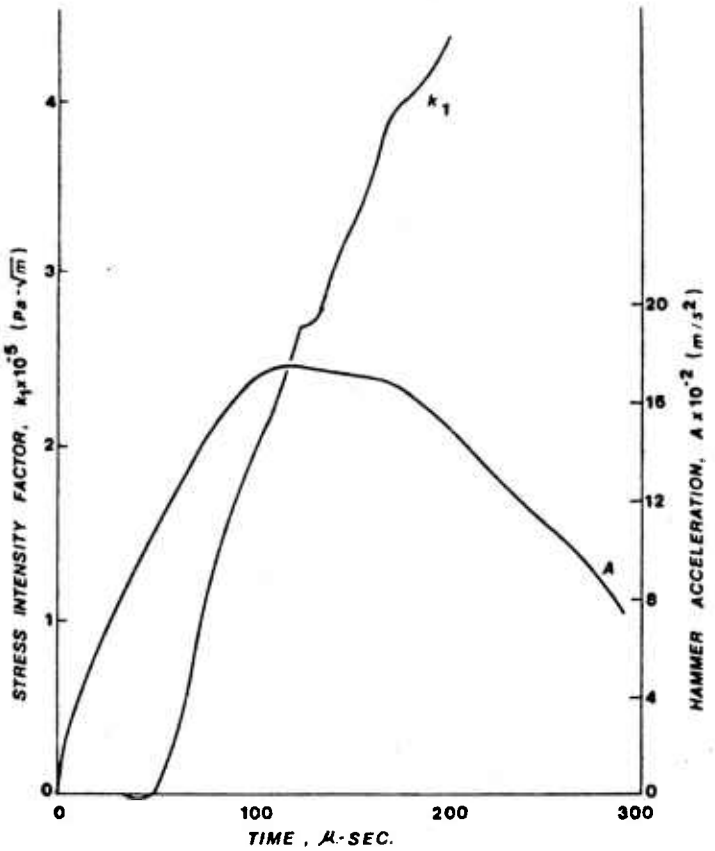

FIGURE IV-71 Stress Intensity Factor and Hammer Acceleration for a Dynamic-Tear-Test

SOURCE: Aberson et al, 1976

Figure IV-73 illustrates the comparison between the computed and measured applied load-time curve for the case when the specimen is loaded at a constant velocity. Although not perfect, comparison seems to show reasonable agreement. In the same analytical study, Ayres also showed that the dynamic crack opening displacement near the crack tip ($.01\alpha$) is much greater than the statically computed value.

Applicability of the MARC type finite element analysis is apparent from Ayres' numerical studies. In

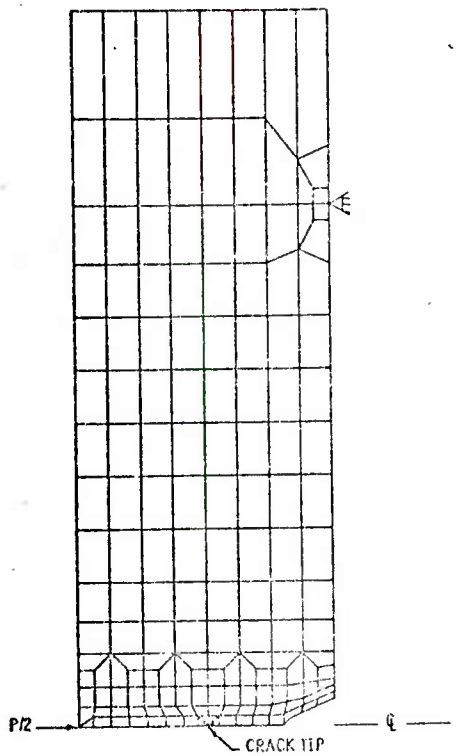

FIGURE IV-72 Finite Element Model of Precracked Charpy Specimen

SOURCE: Ayres, 1976

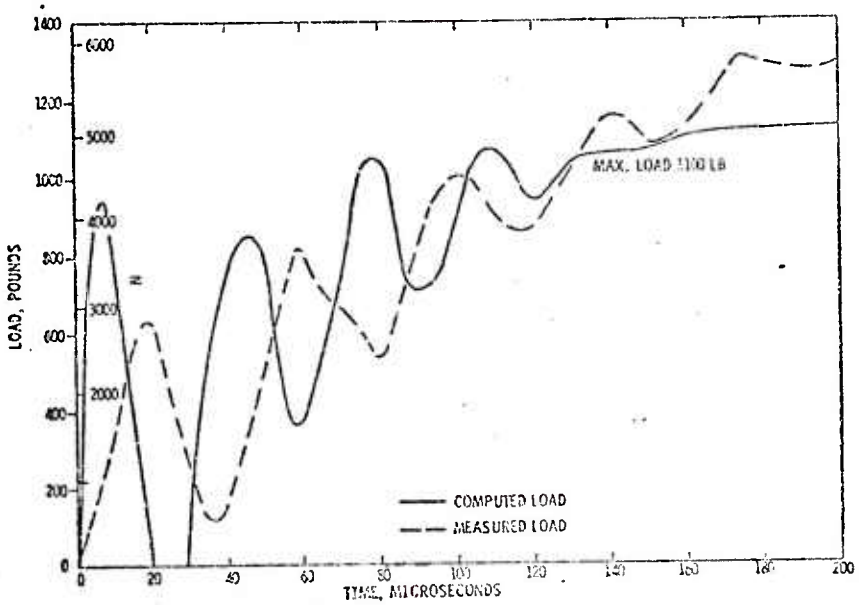

FIGURE IV-73 Load-Time Curve Computed from Elastic-Dynamic Analysis with Constant Velocity of Loaded Point

SOURCE: Ayres, 1976

principle, similar three-dimensional elasto-plastic, dynamic analyses can be performed using the same program. Constitutive properties for elasto-plastic behavior can be input; rate dependence can be incorporated only through a specified constant strain rate. Furthermore, a crack propagation criterion is not used in MARC (1976).

d. Discussion of the Finite Element Method.

As indicated earlier in this section, the FEM is the most versatile tool of structural analysis that is available today. As the field of analytical fracture mechanics grows and the practical application of analysis to important design problems spreads, greater development and use of this method is inevitable. The basics of the finite element method are amply described in textbooks (e.g., Zienkiewicz, 1971). However, for reference purposes, it will be desirable to describe them very briefly. Important aspects of the crack tip finite element will be reviewed in more detail.

For linear media, the equation of motion to be solved is

$$M \ddot{U} + C \dot{U} + K U = F(t) \qquad \text{(IV-69)}$$

where

M = mass matrix
U = displacement vector
C = damping matrix
K = stiffness matrix
F = force vector
$(\dot{})$ = time derivative

Let us consider a continuum finite element (2 or 3 dimensional) with M degrees of freedom. The displacement at any point within the element is given by

$$u_i = N^m u_i^m \qquad \text{(IV-70)}$$

where

N^m = shape function (or interpolation function) at node m
u_i^m = value of displacement u_i at node m

The repeated sub- or superscripts imply summation. The subscript 'i' is for spatial directions in the Cartesian space. In 2D, i = 1,2; whereas in 3D, i = 1,2,3. The strain is given by

$$\epsilon_{ij} = Z^{m}_{ijk} u^{m}_{k} \qquad \text{(IV-71)}$$

where

$$Z^{m}_{ijk} = 1/2\left(\frac{\partial N^{m}}{\partial x_i}\,\delta_{jk} + \frac{\partial N^{m}}{\partial x_j}\,\delta_{ik}\right) \qquad \text{(IV-72)}$$

in which δ_{ij} represents a Kronecker delta.

The linear elastic stress-strain relationship is

$$\sigma_{ij} = E_{ijk\ell}\epsilon_{kL} \qquad \text{(IV-73)}$$

The nodal forces can be obtained from the principle of virtual work for an element; there results

$$P^{m}_{k} = \int Z^{m}_{ijk}\,\sigma_{ij}\,dV \qquad \text{(IV-74)}$$

where the integral is over the volume of the element. Equations IV-69 to IV-74 yield an element nodal force-displacement relationship,

$$P^{m}_{i} = K^{mn}_{ij}\,u^{n}_{j} \qquad \text{(IV-75)}$$

in which K^{mn}_{ij} is the stiffness matrix,

$$K^{mn}_{ij} = \int E_{ijk\ell}\,\frac{\partial N^{m}}{\partial x_k}\,\frac{\partial N^{n}}{\partial x_\ell}\,dV \qquad \text{(IV-76)}$$

The so-called consistent mass matrix for the element is obtained from

$$M^{mn} = \int \rho N^m N^n dV \qquad \text{(IV-77)}$$

The lumped mass matrix is derived by lumping the off-diagonal terms; viz.,

$$M^m = \int \rho \, N^m \, dV \qquad \text{(IV-78)}$$

The overall structural mass and stiffness matrices are obtained by appropriately combining the element mass and stiffness matrices. There are various methods of specifying the damping matrix, which are described in the literature. The following observations are made on the above discussion:

(1) If all the finite elements, including those at the crack tip, are displacement type, then the above procedure directly applies to fracture mechanics problems. If the stress intensity factor is included as an unknown, then the vector U can be treated as a generalized quantity which consists of the unknown displacement and the stress intensity factors.

(2) In a nonlinear material problem, Equations IV-70, 71, 72, 74, 77 and 78 still hold. Equation IV-73 holds in an incremental linear representation provided $E_{ijk\ell}$ is the tangent material property tensor. Then Equation IV-76 yields a tangent stiffness matrix. In this case, Equation IV-69 becomes

$$M\Delta\ddot{u} + C\Delta\dot{u} + K\Delta u = \Delta F$$

In the case of a large displacement/large strain problem, K must be further modified to include nonlinear geometric effects (Zienkiewicz, 1971).

(3) In case of a crack propagation problem, the net effect is change in the connectivity of the finite element model. Appropriate logic to reorganize Equation IV-69 or Equation IV-79 can be easily implemented in a computer program.

Crack Tip Elements

It is well known that a crack tip exhibits a singularity. For a linear elastic material, the stress and strain singularity is of order $1/r$, and for the perfectly plastic material, the stress singularity is of order $1/r$ (Hutchinson, 1968). This means that theoretically strains are infinite at the crack tip, and that they vary rapidly in the vicinity of the crack tip. Some of the earlier attempts in finite element application had been with the help of conventional finite elements without the required singularity. The elements were very small in the vicinity of the crack tip. However, it was found that such a procedure resulted in an unsatisfactory stress field (Hilton and Sih, 1973). In addition, this procedure is very inefficient computationally because of having an unnecessarily high number of degrees of freedoms. The answer to the problem was development of finite elements which would include the appropriate singularity. Use of such elements enables one to predict accurately stress or strain intensity factors which, in turn, may be employed in crack initiation and growth criteria.

A number of special crack tip finite elements have been presented in the literature. They can be classified into two groups. In the first group the crack tip is imbedded in the interior of the element; in the second group the crack tip is enclosed by a number of special elements, all of which have one of their nodal points at the crack tip.

Elements of the first type were first developed by Wilson (1968), and by Hilton and Hutchinson (1971). These elements are circular in shape. Wilson's element had prescribed displacements representing the mode III (antiplane) elastic singularity. Hilton and Hutchinson's element displacements were those associated with the singularity for an elastic-plastic power hardening material under mode I plane stress and mode III antiplane conditions. Byskov (1970) and Wilson (1971) later presented improved elements

by adding more terms to the displacement function of the element. The displacement coupling between the circular element boundary and its neighboring triangular elements is maintained by imposing a displacement constraint on the triangular elements: The displacements of nodal points of the neighboring elements which lie upon the perimeter of the circular element are set equal to those of the circular element. A minor incompatibility still persists - the edge of the Wilson element is circular and the displacements vary along it linearly with the angle θ, whereas the edge of the neighboring element is straight, and the displacement in this element varies linearly along the edge. However, it is easy to see that as the number of nodes along the circle increases, the incompatibility diminishes. Holston (1976) has extended the Wilson element to the mixed mode I and II problem by including additional terms in the displacement expansion.

Tracey (1971) and Wilson (1971) developed triangular elements which enclose the crack tip in a fan-type arrangement (cf. Figure IV-74). They both include a term proportional to $\sqrt{r}$ in the displacement expansion, which gives a $1/\sqrt{r}$ singularity in the stress field appropriate for the mode I elastic singularity. The main difference between the Tracey and the Wilson elements is in the manner in

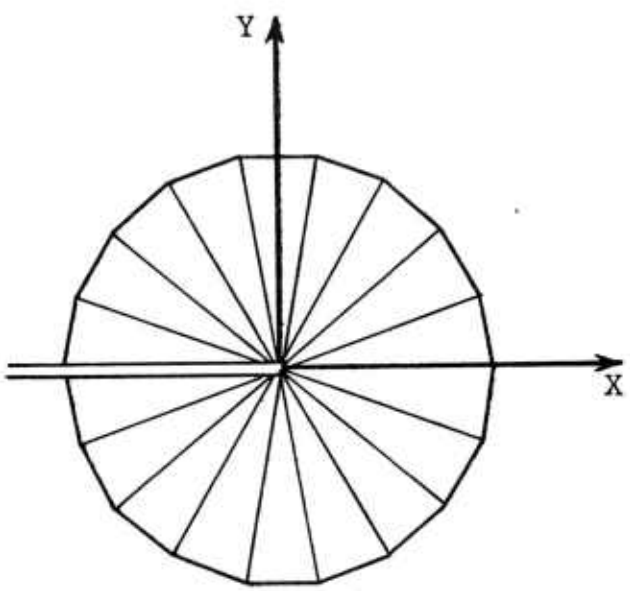

FIGURE IV-74 Crack Tip Enclosed by Triangular Crack Tip Elements

which the interpolation is performed in the circumferential direction. Wilson uses interpolation functions which are linear in the polar angle θ. This approach causes a minor incompatibility depending upon the number of nodes on the circle. Tracey uses an interpolation function which is linear along the straight line joining the two circumferential nodes.

Wilson has shown that his higher order circular element (1971) is superior in performance to other candidates discussed above (1973).

During the last two years, a new breed of crack tip elements has been proposed. Basically, these elements are the regular isoparametric elements (Ergatoudis, 1968) which, with a special arrangement of nodes, yields the desired singularity. The first such attempt was published by Henshell and Shaw (1975). They showed that a $1/\sqrt{r}$ stress singularity develops in the 8 node isoparametric finite element if the midside nodes of two adjacent edges are moved to quarter points, as indicated in Figure IV-75. Soon after the paper by Henshell and Shaw, Barsoum (1976a) published

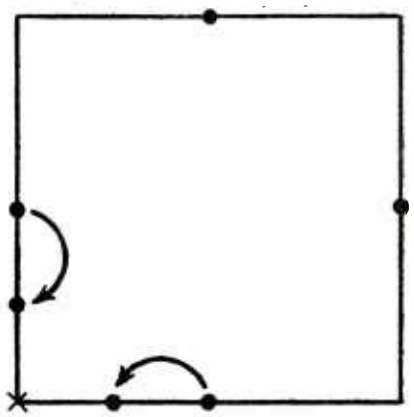

FIGURE IV-75 Eight Node Isoparametric Element

a similar paper. He showed that by collapsing one of the sides of the 8 node isoparametric elements and moving the midside nodes of the edges adjacent to the collapsed edge to the quarter point, a $1/\sqrt{r}$ stress singularity is again obtained (cf. Figure IV-76). The same approach is also applicable to the 3D element. He later extended his method to plate bending and general shell elements (Barsoum, 1976). Recently, Barsoum (1977) has suggested that if 3 common nodes in his degenerate 8 node element are left unconstrained, a 1/r strain singularity results, which is appropriate for mode I plastic strain field. The obvious advantage of using Barsoum's approach is that many computer programs already have isoparametric element. Therefore, no new program development is required in their use in the fracture problem.

Hellen (1977) in his discussion of papers by Henshell and Shaw (1976) and Barsoum (1976) proposes to use a special isoparametric element which uses a slightly different displacement field than the one aimed at by the referenced authors. Hellen's element gives results which are almost identical to those of Barsoum.

For most cases the degenerate isoparametric elements discussed above appear to be very attractive. However, neither these nor other elements provide all the crack and corner singularities that may be encountered in practice. Therefore the work on new elements continues.

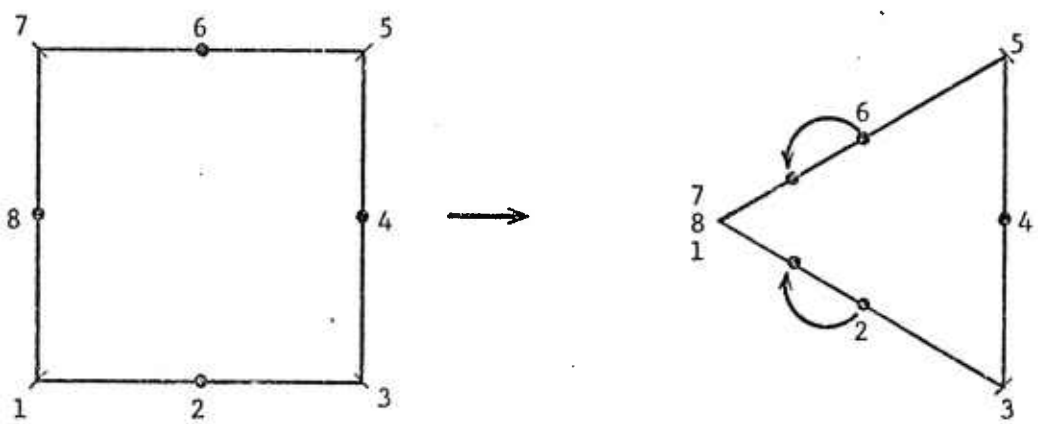

FIGURE IV-76 Barsoum's (1976a) Eight Node Isoparametric Element for Crack Tip Analysis

e. Conclusions on Fracture Analysis

(1) Several problems have been solved using the classical (analytical) methods of analysis. The problems solved are for bodies of simple shapes and are otherwise limited in scope. As noted in the text, solution of such problems is useful in studying physical phenomena. On the other hand, these methods cannot be applied to most realistic engineering problems.

(2) It is possible to solve a quite general problem using the finite difference method. Application of this method has been demonstrated by the use of HEMP and HEMP 3D codes. The main problem with running cracks is in the definition of the propagation criterion.

(3) There is extensive literature available in the application of the finite element method to simple geometry problems. Programs like MARC can be applied to complicated dynamic problems, after sufficient confidence has been achieved.

(4) In the case of both the finite difference and the finite element methods of analysis, the material can be either elastic or elasto-plastic, or practically any other type. Conceptually, strain rate effects can be incorporated. However, the applications made so far are limited to the use of material properties for an assumed constant strain rate.

(5) Special crack tip finite elements have been developed for singularities in elastic and perfectly plastic materials. By suitably locating the nodes, one can use a planar and three-dimensional isoparametric element for both materials. Similar formulation is possible for the plate bending and general shell elements. All of these elements are based on asymptotic expansions to represent the crack tip singularity. These expansions have been established so far for only elastic and uniform plastic behavior near the crack tip, whereas in reality there is a nonuniform elastic-plastic zone.

C. Scale Modeling

One of the three major purposes of this study is to recommend areas where current practices should be strengthened with regard to small scale tests. It is expected that improvements in scale modeling techniques will reduce the need for expensive and time-consuming full-scale testing.

Modeling is a procedure in which similitude analysis is used to design tests conducted to predict the structural or material behavior of a prototype structure subjected to various loadings. This procedure may be used for a number of purposes: (1) evaluate the structural and material limitations of the proposed prototype; (2) experimentally evaluate and guide analysis procedures; (3) obtain response information that no other engineering techniques can provide; and (4) develop empirical damage rules to improve designs to resist dynamic loading.

Large and full-scale models are frequently employed simply because of a lack of confidence in smaller-scale models, despite the cost and time consumption. This lack is due to a belief that small-scale models will not duplicate the many critical structural and material conditions that interact under dynamic loading. However, through careful application of scaling principles, models can be very effective for the purposes listed above.

Basically, there are four types of similarities*

- Geometric similarity - The geometric dimensions of the prototype are scaled by a constant scale factor.
- Kinematic similarity - The pure motion, without reference to masses or forces, is duplicated.
- Dynamic similarity - The responses such as displacements, velocities, accelerations, forces, strain rates, etc. are scaled.
- Constitutive similarity - All relevant material response parameters, such as fracture toughness, are scaled.

* See Baker et al. (1973) for a detailed treatment of theory and practice of scale modeling.

In many cases, all similitude parameters for a given problem cannot be satisfied simultaneously. This leads to the selection of alternate types of modeling, such as replica versus nonreplica. By definition, a replica model has geometrical similarity and is constructed of the same material as the prototype. The scaling is in size alone. Replica models are valid for a broad range of material behavior, including linear elastic, nonlinear elastic and elastic-plastic; fracture as well may be included when it can be defined by global quantities such as maximum stress or maximum strain. However, in replica modeling certain important parameters are not scaled properly; the most significant of these relate to strain-rate dependence and fracture toughness. Nonreplica models, by definition, use materials which are different from those in the prototype. This feature provides flexibility in fabricating the models and in satisfying the required similitude parameters.

If response depends on fracture toughness, a good prospect is to seek materials which preserve the ratio of the plastic zone size to the plate thickness; as an approximation one might use

$$\left(\frac{K_d^2}{t\sigma_Y^2}\right)(\text{model}) = \left(\frac{K_d^2}{t\sigma_Y^2}\right)(\text{prototype})$$

where K_d is dynamic fracture initiation toughness, t is plate thickness and σ_Y is yield stress. A program of experiment and analysis could be conducted to select appropriate scaling parameters using this rule (or other more suitable rules) and to verify that model tests using toughness-scaled materials will give reliable information on actual structures with flaws.

The justification for using small-scale models has been greatly enhanced by the rapid improvements in computer coded analytical methods of predicting dynamic response. If the analysis can accurately predict the response for the model, there is good reason to believe that the prototype will respond in a similar manner, providing the model correctly represents the prototype; depending on the problem, it may be necessary to account in the model for the effect of imperfections (flaws and/or geometric distortions) and residual stresses. As discussed in earlier sections,

proven analytical codes describing linear and nonlinear elastic behavior are numerous, and recently there has been good progress in developing analyses for elastic-plastic response.

The capability to predict dynamic fracture of a full-scale fabricated flawed structure solely by analytical methods is not likely in the near future. For certain structures, nondestructive testing (NDT) procedures, applied in service, can alleviate this problem. In the interim, it is believed to be more realistic to use analytical techniques to determine overall response of a structure and to make a full thickness model of a small segment, or substructure, for fracture toughness testing. In all these situations, there is no doubt that continued improvements in analysis directly enhances the use of small-scale models and substructure models.

REFERENCES - SECTION IV

Aberson, J. A., Anderson, J. M. and King, W. W., "Finite Element Analysis of Dynamic Fracture," Advances in Engineering Sciences, Vol. 1, Proceedings, 13th Annual Meeting, Soc. of Eng. Sc., Hampton, Virginia, November 1-3, 1976.

Achenbach, J. D., "Bifurcation of a Running Crack in Anti-plane Strains," Int. J. Solids Structures, Vol. 11, 1975.

Akkas, N., "Bifurcation and Snap-through Phenomena in Asymmetric Dynamic Analysis of Shallow Spherical Shells," J. Computers and Structures, Vol. 6, 1976, pp 241-251.

Almroth, B.O., Meller, E., and Brogan, F. A., "Computer Solutions for Static and Dynamic Buckling Criteria", IUTAM Symposium: Buckling of Structures, Bernard Budiansky, Ed., Springer, 1976.

ASTM Special Technical Publication, Plane Strain Crack Toughness Testing of High Strength Metallic Materials, No. 410, edited by W. F. Brown, Jr. and J. E. Strawley, 1966.

Anderson, J. M., Aberson, J. A., and King, W. W., "Finite-Element Analysis of Cracked Structures Subjected to Shock Loads," Computational Fracture Mechanics, Edited by E. F. Rybicki and S. E. Benzley, American Society of Mechanical Engineers, New York, 1975, pp 173-184.

Anon, "Rapid Inexpensive Tests for Determining Fracture Toughness," Report of the Committee on Rapid Inexpensive Tests for Determining Fracture Toughness, National Materials Advisory Board, Washington, D. C., 1976.

Ashby, M. F., "A First Report on Deformation Mechanism Maps," Acta Met., Vol. 20, 1972, p 887.

Ashby, M.F., "Progress in the Development of Fracture-Mechanism Maps," Fracture 1977, Vol. 1, IC4F, Waterloo, Canada, 1977.

Ayres, D. J., "Dynamic Plastic Analysis of Ductile Fracture--The Charpy Specimen," Int. J. Fracture, 12, Aug. 1976, pp 567-578.

Baker, W. E., Westine, P.S. and Dodge, F. T., "Similarity Methods in Engineering Dynamics," Hayden Book Co., 1973.

Barsom, J. M., "Development of the AASHTO Fracture Toughness Requirements for Bridge Steels," Eng. Fract. Mech., 7, 1975, p 605.

Barsom, J. M., and Rolfe, S. T., "Correlations Between K_{Ic} and Charpy V-Notch Test Results in the Transition-Temperature Range," Impact Testing of Metals, ASTM STP-466, 1970, p 281.

Barsoum, R. S., "On the Use of Isoparametric Finite Elements in Linear Fracture Mechanics," Int. J. Num. Meth. Engg., Vol. 10, 1976.

_____, "A Degenerate Finite Element for Linear Fracture Analysis of Plate Bending and General Shell," Int. J. Num. Meth. Engg., Vol. 10, 1976.

_____, "Triangular Quarter Point Elements as Elastic and Perfectly Plastic Crack Tip Elements,", Int. J. Num Meth. Engg., Vol. 11, 1977.

Basinski, Z. S., Phil Mag., 4, 1959, p 393.

Basinski, Z. S. and Christian, J. W., Australian J. Phys., 13, 1960, p 299.

Begley, J. A. and Landes, J. D., "The J-Integral as a Fracture Criterion," Fracture Toughness, ASTM STP-514, 1972, p 1.

Bennett, P. E. and Sinclair, G. M., J. Basic Dng., Trans., American Society of Mechanical Engineers, Series D, 88, 1966.

Bodner, S. R., "Constitutive Equations for Dynamic Material Behavior," Mechanical Behavior of Materials Under Dynamic Loads, U. S. Lindholm, Ed., Springer, New York, 1968.

Broek, D., Elementary Engineering Fracture Mechanics, Noordhoff, Leyden, The Netherlands, 1974.

Bromovsky, M., Filip, R., Kalna, K., Stepanek, S., and Urban, A., "Study of Crack Initiation-Arresting Conditions in Pressure Vessel Models with Respect to Accumulated Energy," Proceedings, Second International Conference on Pressure Vessel Technology, Part II, American Society of Mechanical Engineers, 1973, p 953.

Buchalet, C. and Mager, T. R., "Experimental Verification of Lower Bound K_{Ic} Values Utilizing the Equivalent Energy Concept," Progress in Flaw Growth and Fracture Toughness Testing, ASTM STP-536, 1973, p 281.

Budiansky, B. and Roth, R. S., "Axisymmetric Dynamic Buckling of Clamped Shallow Spherical Shells," Collected Papers on Instability of Shell Structures-1962, NASA Langley Research Center, TN D-1510, 1962.

Burns, S. J., Bilek, Z.J., "The Dependence of the Fracture Toughness of Mild Steel on Temperature and Crack Velocity," Met. Trans., 4, 1973, p 975.

Byskov, E., Int. J. Fracture, Vol. 6, No. 2, 1970.

Campbell, J.D. and Harding, J., Response of Metals in High Velocity Deformation, 51, Interscience, New York, 1961.

Chen, E. P. and Sih, G. C., "Scattering of Plane Waves by a Propagating Crack," J. Applied Mech., American Society of Mechanical Engineers, Vol. 42, No. 3, September 1975.

_____, "Influence of Specimen Boundary on Dynamic Stress Intensity Factor," Advances in Engineering Sciences, Vol. 1, Proceedings, 13th Annual Meeting, Soc. of Engg. Sc., Hampton, Virginia, November 1-3, 1976.

Chen, Y.M. and Wilkins, M. L., "Application of Novel Finite Difference Method to Dynamic Crack Problems," Advances in Engineering Sciences, Vol. 1, Proceedings, 13th Annual Meeting, Soc. of Engg. Sc., Hampton, Virginia November 1-3, 1976.

_____, "Stress Analysis of Crack Problems With Three-Dimensional Computer Program," Int. J. Fr., Vol. 12, No. 4, August 1976.

_____, "Numerical Analysis of Dynamic Crack Problems," Mechanics of Fracture, Vol. IV, Ed., G. C. Sih, Noordhoff, 1977.

Corten, H. T. and Shoemaker, A. K., American Society of Mechanical Engineers Paper No. 66-WA/Met-8, 1966.

_____, "Fracture Toughness of Structual Steels as a Function of the Rate Parameter T $\ell n(A/\dot{\epsilon})$", Trans., American Society of Mechanical Engineers, J. Basic Eng., 89, 1967, p 86.

Costin, L. S., Duffy, J., and Freund, L.B., "Fracture Initiation in Metals Under Stress Wave Loading Conditions," ASTM Special Technical Publication 627, Fast Fracture and Crack Arrest, edited by G. T. Hahn and M. F. Kanninen, 1977, p 301.

Crosley, P. B. and Ripling, E. J., "Crack Arrest Toughness of Pressure Vessel Steels, " Nuclear Eng. and Design, 17, 1971, p 32.

_____, "Crack Arrest in an Increasing K-Field," Proceedings of the Second International Conference on Pressure Vessel Technology-Part II, American Society of Mechanical Engineers, 1973, p 995.

_____, "Plane Strain Crack Arrest Characterization of Steels," American Society of Mechanical Engineers, Paper No. 75-PVP-32, 1975.

Davies, R. G. and Magee, C. L., Trans. American Society of Mechanical Engineers, J. Eng. Mats. and Tech., 97, Series H, 1975, p 151.

de Meester, B., Doner, M. and Conrad, H., Met. Trans, 6A, 1975, p 65.

Doll, W., "Application of an Energy Balance and an Energy Method to Dynamic Crack Propagation,", Int. J. Fracture, 12, 1976, pp 595-605.

Dresburg, D. E., "Prediction of Toughness Behavior Using Precracked Charpy Specimens," American Society of Mechanical Engineers Preprint 75-PET-25, 1975.

Edmonson, B., Formby, C. L., and Stagg, M. S., "Dynamic Fracture Toughness Measurements," in Practical Fracture Mechanics for Structural Steel, Chapman and Hall, 1969.

Eftis, J. and Krafft, J. M., "A Comparison of the Initiation with the Rapid Propagation of a Crack in a Mild Steel Plate," Trans. American Society of Mechanical Engineers, Basic Eng., 87, 1965, p 257.

Erdogan, F., "Crack Propagation Theories," Fracture, an Advanced Treatise, II, Academic Press, 1969.

Erdogan, F. and Sih, G. C., "On the Crack Extension in Plates Under Plane Loading and Transverse Shear," Journal of Basic Engineering, Vol. 85, 1963, p 519.

Ergatoudis, J. and Irons, B. M., "Curved, Isoparametric 'Quadrilateral' Elements for Finite Element Analysis," Int. J. Solids Structures, Vol. 14, 1968.

Eshelby, J. D., "The Calculation of Energy Release Rates," Prospects of Fracture Mechanics, edited by G. C. Sih et al, Noordhoff International Publishing, 1974, p 69.

Freund, L. B., "Crack Propagation in an Elastic Solid Subjected to General Loading - I. Constant Rate of Extension," J. Mech. Phys. Solids, 20, 1972a, p 129.

_____, "Crack Propagation in an Elastic Solid Subjected to General Loading - II. Nonuniform Rate of Extension," J. Mech. Phys. Solids, 20, 1972b, p 141.

Freund, L. B., "Crack Propagation in an Elastic Solid Subjected to General Loading - III. Stress Wave Loading," J. Mech. Phys. Solids, 21, 1973, p 41.

_____, "The Motion of a Crack in an Elastic Solid Subjected to General Loading," Proc. Int. Conf. on Dynamic Crack Propagation, Noordhoof, Leyden, 1973, p 553.

Freund, L. B. and Rice, J. R., "On the Determination of Elasto-Dynamic Crack Tip Stress Fields," Int. J. Solids Structures, Vol. 10, 1974.

Freund, L. B., "The Analysis of Elasto-Dynamic Crack Tip Stress Fields," Mechanics Today, Vol. 3, edited by S. Nemat-Nasser, Pergamon Press, 1976, p 55.

_____, "A Simple Model of the Double Cantilever Beam Crack Propagation Specimen," J. Mech. Phys. Solids, Vol. 25, 1977, p 69.

Gray, I. and Priest, A. H., "The Arrest of Propagating Cracks," Practical Applications of Fracture Mechanics to Pressure Vessel Technology, Inst. Mech. Eng., London, 1971, p 225.

Griffis, C. A., "Approximate One-Dimensional Elastic Analysis of Notched, Three Point Bend Specimens Subjected to Impact Loads," NRL Memorandum Report, 1975.

Hahn, G. T., Hoagland, R. G., Rosenfield, A. R., and Sejnoha, R., "Rapid Crack Propagation in a High Strength Steel," Met. Trans., 5, 1974, p 475.

Hahn, G. T., Hoagland, R. G., Kanninen, M. F., and Rosenfield, A. R., "Pilot Study of the Fracture Arrest Capabilities of A533B Steel," Presented at Ninth National Symposium on Fracture Mechanics, Pittsburgh, August 1975.

Hahn, G. T., Hoagland, R. G., Kanninen, M. F., and Rosenfield, A. R., "The Characteristics of Fracture Arrest in a Structural Steel," ibid, p 981.

Hahn, G. T., Gehlen, P. C., Hoagland, R. G., Marschall, C.W., Kanninen, M. F., Popelar, C., and Rosenfield, A. R., "Critical Experiments, Measurements and Analyses to Establish a Crack Arrest Methodology for Nuclear Pressure Vessel Steels," Reports Prepared for the U. S. Nuclear Regulatory Commission by Battelle Columbus Laboratories, Ohio, 1975-1976.

Hatch, A. J., TMCA, Tech Dept. (Oct. 6, 1958) cited in Aerospace Structural Metals Handbook, Code 3707, Mech. Properties Data Center, Traverse City, Michigan, March 1965, p 12.

Hauser, F. E., Simmons, J. A., and Dorn, J. E., in Response of Metals in High Velocity Deformation, 93, 1961.

Hellan, K., "Griffith-type Fracture Analysis for Large-Scale Yielding Conditions," Eng. Fracture Mech., 8, 1976, pp 501-506.

Hellen, T.K., "On Special Isoparametric Elements for Linear Elastic Fracture Mechanics," Int. J. Num. Meth. Engg., Vol. 11, 1977.

Henshell, R. D. and Shaw, K. G., "Crack Tip Finite Elements are Unnecessary," Int. J. Num. Meth. Engg., Vol. 9, 1975.

Hertzberg, R. W., Deformation and Fracture Mechanics of Engineering Materials, Wiley, New York, 1976.

Hilton, P. D. and Hutchinson, J. W., "Plastic Intensity Factor for Cracked Plates, Engineering Fracture Mechanics, Vol. 3, No. 4, 1971, pp 435-451.

Hilton, P. D. and Sih, G. C., "Application of the Finite Element Method to the Calculation of Stress Intensity Factors," Mechanics of Fracture, Vol. 1, Ed.: G. C. Sih, Noordhoff, 1973.

Hockett, J. E., "Compression Testing at Constant True Strain Rates," American Society Testing Mater. Proc., Vol. 59, 1959, p 1309.

Hockett, J. E. and Zukas, E. G., Institute of Physics, Conf. Ser. No. 21, 1973, 53.

Holston, A., Jr., "A Mixed Mode Crack Tip Finite Element," Int. J. Fracture, Vol. 12, No. 6, December 1976.

Hutchinson, J. W., "Singular Behavior at the End of a Tensile Crack in Hardening Material," J. Mech. Phys. Solids, Vol. 16, 1968.

Johnson, F. A., Glover, A. P. and Radon, J. C., "Fracture Toughness and Fracture Energy Measurements on Aluminum Alloys," Eng. Fracture Mech., 8, 1976, pp 381-390.

Jones, N. and Okawa, D. M., "Dynamic Plastic Buckling of Rings and Cylindrical Shells," Nuclear Engineering and Design, Vol. 37, 1976, p 125.

Kanninen, M. F., "An Analysis of Dynamic Crack Propagation and Arrest for a Material Having a Crack Speed Dependent Fracture Toughness," Prospects Fracture Mechanics, Noordhoff, Leyden, 1974, p 251.

_____, "An Augmented Double Cantilever Beam Model for Studying Crack Propagation and Arrest," 9, 1973, p 83.

_____, "A Dynamic Analysis of Unstable Crack Propagation and Arrest in the DCB Test Specimen," 10, 1974, p 415.

Kanninen, M., Mills, E., Hahn, G., Marschall, C., Broek, D., Coyle, A., Masubushi, K. and Itoga, K., "A Study of Ship Hull Crack Arrester Systems," Ship Structure Committee Report SSC-265, Naval Sea Systems Command, Washington, D. C., 1977.

Kennedy, T. C. and Achenbach, J. D., "Rapid Extension of Penny-Shaped Crack Under Torsion," Int. J. Solids Structures, Vol. 18, 1972.

Kobayashi, A. S., Emery, A. F. and Mall, S., "Dynamic-Finite Element and Dynamic-Photoelastic Analyses of Two Fracturing Homalite-100 Plates," Exp. Mech., Sept. 1976, pp 321-328.

Kolsky, H., "An Investigation of Mechanical Properties at Very High Rates of Loading," Proc. Phys. Soc. (London), Sev. B., Vol. 62, 1949, p 676.

Krafft, J. M. and Irwin, G. R., "Crack-Velocity Considerations," Fracture Toughness Testing and Its Applications, ASTM STP-381, 1964, p 114.

Krafft, J. M., Hettche, L. R., Sullivan, A. M. and Loss, F.J., "Fracture-Flow Relationships for A533B Pressure Vessel Steel," Trans. American Society of Mechanical Engineers, J. Eng. for Industry, 92, 1970, p 330.

Lange, E. A., "Dynamic Fracture-Resistance Testing and Methods for Structural Analysis," NRL Report 7979, Naval Research Laboratory, Department of the Navy, Washington, D. C., April 27, 1976.

Lindholm, U. S., "High Strain Rate Tests," Techniques of Metals Research, Vol. 5, R. F. Banshak, Ed., John Wiley & Sons, Inc., 1971.

MacGregor, C. W. and Fisher, J. C., J. Appl. Mech., 12, 1945, A217.

Malvern, L. E., "The Propagation of Longitudinal Waves in a Bar Exhibiting a Strain-Rate Effect," J. Appl. Mech., Vol. 18, 1951, p 203.

MARC Analysis Research Corporation, MARC User's Manual, Vols. I-IV, Revision H, 1976.

Morgan, J. D., Anderson, J. M., and King, W. W., "Elastodynamics of Cracked Structures Using Finite Elements," AIAA Journal, 12, pp 1767-1769.

Mostovoy, S., Crosley, P.B. and Ripling, E. J., "Use of Crack-Line-Loaded Specimens for Measuring Plane-Strain Fracture Toughness," J. Materials, 2, 1967, p 661.

Palinswamy, K. and Knauss, W. G., "Crack Extension in Brittle Solids Under General Loading," Mechanics Today, Vol. 4., S. Nemat-Nasser, Ed., 1977.

Perrone, N., "On a Simplified Method for Solving Impulsively Loaded Structures of Rate-Sensitive Materials," J. Appl. Mech., Vol 32, 1965, p 489.

Perzyna, P., "The Constitutive Equations for Rate Sensitive Plastic Materials," Quarterly Appl Math., Vol. 20, 1963, p 321.

Pilkey, W., Saczalski, K. and Schaeffer, H., "Structural Mechanics Computer Programs - Surveys, Assessments, and Availability," University Press of Virginia, Charlottesville, 1974.

Popelar, C., Rosenfield, A. R. and Kanninen, M. F., "Steady-State Crack Propagation in Pressurized Pipelines," J. Pressure Vessel Technology, Vol. 99, 1977, pp 112-121.

"PVRC Recommendations on Toughness Requirements for Ferritic Materials," Welding Research Council Bulletin No. 175, August 1972.

Rice, J. R., "A Path Independent Integral and the Approximate Analysis of Strain Concentration by Notches and Cracks," J. Appl. Mech., 1968, p 379.

Robinson, J.N. and Tetelman, A. S., "Comparison of Various Methods of Measuring K_{Ic} on Small Precracked Bend Specimens that Fracture After General Yield," Eng. Fracture Mech., 8, 1976, pp 301-313.

Rolfe, S.T. and Barsom, J. M., Fracture and Fatigue Control in Structures, Prentice-Hall, Englewood Cliffs, N.J., 1977.

Schapery, R.A., "On a Thermodynamic Constitutive Theory and Its Application to Various Nonlinear Materials," Proc. IUTAM Symposium, B. A. Boley, Ed., Springer-Verlag, 1968.

Seeger, A., in Dislocations and Mechanical Properties of Crystals, J. Wiley and Sons, New York, 1957, p 243.

Shabbits, W. O., "Dynamic Fracture Toughness Properties of Heavy Section A533 Grade B Class 1 Steel Plate," Heavy Section Steel Technology Program Tech. Report No. 13 (WCAP-7623), Oak Ridge National Laboratory, December 1970.

Shabbits, W. O., Pryle, W. H. and Wessel, E. T., "Heavy Section Fracture Toughness Properties of A533 Grade B Class 1 Steel Plate and Submerged-ARC Weldment," Heavy Section Steel Technology Program Report No. 6. (WCAP-7414), Oak Ridge National Laboratory, December 1969.

Shmuely, M. and Peretz, D., "Static and Dynamic Analysis of the DCB Problem in Fracture Mechanics," Int. J. Solids Structures, Vol. 12, 1976.

Shockey, D. A. and Curran, D. R., "A Method for Measuring K_{Ic} at Very High Strain Rates," Progress in Flaw Growth and Fracture Toughness Testing, ASTM STP-536, 1973, p 297.

Shoemaker, A.K., and Rolfe, S. T., "The Static and Dynamic Low-Temperature Crack Toughness Performance of Seven Structural Steels," Eng. Fracture Mech., 2, 1971, p 319.

Sih, G. C., "Some Elastodynamic Problems of Cracks," International Journal of Fracture Mechanics, Vol. 4, 1968, pp 51-68.

_____, "Dynamic Aspects of Crack Propagation," Inelastic Behavior of Solids, M. F. Kanninen et al., Editors, McGraw-Hill, 1970, p 607.

_____, "A Special Theory of Crack Propagation," Methods of Analysis and Solution of Crack Problems, Vol. 1, edited by G. C. Sih, Noordhoof International Publishing, Leyden, the Netherlands, 1973, p 21.

_____, "Fracture Toughness Concept," ASTM Special Technical Publication No. 605, 1976, p 3.

_____, "Mechanics of Ductile Fracture," Technical Report IFSM-77-78, Lehigh University, Bethlehem, PA, June 1977.(a)

Sih, G. C., "Dynamic Crack Problems - Strain Energy Density Fracture Theory," Elastodynamic Crack Problems, Mechanics of Fracture IV, edited by G. C. Sih, Noordhoff International Publishing, 1977, p 17.(b)

Sih, G. C. and Embly, G. T., "Impact Response of a Finite Crack in Plane Exterior," Int. J. Solids Structures, Vol. 8, 1972.

Stöckel, H. and Auer, F., "Dynamic Behavior of Tensile Cracks - Finite Difference Simulation of Fracture Experiments," Int. J. Fracture, Vol. 12, June 1976.

Stricklin, J. A., Haisler, W. E. and Von Riesermann, W. R., "Large Deflection Elastic-Plastic Dynamic Response of Stiffened Shells of Revolution," J. Pressure Vessel Technology, 1974, p 87.

Stricklin, J. A. and Saczalski, K. J., Constitutive Equations in Viscoplasticity: Computational and Engineering Aspects, American Society of Mechanical Engineers, Pub. No. AMD-Vol. 20, 1976.

Taylor, D. B. C. and Malvern, L. E., "Response of Metals in High Velocity Deformation," 1961, p 77.

Tracey, D. M., Engineering Fracture Mechanics, Vol. 3, 1971

Tsai, Y. M., "Propagation of a Brittle Crack at Constant and Accelerating Speeds," Int. J. Solids Structures, 9, 1973, p 625.

_____, "Dynamic Ductile Fracture of a Critical Crack," Advances in Engineering Sciences, Vol. 1, Proceedings, 13th Annual Meeting, Soc. of Engg. Sc., Hampton, Virginia, November 1-3, 1976.

Turner, C. E., "Dynamic Fracture Toughness Measurement by Instrumental Impact Testing," ISPRA Advanced Seminar on Fracture Mechanics, October 1975.

Valanis, K. C., "Observed Plastic Behavior of Metals vis-a-vis the Endochronic Theory of Plasticity," Proc. Int. Symp. on Plasticity, Warsaw, 1972.

Valanis, K. C., Constitutive Equations in Viscoplasticity: Phenomenological and Physical Aspects, American Society of Mechanical Engineers, Pub. No. AMD-Vol 21, 1976.

Wilkins, M. L., "Fracture Studies with Two- and Three-Dimensional Computer Simulation Programs," Conference on Fracture Mechanics and Technology, Hong Kong, 1977.

Wilson, W. K., Combined Mode Fracture Mechanics, Ph. D. Thesis, University of Pittsburgh, 1969.

_____, "Some Crack Tip Finite Elements for Plate Elasticity," Fifth National Symposium on Fracture Mechanics, University of Illinois, 1971.

_____, "Finite Element Methods for Elastic Bodies Containing Cracks," Mechanics of Fracture, Vol. 1, Ed: G. C. Sih, 1973.

Wullaert, R. A., Oldfield, W. and Server, W. L., "Fracture Toughness Data for Ferritic Nuclear Pressure Vessel Materials," Report to EPRI by Effects Technology, Santa Barbara, California, April 1976.

Yeung, K. S. and Welch, R. E., "Refinement of Finite Element Analysis of Automobile Structures under Crash Loading," IITRI Project No. J6384, U. S. DoT Contract DoT-HS-6-01364, October 1977.

Zienkiewicz, O. C., The Finite Element Method in Engineering Science, McGraw Hill, 1971.

THE NATIONAL ACADEMY OF SCIENCES was established in 1863 by Act of Congress as a private, non-profit, self-governing membership corporation for the furtherance of science and technology, required to advise the federal government upon request within its fields of competence. Under its corporate charter the Academy established the National Research Council in 1916, the National Academy of Engineering in 1964, and the Institute of Medicine in 1970.

THE NATIONAL ACADEMY OF ENGINEERING was founded in 1964 as a non-profit membership institution, by action of the National Academy of Sciences under the authority of its congressional charter of 1863 establishing it as a private, self-governing corporation to further science and technology and to advise the federal government. The two Academies share those purposes in their fields.

THE NATIONAL RESEARCH COUNCIL was established in 1916 by the National Academy of Sciences to associate the broad community of science and technology with the Academy's purposes of furthering knowledge and of advising the federal government. The Council operates in accordance with general policies determined by the Academy by authority of its Congressional charter of 1863 as a non-profit, self-governing membership corporation. Administered jointly by the National Academy of Sciences, the National Academy of Engineering, and the Institute of Medicine (all three of which operate under the charter of the National Academy of Sciences), the Council is their principal agency for the conduct of their services to the government and the scientific and engineering communities.

THE COMMISSION ON SOCIOTECHNICAL SYSTEMS is one of the major components of the National Research Council and has general responsibility for and cognizance over those program areas concerned with physical, technological, and industrial systems that are or may be deployed in the public or private sector to serve societal needs.

THE NATIONAL MATERIALS ADVISORY BOARD is a unit of the Commission on Sociotechnical Systems of the National Research Council. Organized in 1951 as the Metallurgical Advisory Board, through a series of changes and expansion of scope, it became the Materials Advisory Board and, in January 1969, the National Materials Advisory Board. In consonance with the scope of the two Academies, the general purpose of the Board is the advancement of materials science and engineering, in the national interest. The Board fulfills its purpose by: providing advice and assistance, on request, to government agencies and to private organizations on matters of materials science and technology affecting the national interest; focusing attention on the materials aspects of national problems and opportunities, both technical and nontechnical in nature, and making appropriate recommendations as to the solution of such problems and the exploitation of these opportunities; performing studies and critical analyses on materials problems of a national scope, recommending approaches to the solution of these problems, and providing continuing guidance in the implementation of resulting activities; identifying problems in the interactions of materials disciplines with other technical functions, and defining approaches for the effective utilization of materials technologies; cooperating in the development of advanced educational concepts and approaches in the materials disciplines; communicating and disseminating information on Board activities and related national concerns; promoting cooperation with and among the materials-related professional societies; maintaining an awareness of trends and significant advances in materials technology, in order to call attention to opportunities and possible roadblocks, and their implications for other fields, and recognizing and promoting the development and application of advanced concepts in materials and materials processes.